

Transport Infrastructure Improvements and Spatial Sorting: Evidence from Buenos Aires *

[Click here for the latest version](#)

Pablo Ernesto Warnes[†]

November 8, 2020

Abstract

How do improvements in the urban transport infrastructure affect the spatial sorting of residents with different levels of income and education within a city? What are the welfare effects of improving urban transit once we take into account these patterns of spatial sorting? In this paper, I study the effects of the construction of a bus rapid transit system (BRT) on the spatial reorganization of residents within the city of Buenos Aires, Argentina. To do so, I leverage an individual level panel data set of more than two million residents that with which I can describe intra-city migration patterns. I first find reduced form evidence that the construction of the BRT increased the spatial segregation between high and low-skilled residents within the city. I then develop a dynamic quantitative spatial equilibrium model of a city with heterogeneous workers that allows me to quantify the welfare effects of this BRT system while taking into account these spatial sorting patterns. With this quantitative framework, I can measure the average welfare gains for residents that were living near the BRT lines before these were built. I find that welfare gains were very similar between high- and low-skilled workers living in the same locations, but very different within skill levels across locations. Residents living near a BRT line in neighborhoods with the lowest share of high-skilled residents saw welfare gains close to 1% on average, while residents living near a BRT line in neighborhoods with the highest high-skilled share saw welfare gains around 0.5% on average.

* I am grateful to David Weinstein, Donald Davis, and Réka Juhász for their guidance and support. I thank Iain Bamford, David Alfaro Serrano, Timur Abbiasov, Yue Yu, Howard Zhang, Sang Hoon Kong, Yi Jie Gwee, Vinayak Iyer, Motaz Al-Chanati, and all the participants at the International Trade Colloquium at Columbia for their invaluable comments and suggestions. I thank the Institute for Latin American Studies at Columbia University, the Center for Development Economics and Policy, and the CAF-Development Bank of Latin America for providing financial support for this project. I would also like to thank Andrea Quijano and Alejandro Diaz Tur for their excellent research assistance. All errors are my own.

[†]Columbia University (PhD candidate). Email: pew2116@columbia.edu

1 Introduction

How do improvements in the urban transport infrastructure affect the spatial sorting of residents with different levels of income and education within the city? What are the welfare effects of these improvements in transport infrastructure once we take into account these patterns of spatial sorting? Given the world's rapid urban growth of the last decades,¹ it is no surprise that many cities (especially in the developing world) are investing large sums in improving their public transport infrastructure.² The literature on public transport improvements has shown that these projects tend to increase population density, land rents, and output in the neighborhoods that are close to the improved infrastructure.³ However, one concern that arises is that these improvements in public transport may displace incumbent low-skilled residents through rent increases, a process often referred to as "transit-induced gentrification." As a consequence, these low-skilled incumbent residents might suffer welfare losses.⁴ In this paper, I study how the construction of a bus rapid transit system⁵ (BRT) in the city of Buenos Aires, Argentina, affected the spatial sorting of high- and low-skilled residents,⁶ as well as the welfare consequences of these transport infrastructure improvements for the incumbent residents of the neighborhoods near the new transit lines.

A distinguishing feature of this paper is that it leverages individual level panel data on the addresses of more than two million residents. By using a panel data set at the individual level, I can follow residents as they move within the city, which allows me to describe intra-city migration patterns at a very fine spatial scale. I use these data to contribute to the literature on the effects of urban transit infrastructure in three ways. First, I document the heterogeneous response by high- and low-skilled residents in their intra-city migration decisions to the improvements in market access generated by the new BRT system. Second, I develop one of the first dynamic quantitative spatial equilibrium models of a city that combines commuting and migration decisions taken by forward-looking agents. Third, I use the dynamic quantitative spatial equilibrium framework with heterogeneous workers to estimate the welfare effects for high- and low-skilled incumbent residents in the city. The crucial difference with previous welfare estimates of transport infrastructure improvements is that, by relying on individual level panel data, I can account for the changes in migration decisions as a consequence of these infrastructure improvements. In doing so, I can differentiate between the welfare gains of the residents that were already living in affected areas before the improvements, and the welfare gains of the residents who live in the affected areas after a new steady state equilibrium is reached.

¹The world's urban population accounted for 34% of total global population in 1960, 55% in 2018, and is expected to account for 68% of total global population by 2050 (UN, 2018).

²According to Hannon et al. (2020), more than \$1.4 trillion will be spent in new light-rail and metro projects in cities around the world between 2019 and 2025.

³See Redding and Turner (2015), Berg et al. (2017), and Roberts et al. (2020) for surveys of the literature on the effects of transport infrastructure improvements.

⁴The phenomenon referred to as "transit-induced gentrification" has been extensively studied in the urban planning and transportation engineering literature (Chapple and Loukaitou-Sideris, 2019, Dawkins and Moeckel, 2016, Chapple and Loukaitou-Sideris, 2019, Bardaka et al., 2018, Tehrani et al., 2019), with varying results, and often not accounting for the endogeneity concerns that might arise from the placement of the transport infrastructure (see Padeiro et al. 2019 for a review of the literature).

⁵A bus rapid transit system is a bus-based public transport system that includes dedicated roadways for buses, platform-level boarding, and assigns priority to buses at intersections where buses may interact with other traffic.

⁶I define a resident as low-skilled if she has no post-secondary education, and as high-skilled if she has at least some post-secondary education.

Between 2011 and 2017, the city of Buenos Aires opened six lines of a BRT network, the *Metrobus*. This network spans 51 kilometers and transports close to a million passengers a day. Although Buenos Aires already had a robust network of buses and subway lines that provided coverage for most of the city's neighborhoods, the new BRT lines resulted in an average increase in speed of 30% for the buses that went through those avenues (Kamrowska-Zaluska, 2017). These increases in transport speed led to increases in market access for commuters located in neighborhoods that were originally less well connected to locations in the city with high employment density. The effects of this change in market access are the main focus of this study.

In order to analyze the sorting patterns of residents by skill type, I leverage a uniquely detailed data source: the electoral register for all election years between 2011 and 2017 for the city of Buenos Aires, which allows me to track individuals as they change their residential location within the city. Since voting is compulsory in Argentina, the government maintains a register with residential addresses for all eligible voters. I have processed this register for the city of Buenos Aires, and geocoded⁷ all addresses for more than two million eligible voters that reside in the city. I use this register, along with other data sources, such as census data and household surveys, to implement a reduced form analysis that relies on a historical IV identification strategy. In order to capture the full general equilibrium effects of the changes in the transport network on every location of the city, I construct a measure of commuter market access developed by Ahlfeldt et al. (2015) and Tsivanidis (2019).⁸ I then examine how changes in this measure of market access affected the change in the share of high-skilled workers⁹ in each neighborhood, the change in high- and low-skilled population, the change in population density in each neighborhood, and the change in residential floorspace prices. I address the endogeneity concerns regarding the placement of the BRT lines by constructing an instrumental variable for the changes in market access that relies on the placement of a tram system built in the first half of the twentieth century, that was dismantled by 1963. The identifying assumption behind this strategy¹⁰ is that the placement of a tram system that had been decided prior to 1938 should not be correlated with changes in unobservable confounders between 2011 and 2017. Through this reduced form analysis, I find that the BRT system increased the high-skilled population relatively more in places that already had a high-skilled share, while it did the opposite in places with the lowest initial shares of high-skilled residents. This pattern of spatial sorting increased segregation by skill type within the city.

Having described these sorting patterns between high- and low-skilled workers in a reduced form setting, I develop a dynamic model of a city in which residents who are forward-looking must make migration and commuting decisions each period. On the production side, I assume that each location produces a location-specific variety of the consumption good under perfect competition. To do so, they must employ both types of labor (high- and low-skilled). These assumptions lead to labor demand being spatially distributed across the city, which in turn motivates the commuting decisions of the residents. This model draws from the dynamic structure used by Caliendo et al. (2019) and Balboni (2019) to study questions of

⁷Geocoding is the process of assigning geographical coordinates to an address.

⁸This measure summarizes the total impact of the transit network on firms and residents, and can be derived from a wide class of models, as long as they imply a gravity equation for commuting flows (Tsivanidis, 2019).

⁹The share of high-skilled residents is defined as the population of high-skilled residents divided by the total population.

¹⁰This type of historical route IV approach was developed by Duranton and Turner (2012) and has been used frequently in the transportation economics literature (Redding and Turner, 2015).

regional economics, and from the commuting structure present in the static models of a city developed by Ahlfeldt et al. (2015) and Tsivanidis (2019), which allow for residents to live and work in different locations. I rely on the individual level migration data constructed from the electoral register to estimate key parameters of the model. I develop a numerical solution algorithm for the model, which is based on Caliendo et al. (2019). Having solved the model, I show that it predicts very similar patterns of spatial sorting as a response to the transport improvements as the ones found by the reduced form analysis.

Using this framework, I estimate the welfare impact of implementing this BRT system in the city of Buenos Aires on the residents that were already living near the BRT lines before they were put in place, which I refer to as incumbent residents. Welfare gains are measured as the difference in aggregate expected utility in the period prior to the implementation of the new transport infrastructure between a scenario where the changes in the transport infrastructure are implemented and a scenario where no change in the transport infrastructure is implemented. I find that incumbents in different parts of the city benefit differently from this new BRT. In particular, both high- and low-skilled residents that were living in the neighborhoods with the lowest high-skilled shares benefited more from the new BRT lines than the residents that were living in neighborhoods with a higher initial high-skilled share. This result is consistent with the fact that places with a higher initial high-skilled share saw higher increases in population and floorspace prices, which could have reduced the welfare gains from the increased market access for the incumbent residents. Finally, it is worth mentioning that, consistent with what Tsivanidis (2019) finds for the aggregate gains of a transport improvement for high- and low-skilled workers, I find that welfare gains for high- and low-skilled incumbents are also very similar.

Finally, I use the dynamic quantitative framework to study how different counterfactual configurations of the BRT system would have produced different results in terms of spatial sorting and welfare gains. To do so, I solve for the full equilibrium path of endogenous variables under different assumptions on which BRT lines were built. I then compare, in different parts of the city, the welfare gains for incumbents in these counterfactual scenarios to the welfare gains for incumbents obtained from having built the entire BRT system. I find that if the government had only built a line that improved market access to the neighborhoods with the lowest share of high-skilled residents, this would have led to an increase in the share of high-skilled residents in the neighborhoods closest to the new line. This result suggests that transport improvements that only target low-income neighborhoods (with a high share of low-skilled residents) could end up displacing some of the low-skilled residents to which the policy was initially targeted. However, even in this case, both high- and low-skilled incumbents living in predominantly low-skilled neighborhoods benefit, on average, from these more targeted transport improvements.

This paper presents four main findings. First, contrary to the hypothesis of transport-induced gentrification, I find that the transport infrastructure improvements led to increases in the high-skilled share mostly in neighborhoods that already had a relatively high level of high-skilled share, while neighborhoods in the lowest quintile of the distribution of high-skilled share saw a decrease in their high-skilled share as a consequence of the improvements in transport infrastructure. For the same increase in market access, a neighborhood at the eightieth percentile of the initial distribution of high-skilled share saw a proportional increase in its share of high-skilled residents six times higher than a neighborhood in the

twentieth percentile. These patterns of spatial sorting between high- and low-skilled workers led to an increase in the segregation by skill type in the city.

Second, I find that on average, high-skilled incumbent residents, who lived near¹¹ the route of a BRT line before the line was put in place, benefited slightly more than low-skilled incumbent residents, with high-skilled incumbents seeing an average welfare gain of 1.04%, and low-skilled incumbent residents seeing an average welfare gain of 0.94%.

Third, I find that, although the average welfare gains for high- and low-skilled incumbent residents are quite similar on average, there is a significant difference in how these gains are distributed across space. Both high- and low-skilled residents that lived near the BRT line that served the neighborhoods with the lowest proportion of high-skilled residents saw increases in welfare that were, on average, around twice¹² the welfare gains perceived by residents that lived near the BRT line that served the neighborhoods with the highest proportion of high-skilled residents. Suggesting that the larger increases in population and, consequently, in housing prices produced by the transport improvements in neighborhoods with higher high-skilled share offset a larger fraction of the welfare gains for the residents that were already living there.

Fourth, I find that, had the government chosen to built only a BRT line going through low-skilled neighborhoods, the policy would have had a gentrification effect. Budgetary and political consideration might lead governments to prioritize infrastructure improvements in poorer areas, where the share of low-skilled workers is higher. According to my quantitative analysis, doing so would have led to an increase in the share of high-skilled workers in the areas that initially had a low presence of this type worker. Moreover, both high- and low-skilled incumbents in the neighborhoods that initially had a low share of high-skilled population would have benefited around 30% less¹³ than if the the full BRT system had been built.

This paper contributes to several strands of literature. There is a large body of work that studies the impact of transport infrastructure improvements on the spatial distribution of residents and economics activity (Allen and Arkolakis, 2019, Baum-Snow, 2007, Duranton and Turner, 2012, Gonzalez-Navarro and Turner, 2018, Baum-Snow et al., 2018, Gibbons and Machin, 2005, Glaeser et al., 2008, Tsivianidis, 2019, Pathak et al., 2017). This paper contributes to this body of research by providing a general equilibrium framework that incorporates intra-city migration decisions, and using this framework to study the welfare effects for incumbent residents of the areas that were close to the transport improvements.

There is also a substantial body of work, especially in recent years, that develops quantitative spatial equilibrium models of cities that incorporate commuting (Allen et al., 2016, Severen, 2018, Hebllich et al., 2020, Tsivianidis, 2019). These studies, however, lack migration data at the level of spatial aggregation necessary to study intra-city migration within the context of these models. As a consequence, these papers have not included agents that must make migration decisions in a dynamic setting. Because I

¹¹Within half a mile of a BRT line.

¹²The increase was 2.1 times higher for high-skilled residents and 1.8 times higher for low-skilled residents.

¹³31% less for high-skilled incumbents, and 30% less for low-skilled incumbents.

can track individuals within the city as they change residential location, I am able to develop a dynamic quantitative spatial equilibrium model, where residents choose their residential location in a forward-looking manner.

This paper also contributes to the growing body of work that develops dynamic quantitative spatial equilibrium models for regions or countries (Caliendo et al., 2019, Balboni, 2019, Morten and Oliveira, 2018, Desmet et al., forthcoming, Bryan and Morten, 2019). Within this body of work, this paper is the first to incorporate commuting, which allows for workers to live and work in different locations.

A fourth strand of literature to which this paper contributes is the large body of research on the determinants of gentrification (Almagro and Domínguez-Iino, 2019, David et al., 2017, Couture et al., 2018, Dragan et al., 2019, Su, 2020). This paper contributes to this body of research by evaluating the hypothesis that transport infrastructure improvements might have led to gentrification of neighborhoods that were initially populated predominantly by low-skilled residents. I do not find that the BRT system implemented in Buenos Aires led to gentrification (defined as an increase in the share of high-skilled residents) in the neighborhoods that had an initially low level of high-skill share. I do, however, find that a more localized transport improvement, targeted only to neighborhoods with low high-skilled share, would have lead to gentrification.

Finally, I contribute to the growing body of literature that studies the effects of improvements in transport infrastructure in developing countries¹⁴ (Baum-Snow and Turner, 2017 Fajgelbaum and Redding, 2018, and Tsivanidis, 2019) by examining the impact of the BRT system implemented in the city of Buenos Aires. This is particularly important, given that most of the urban growth in the next thirty years will likely take place in developing countries (UN, 2018), and therefore, understanding the effects of urban transport infrastructure improvements in the specific context of developing countries has become increasingly relevant.

The paper is organized as follows. In Section 2, I provide a brief background on the city of Buenos Aires, and on the BRT project that will serve as the main focus of this paper; in Section 3, I describe the main sources of data used in this paper; in Section 4, I conduct a reduced form analysis to study the effects of the BRT system on key outcomes; in Section 5, I develop a dynamic quantitative spatial equilibrium model that allows me to study the welfare effects of the transport infrastructure improvements, as well as analyze counterfactual scenarios; in Section 6, I explain the estimation procedure for the parameters of the model; in Section 7, I present the results of the model, and contrast the predictions from the model with the reduced form results; in Section 8, I analyze the welfare effects of the transport infrastructure improvements; in Section 9, I examine different counterfactual scenarios where only a subset of the BRT lines were built; finally, Section 10 concludes.

¹⁴See Bryan et al. (2020) for a review of the literature on urban economics in developing countries.

2 Background

The city of Buenos Aires is the capital and largest city of Argentina, with 2.9 million inhabitants.¹⁵ Representing 28% of the country's GDP, it is the economic, political, and cultural center of Argentina. In this section, I will provide a brief overview of the city's demographic composition, as well as of the spatial distribution of economic activity and residents by skill type. I will also analyze the commuting patterns of residents of the city prior to the construction of the BRT system. I will then describe the BRT system that was put in place between 2011 and 2017 in the city, which will be the main focus of my analysis.

2.1 City Structure

Economic activity in the city of Buenos Aires, measured by employment, is highly concentrated around the city's central business district (CBD). Alves et al. (2018) find that 50% of the formal employment in the city is located within a 4 kilometer radius of the CBD, in an area that constitutes less than 19% of the surface area of the city. From Figure 1 we can see that most of the employment is concentrated in 4 of the 15 communes, with 31% of employment located in commune 1, where the CBD is located.

We can then separate workers between those with at least some post-secondary education (which I will call high-skilled), and those with at most a completed secondary education (which I will call low-skilled). Figure 2 shows the fraction of workers by skill type that work in each commune. We can see that high-skilled workers are more spatially concentrated in commune 1, around the CBD, while low-skilled workers are more spatially dispersed. This is consistent with high-skilled workers being employed more intensively in industries that tend to be more spatially concentrated around the CBD.

In terms of the spatial distribution of residents by residential location, we can see in Figure 3 that there is a clear decreasing gradient in the high-skilled share—defined as the share of residents that are high-skilled in a location—from the north-east to the south-west. This exact same pattern can be seen by looking at Figure 4, that shows the average housing prices (in terms of US dollars per square meter) by district. We can see that the most expensive districts are in the north-eastern side of the city, while the least expensive parts of the city are in the southern and south-western districts.

2.2 Commuting in Buenos Aires

With over 130 bus lines running through the city and six subway lines connecting the periphery of the city with the CBD (see Figure 5), Buenos Aires already had a robust urban transportation network prior to the construction of the Metrobus. As a result, almost 80% of trips within the city done in 2010 were done either by public transport (bus, subway or train), or by walking or biking. Table 1 shows the percentage

¹⁵The entire metropolitan area surrounding the city of Buenos Aires constitutes the third largest metropolitan area in Latin America, with a population of 14.8 million, and represents 33% of the country's population.

of trips done in 2010 within the city by mode of transport by both high-skilled and low-skilled residents. We can see that although high-skilled residents used cars at a slightly higher rate, the majority of trips for both high- and low-skilled residents were done by public transit, walking, or biking (81% of trips for low-skilled residents, and 73% of trips for high-skilled residents).

2.3 *Metrobus*: The BRT System of the City of Buenos Aires

Between 2011 and 2018, the city of Buenos Aires built a system of bus rapid transit (BRT) lines that spans 50.5 km (31.4 mi). The main objective of this infrastructure project was to improve commute times by bus between the residential areas in the periphery of the city and the neighborhoods with the highest employment density. Each line in the system is composed of two to four dedicated bus lanes, with physical separation from regular traffic, and platform-level boarding. By 2016, the system was composed of five lines that functioned full time.¹⁶ Figure 6 shows the placement of these five lines in the city.

The first line of the Metrobus, the *Juan B. Justo* Line, was inaugurated in May 2011. This line is estimated to transport around 100,000 passengers a day, and reduce commuting costs along the *Juan B. Justo* Avenue by 40% according to government estimates¹⁷. The *9 de Julio* Line and the *Sur* Line were inaugurated in 2013. The *9 de Julio* Line joins the two main train stations of the city, and goes across the CBD. This line transports an estimated 250,000 passengers a day, and reduces bus travel time by 50% along the *9 de Julio* Avenue according to the government's estimates. The *Sur* Line serves the southern part of the city (which includes most of the lowest income neighborhoods in the city). The *Metrobus Sur* Line also serves approximately 250,000 passengers a day, it has reduced travel times by 15% according to the government's estimates, and has increased ridership by 30%. The *Cabildo* Line and the *25 de Mayo* Line were inaugurated in 2015. The *Cabildo* Line is estimated to serve around 200,000 passengers and was designed to connect the periphery of the city with the subway line D (see Figure 2 for a map of both the subway lines and the Metrobus lines). The *San Martín* line was inaugurated in 2016, and is estimated to have decreased transport times for buses along the line by 20%.

3 Data

The two main geographic units used in the analysis are the census tracts (*radio censal*) for the city of Buenos Aires, and the voting districts (*círculo electoral*) for the city of Buenos Aires. The city is divided into 3555 census tracts, which are the smallest geographical unit at which the data from the national census is reported. Census tracts in the city have an average surface area of 0.05 square kilometers (0.02 square miles), and an average population of 813 people. Voting districts are much larger, and divide the

¹⁶A sixth line, the *25 de Mayo* line operates only during rush hour, was built on a highway, and runs mid-distance and long-distance buses that connect the suburban metropolitan region to the city center. Since this line does not have any intermediary stops within the city proper, I will not include it in my main analysis.

¹⁷This would translate to a reduction of 44 minutes a day, or 7 days per year for the average commuter of this line, according to government estimates.

city into 167 regions, with an average surface area of 1.21 square kilometers (0.47 square miles), and an average population of 14952.

As my main source of data on residential location at the individual level, I use the electoral registries for the years 2011, 2013, 2015, and 2017. Voting is compulsory for all Argentine citizens between the ages of 18 and 70, and the polling place for each citizen is decided based on their residence, so the government keeps an up-to-date record of every person's address, which is updated for every election. I have obtained the electoral register for the city of Buenos Aires for the years 2011, 2013, 2015, and 2017. These registers include the National ID number, name, sex at birth, birth year, residential address as free text, and a description of occupation or profession for every person that is eligible to vote. I have cleaned and geocoded (assigned GPS coordinates) almost all addresses¹⁸ in the city of Buenos Aires (which account for approximately 2.5 million people).

One potential concern with these data arises from the fact that residence changes are self-reported, which might imply under-reporting of changes in residence or a lag in the change of residential addresses. Although I cannot rule out this possibility, and in fact it is highly likely that these data does not reflect the exact residential location of every citizen at each point in time, I show that the cross-sectional distribution of population in 2011 for the city of Buenos Aires that is implied in the electoral register data is highly correlated with the census data from the 2010 census. Figure 7 shows a binscatter plot that compares the number of voters from the electoral registry data that were geocoded in each census tract in 2011 with the population in each census tract in 2010, obtained from the 2010 national census. As we can see in this figure, there is a positive correlation between the 2010 census population and the number of voters geocoded from the electoral registry, with the 2010 census population being above the geocoded population for every bin average, which is consistent with the number of eligible voters being a fraction of the total population in each census tract.

I have obtained a restricted version of the the Annual Household Survey for the city of Buenos Aires (*Encuesta Anual de Hogares*) that details the employment location of each household member surveyed that is employed for every year between 2010 and 2019. With these data, I estimate the fraction of high-skilled and low-skilled workers that work in each commune of the city. I then employ the land use data census for the year 2011 to build a measure of employment by district within each commune, under the assumptions that employment is distributed in proportion to the fraction of land used for commercial and productive purposes within each district, and that the skill-share is constant across districts within a commune.¹⁹

I use ArcMap's Network Analysis tool to construct a model of the city's transportation network before and after the BRT lines were built. I then calculate the minimum commute time between census tracts using Dijkstra's algorithm to measure the changes in commute times after the BRT was put in place.²⁰

¹⁸One limitation with these data is that I require a full address (street name and number) in order to assign geographical coordinates to a citizens residential location. Therefore, I cannot locate citizens that live in disadvantaged low-income settlements that do not have a formal address. Because of this limitation, I can only geo-locate approximately 95% of the electoral register. See Appendix A for more information on this process.

¹⁹See Appendix A for details.

²⁰See Appendix A for more information on how the commute times are calculated.

I also use the 2010 mobility survey for the City of Buenos Aires (*Encuesta de Movilidad Domiciliaria*) to calculate average travel speeds by mode before the BRT was put in place, as well as to estimate the semi-elasticity of commuting with respect to travel times for high- and low-skilled residents in the model.

Regarding floorspace prices, I use the ask price for a subset of all listings from a major online marketplace from 2009 to 2017, as well as additional information such as the number of bedrooms, surface area, address, and GPS coordinates. With these data, I estimate the average housing price per square meter by district and by census tract.

As mentioned above, I employ the land use data from the 2011 land use map (*Relevamiento de Usos del Suelo*) produced by the government of the city of Buenos Aires. This data set contains land use information on every parcel of land in the city and, crucially, allows me to distinguish between land used for commercial and productive purposes from land used for residential purposes or other uses.

Finally, I use data from the 2010 national census,²¹ as well as from the National Household Survey (*Encuesta Permanente de Hogares*) to supplement the previously described sources of data.

3.1 Defining High- and Low-Skilled Residents

The electoral registry data includes a free text description of the occupation of each citizen. I processed this information and matched each description to a one-digit occupation group in the International Standard Classification of Occupations (ISCO).²² Table 11 shows the ten one-digit occupation groups of the ISCO.

I define a high-skilled worker as a worker who has at least some post-secondary education. From the National Household Survey for the city of Buenos Aires in 2010, we can calculate the fraction of workers within each one-digit ISCO occupation group that is high-skilled in the city of Buenos Aires according to this classification. We can see in Figure 8 that for five of the occupation groups,²³ the majority of workers in those occupations are low-skilled. For the remaining five occupation groups,²⁴ the majority of the workers in those occupations are high-skilled in the city of Buenos Aires. Therefore, I classify as a high-skilled worker every resident of the city categorized as being in an occupation group where the majority of the workers in that occupation are high-skilled, and I classify as a low-skilled worker every resident of the city in an occupation group where the majority of the workers in that occupation are low-skilled. Figure 9 compares the share of high-skilled residents by census tract calculated using the electoral register data from 2011 to the share of high-skilled residents by census tract obtained from the

²¹The following census was scheduled to occur in 2020, but has been postponed due to the emergency sanitary measures put in place as a consequence of the COVID-19 pandemic.

²²See the Appendix A for more information on this matching process.

²³These are: armed forces, elementary occupations, plant and machine operators, and assemblers, craft and related trades workers, and service and sales workers.

²⁴Which are: managers, professionals, technicians and associate professionals, clerical support workers, and skilled agricultural, forestry and fishery workers.

2010 census.²⁵ We can see in this graph that there is a positive and significant correlation between both measures.

4 Reduced Form Analysis

4.1 Commuter Market Access: Using the Model to Measure the Impact of the BRT System

In order to capture the full general equilibrium effects of the changes in the transport network due to the construction of the *Metrobus* BRT on every location of the city, I construct a measure of commuter market access developed by Ahlfeldt et al. (2015) and Tsivanidis (2019). This measure summarizes the total impact of the transit network on firms and residents, and can be derived from a wide class of models, as long as they imply a gravity equation for commuting flows (Tsivanidis, 2019). In Section 5, I derive this measure within the dynamic framework developed in this paper. I show that the commuter market access (CMA) for a resident of skill-type g living in a residential location (district or census tract) n at time t can be defined as

$$CMA_{gn,t} = \sum_j \left(\frac{w_{j,t}^g}{d_{nj,t}} \right)^{\theta_g}.$$

Where $d_{nj,t} = \exp(\kappa\tau_{ij,t})$ are the commute costs associated with commuting between i and j , with τ_{ij} being the minimum commute time between i and j calculated using Dijkstra's algorithm, and κ being the semi-elasticity of commute costs to commute times; $w_{gj,t}$ is the model-consistent wage for a worker of type g that works in workplace location j at time t , and can be calculated with information on the spatial distribution of employment population and residential population by skill type at a given year (given parameter estimates); and θ_g is the semi-elasticity of commute shares with respect to commute costs ($d_{nj,t}$).

Given parameter estimates²⁶ for θ_g and κ , we can calculate these measures of market access for 2011 by using data on employment population at the district level and residential population at the census tract level, as well as commute times calculated through a commuting model before the BRT was put in place. This will result in a vector of market access $\{CMA_{gn,2011}\}_{g \in \{h,l\}, n \in I}$ for every residential location n and both skill types g in 2011. Following Tsivanidis (2019), I then calculate $\{CMA_{gn,2017}\}_{g \in \{h,l\}, n \in I}$ by fixing the employment and residential population at 2011 levels and by changing the commute costs to reflect the new commute times with the full BRT put in place. I fix the employment and residential population at 2011 levels in order to abstract from endogenous changes in population that might bias the estimation.²⁷ I then calculate the change in the logged market access, $\Delta_{2011-2017} CMA_{gn,t}$, as the measure

²⁵Where high-skilled is defined as having at least some post-secondary education.

²⁶See Section 6 for details on how these parameters are estimated.

²⁷In Appendix B I show that this assumption does not affect the main results from the reduced form analysis.

that will allow me to capture the full general equilibrium effects of changes in the transport network on the outcomes analyzed in this section.

Figures 10 and 11 show the market access measure estimated for every census tract in the city in 2011. We can clearly see two things in these maps: first, market access is higher near the subway lines and closer to the CBD, where most subway lines converge; second, although the market access measure for high- and low-skilled workers are clearly not identically distributed across census tracts, there is a strong correlation between these measures. In fact, the estimated Pearson correlation coefficient between these two measures at the census tract level in 2011 is 0.99.

In Figures 12 and 13, we can see that the change in commuter market access for both high- and low-skilled workers decreases with distance to the new BRT lines, and increases with distance to the CBD. This is consistent with the fact that places closer to the BRT saw a larger proportional increase in their commute speeds, while places further from the CBD were able to benefit relatively more from these increases in speed, since they translated into larger decreases in commute times towards the major areas of employment. Moreover, the changes in market access for high- and low-skilled workers are highly correlated. In fact, the estimated correlation coefficient between changes in market access for high- and low-skilled workers is 0.98. Due to this high degree of correlation between both measures, I conduct the main reduced form analysis by regressing changes in the outcomes of interest on changes in the commuter market access measure for high-skilled workers. All the main results hold when changes in market access for low-skilled workers are used instead.²⁸

4.2 Identification Strategy: Instrumenting BRT Placement With Historical Tramway

The main identification concern when studying the effects of transport infrastructure is that the placement of this infrastructure is clearly not randomly allocated. In particular, one might worry that the BRT lines were placed such that they served neighborhoods that had specific unobserved characteristics, such as a secular population trend (either decreasing or increasing), that would bias the OLS results. In order to address these concerns, I use a historical route IV approach²⁹ based on Duranton and Turner (2012).

In the early twentieth century, Buenos Aires had a vast system of electric trams that connected the city center to the suburbs of the city. In the 1920s, privately operated buses started competing with the trams by running parallel to the tramways and often outpacing the trams in order to lure passengers that were waiting for the trams (Singh, 2018). Due in part to this competition and in part to the construction of five subway lines in the following decades, the trams saw a steady decrease in ridership between the late 1930s and the 1960s. In 1963, the tramway system was finally dismantled. The bus lines, however, continued operating on essentially the same routes that the old tramway system followed. When the Metrobus BRT lines were built, they were chosen so as to follow existing bus routes, with the added re-

²⁸See Appendix B for reduced form results using changes in the commuter market access measure for low-skilled workers.

²⁹This type of identification strategy has been used frequently in the transportation economics literature (Redding and Turner, 2015)

striction that they had to be built on large two-way avenues that allowed for the construction of boarding platforms and exclusive lanes for buses.

Given that many of the bus routes were historically determined by the placement of the tram system, I construct an instrument based on the tramway routes that were built before 1938 and that ran through large two-way avenues. Figure 14 shows the placement of these tramway routes and the *Metrobus* BRT system, we can see that there is a clear spatial correlation between the two. The instrument is constructed by calculating commute times assuming that the BRT was built following the tramway routes, using those times to calculate a measure of market access for each residential location, and then calculating the change in market access between 2011 and this hypothetical scenario. This hypothetical change in market access is used to instrument for the change in market access calculated using the actual placement of the BRT. The identifying assumption is that the placement of the tramway routes decided prior to 1938 is not correlated with contemporary changes in unobservable variables that might correlate with the placement of the BRT and affect the outcomes of interest directly.

In Table 3, we can see the results from the first stage regressions of the 2SLS IV estimation for every specification that is used in the following section. We can see that the historical IV instrument has indeed a very strong first stage, with Cragg-Donald Wald F statistics that range from 1470 to 277. With these values of the F-statistics we can confidently reject the null hypothesis of weak instruments in the test proposed by Stock and Yogo (2005).³⁰ We can also gather from these regressions that the coefficient for the regression of observed changes in market access on instrumented changes in market access is positive and significant, as expected given the spatial correlation between the tram lines and the BRT lines.

4.3 Main Specification and Results

In this section, I analyze the effects of improving the transport infrastructure through the construction of the BRT system in Buenos Aires on the share of high-skilled residents³¹ in each census tract, the average floorspace price in each census tract, the population density, and the population density by skill type in each census tract. In order to do so, I estimate the following equation through OLS and by instrumenting the change in market access (defined in Subsection 4.1) with a historical IV (defined in Subsection 4.2):

$$\Delta Y = \alpha + \beta_1 \Delta CMA + \beta_2 HS\ share_0 + \beta_3 \Delta CMA \times HS\ share_0 + \Lambda + \epsilon. \quad (1)$$

Where ΔY is the change in the outcome of interest; ΔCMA is the change in the commuter market access as defined in Subsection 4.1 between 2011 and 2017 due to the construction of the BRT; $HS\ share_0$ is intended to capture the initial differences in the high-skilled share between census tracts, and is calculated

³⁰The null hypothesis of weak instruments can also be rejected for the F-test proposed by Sanderson and Windmeijer (2016).

³¹The share of high-skilled residents in a census tract i at time t is defined as $\frac{L_{i,t}^h}{L_{i,t}^h + L_{i,t}^l}$ where $L_{i,t}^g$ is the total population of skill type g residing in i at time t .

as the average high-skilled share for all census tracts that are contiguous to a given census tract³²; Λ is a set of potential controls, such as fixed effects at the neighborhood level; and ϵ is the error term in each regression.

Table 4 shows the results of estimating equation 1 both by OLS and IV for the change in the high-skilled share by census tract between 2011 and 2017. We can first see from these results that while the IV estimation in column 2 results in a positive and significant coefficient for the change in market access, the OLS estimation produces a non-significant coefficient (with negative sign). This result suggests that the placement of the BRT might have favored areas where the high-skilled share had a decreasing secular trend, resulting in a negative bias of the coefficient. From the IV estimation, we find that a 1% change in market access leads to a 0.2% change in the high-skilled share. In columns 3 and 4, we can see that once we include an interaction term between the initial high-skilled share and the change in market access, the IV and the OLS estimates become very similar to one another. Both of these estimates show that, although the high-skilled share increased on average as a consequence of the increase in market access, this effect was not equal across neighborhoods. In census tracts with a higher initial high-skilled share, the high-skilled share increased more as a consequence of the increase in market access. In fact, using the results from column 4 we see that the derivative of $\Delta \log(CMA)$ with respect to $\Delta \log(\text{HS share})$ is equal to 0.1 for a census tract at the twentieth percentile of the initial high-skilled share distribution,³³ and equal to 0.6 for a census tract at the eightieth percentile of the distribution of initial high-skilled share. Finally, these results are robust to controlling for neighborhood³⁴ fixed effects (although the significance level decreases due to loss of power in the estimation), which suggests that these results are not driven by differential effects across neighborhoods. Taken as a whole, these results imply that the BRT increased segregation by skill type within the city, by increasing the high-skilled share at a higher rate in census tracts that had an initially higher level of high-skilled share.

As an alternative way to study the different effects that changes in market access had on the share of high-skilled residents for census tracts in different parts of the distribution of initial high-skilled share, I divide the sample of census tracts into five groups according to the quintiles of the distribution of initial high-skilled share, and estimate the following regression for each group:

$$\Delta \text{HS share} = \alpha + \beta_1 \Delta CMA + \epsilon. \quad (2)$$

Figure 15 shows the results for the β_1 coefficient of estimating equation 2 using the historical IV strategy for each quintile of the initial high-skilled share distribution. In this graph, we can see that for census tracts in the lowest quintile of the distribution of the initial high-skilled share, the relationship between changes in market access and change in the high-skilled share is actually negative. Implying that an increase in market access in census tracts in the lowest quintile reduced the high-skilled share. For all

³²I use this measure in order to avoid mechanical correlations between the initial high-skilled share and the change in high-skilled share. All coefficients are not statistically different at 5% level when using the actual high-skilled share instead of this measure in the regressions.

³³Recall that this is not the actual initial high-skilled share distribution, but the average distribution for all the census tracts contiguous to a given census tract in 2011.

³⁴Every census tract is included in a neighborhood, and the city is divided into 48 neighborhoods.

the subsequent quintiles, the point estimates are positive and increasing in the initial high-skilled share (although they are not statistically distinguishable at a 10% level), with the exception of the coefficient for the top quintile.

In Table 5, we can see that the same patterns observed in the effect of market access on the high-skilled share can be observed in the effect of market access on floorspace prices. On average, a 1% increase in market access increased the average price per square meter of residential housing in a census tract by 0.3% (column 2). However, this effect varied by the initial share of high-skilled resident in the census tract (columns 3, 4, and 5). A 1% increase in market access in a census tract at the twentieth percentile of the initial high-skilled distribution increased residential floorspace prices on average by 0.3%, while a 1% increase in market access in a census tract at the eightieth percentile of the initial high-skilled distribution increased residential floorspace prices 1%.

Table 6 shows the results of estimating equation 1 by IV for the changes in total population, population of high-skilled residents, and population of low-skilled residents by census tract. We can see that total population, as well as population by both skill types increased more in census tracts with a higher initial high-skill share. A 1% increase in market access led to an increase of the high-skilled population of 0.6% on average in a census tract at the twentieth percentile of the initial high-skilled share distribution, while the same same 1% increase in market access led to an increase of the low-skilled population of 0.7% on average in a census tract at the same twentieth percentile. Conversely, a 1% increase in the market access in a census tract at the eightieth percentile of the initial high-skilled share distribution led to an increase of the high- and low-skilled population of 1.1% and 1.0% respectively.

5 Model

Most quantitative spatial equilibrium models of a city rely on comparative statics for welfare analysis (e.g. Tsivianidis, 2019, Ahlfeldt et al., 2015). This analysis can tell us the average welfare gains for residents living at a specific location after the changes of interest have occurred, and a new static equilibrium has been reached. We know, however, that residents are mobile within a city, and can change their residential location as a response to changes in the city's fundamentals (such as transport infrastructure improvements). Therefore, in order to analyze the welfare gains for residents living in each location before the improvements in transport infrastructure were put in place, I develop a model that can incorporate migration decision by forward-looking agents explicitly. This model draws from the dynamic structure of Caliendo et al. (2019) and Balboni et al. (2020), and from Ahlfeldt et al. (2015) and Tsivianidis (2019) in terms of the commuting structure, that allows workers to work and live in different locations within the city.

5.1 Setup

A city is composed of I residence locations (indexed by i or n), and J workplace locations, (indexed by j or s). I assume that there is a fixed mass L of atomistic residents in the city³⁵ that are infinitely lived, and who must decide how much to consume, where to work, and where to live each period. These residents can either be high-skilled or low-skilled (indexed by $g \in \{h, l\}$). Each period, residents start in a residence location, which will depend on their choices from the previous period. They then observe a vector of idiosyncratic match productivities for each workplace location. They take wages in each location as given, as well as commute costs from their residence location. With this information, they choose a workplace location for that period. Once they know their workplace location, and have obtained a wage income discounted by the commute cost of commuting from their residence location to their workplace location, they choose how much to consume of the freely traded consumption bundle and of the floorspace (housing services) available in their residence location. Having consumed the consumption bundle and the housing services, they observe a vector of idiosyncratic preference shocks for each residence location for the next period. With this information, they choose a residence location for the next period. If they decide to leave their current location, they pay an origin-destination specific moving cost.

Production in each workplace location is characterized by a static problem. Each location produces a variety of the final consumption good³⁶ under perfect competition, employing both types of labor (high- and low-skilled).

I assume a fixed supply of floorspace in each residence location, which, along with aggregate floorspace demand by each skill-type in each location, determines the floorspace price in that location for that period. I also assume that all floorspace is owned by an absentee landlord to whom all rents are payed.

5.2 Resident's Problem

5.2.1 Consumption Problem

Given a residential location i and a workplace location j , a resident of skill type $g \in \{h, l\}$ will have an intra-period utility function at time t defined as

$$U_{ij,t}^g = \left(\frac{c_{ij,t}^g}{\alpha} \right)^\alpha \left(\frac{H_{R,ij,t}^g}{1-\alpha} \right)^{1-\alpha}.$$

³⁵This is a closed city model. This assumption has been made mostly due to data limitations, since I have limited information on migration patterns for individuals between the city and the rest of the country (or the world), as well as for modeling convenience.

³⁶Consumers will consume a CES bundle of these varieties.

Where $c_{ij,t}^g$ is the level of consumption of the freely traded numeraire consumption good for a resident of skill type g , and $H_{R,ij,t}^g$ is the level of housing services or residential floorspace consumed by a resident of skill type g .

I assume that a resident of i that works in workplace location j earns a wage income $\frac{w_{j,t}^g \varepsilon_{j,t}}{d_{ij,t}}$, where $w_{j,t}^g$ is the competitive wage payed at workplace location j for a worker of skill type g , $\varepsilon_{j,t}^g$ is the idiosyncratic match-productivity shock for location j , and $d_{ij,t}$ is the commuting cost³⁷ between residential location i and workplace location j . The consumer's intra-period problem can be expressed as

$$\max_{\{c_{ij,t}^g, H_{R,ij,t}^g\}} C_{ij,t}^g = \left(\frac{c_{ij,t}^g}{\alpha} \right)^\alpha \left(\frac{H_{R,ij,t}^g}{1-\alpha} \right)^{1-\alpha} \text{ subject to } c_{ij,t}^g + r_{Ri,t} H_{R,ij,t}^g = \frac{w_{j,t}^g \varepsilon_{j,t}^g}{d_{ij,t}}.$$

Where $r_{Ri,t}$ is the price of a square meter of residential floorspace in location i . I assume that the housing rents are payed to an absentee landlord who does not consume goods or services in the city.

The solution of the consumer's intra-period problem implies

$$c_{ij,t}^{g*} = \alpha \frac{w_{j,t}^g \varepsilon_{j,t}^g}{d_{ij,t}}, \quad (3)$$

$$H_{R,ij,t}^{g*} = \frac{(1-\alpha)}{r_{Ri,t}} \frac{w_{j,t}^g \varepsilon_{j,t}^g}{d_{ij,t}}. \quad (4)$$

Which implies an indirect utility function

$$C_{ij,t}^{g*} = \frac{w_{j,t}^g \varepsilon_{j,t}^g r_{Ri,t}^{\alpha-1}}{d_{ij,t}}.$$

5.2.2 Dynamic Problem

The agent's full dynamic problem at time t can be expressed as the following Bellman equation:

$$v_{n,t}^g = \max_{\{i,j\}} \{ C_{nj,t}^{g*} + \beta E_t[v_{i,t+1}^g] - \mu_{ni}^g + \eta_{i,t}^g \} \quad (5)$$

Where i is the residential location that the agent chooses for $t+1$, and j is the workplace location that the agent chooses for period t , μ_{ni}^g is the moving cost required to move from residential location n to location i , which is assumed to be constant over time, and $\eta_{i,t}^g$ is the idiosyncratic preference shock on residential location choices for period $t+1$, which is observed in period t .

³⁷Following Ahlfeldt et al. (2015), I define $d_{ij,t} = \exp(\kappa \tau_{ij,t})$, where $\tau_{ij,t}$ is the average commute time in minutes between i and j at time t , and κ is the semi-elasticity of commute costs with respect to commute times. I make the simplifying assumption that there is only one mode of transport, which includes walking, and public transportation. As discussed in Section 2, the vast majority of trips within the city for both high- and low-skilled workers were done either walking or by taking public transport.

Note that the maximization problem is separable between choosing the optimal workplace at time t , and choosing the optimal residence location for next period i . Therefore, we can write

$$v_{n,t}^g = \max_{\{j\}} \left\{ \frac{w_{jt}^g \varepsilon_{jt}^g r_{Rn,t}^{\alpha-1}}{d_{nj}} \right\} + \max_{\{i\}} \left\{ \beta E_t[v_{i,t+1}^g] - \mu_{ni}^g + \eta_{i,t}^g \right\}.$$

Taking expectations with respect to the joint distribution of both idiosyncratic shocks (ε_j and η_i), we get

$$E_0 v_{n,t}^g = E_0 \left[\max_{\{j\}} \left\{ \frac{w_{jt}^g \varepsilon_{jt}^g r_{Rn,t}^{\alpha-1}}{d_{nj,t}} \right\} \right] + E_0 \left[\max_{\{i\}} \left\{ \beta E_t[v_{i,t+1}^g] - \mu_{ni}^g + \eta_{i,t}^g \right\} \right].$$

Let $V_{n,t}^g = E_0 v_{n,t}^g$, then it follows from the Markovian structure of this dynamic problem that $E_t[v_{n,t+1}^g] = V_{n,t+1}^g$, therefore,

$$V_{n,t}^g = E_0 \left[\max_{\{j\}} \left\{ \frac{w_{jt}^g \varepsilon_{jt}^g r_{Rn,t}^{\alpha-1}}{d_{nj,t}} \right\} \right] + E_0 \left[\max_{\{i\}} \left\{ \beta V_{i,t+1}^g - \mu_{ni}^g + \eta_{i,t}^g \right\} \right]. \quad (6)$$

We can solve both expectations by using the fact that $\varepsilon_{j,t}^g$ is distributed extreme value type I, and $\eta_{i,t}^g$ is distributed extreme value type II (see Appendix C). By solving these expectations we obtain

$$V_{n,t}^g = \tilde{T}_g \Phi_{Rgn,t}^{\frac{1}{\theta_g}} r_{Rn,t}^{\alpha-1} + \nu_g \ln \sum_{i=1}^I \exp(\beta V_{i,t+1}^g - \mu_{i,n}^g)^{\frac{1}{\nu_g}}. \quad (7)$$

Where $\Phi_{Rgi,t} = \sum_j \left(\frac{w_{jt}^g}{d_{ij,t}} \right)^{\theta_g}$, θ_g and \tilde{T}_g are the shape and scale parameters of the CDF of ε_j^g , and ν_g is the scale parameter of the CDF of η_i^g .

5.3 Neighborhood Migration Flows

Let $m_{in,t}$ be the fraction of agents that are residing in location n at the beginning of period t , and move to location i by the end of period t . From the distribution of idiosyncratic preferences $\eta_{n,t}$ we can obtain the following equation.³⁸

$$m_{in,t}^g = \frac{\left[\exp(\beta V_{i,t+1}^g - \mu_{in}^g) \right]^{\frac{1}{\nu_g}}}{\sum_{m=1}^N \left[\exp(\beta V_{m,t+1}^g - \mu_{mn}^g) \right]^{\frac{1}{\nu_g}}} \quad (8)$$

³⁸See Appendix C for derivation.

5.4 Labor Supply

As in Tsivianidis (2019), the probability of a worker that lives in i at time t decides to work in location j is:

$$\Pi_{j|tig} = \frac{(w_{j,t}^g/d_{ij,t})^\theta}{\sum_s \left(\frac{w_{s,t}^g}{d_{is,t}}\right)^\theta} = \frac{(w_{j,t}^g/d_{ij,t})^\theta}{\Phi_{Rgi,t}}. \quad (9)$$

Therefore, labor supply at time t for workplace location j will be

$$L_{Fj,t}^g = \sum_{i=1}^I \Pi_{j|tig} L_{Ri,t}^g, \quad (10)$$

where $L_{Ri,t}^g$ is the residential population at time t in location i of workers of type g .

5.5 Residential Population

Let $m_{in,t}^g$ be the fraction of agents of type g that are residing in location n at the beginning of period t , and move to location i by the end of period t . It must be then that

$$L_{Ri,t}^g = \sum_{n=1}^I m_{in,t}^g L_{Rn,t-1}^g \quad (11)$$

5.6 Production

I will assume there are J varieties of the consumption good, differentiated by location of production, and supplied in a competitive market. Consumers have CES preferences over each variety, with elasticity of substitution $\sigma > 1$. Producers solve a static problem each period t , where they choose their demand for low-skill and high-skill effective units of labor, in order to maximize their profits in that period. I assume firms produce using an Cobb-Douglas production function such that the output of the variety of the final good produced in location j at time t will be:

$$q_j = A_j (\tilde{L}_{jt}^l)^{\rho_j} (\tilde{L}_{jt}^h)^{(1-\rho_j)}$$

Where A_j is the exogenous TFP from producing in j , $\tilde{L}_{Fj,t}^h$ is the demand at time t in location j for effective units of high-skill labor, and $\tilde{L}_{Fj,t}^l$ is the demand at time t in location j for effective units of low-skill labor. I allow ρ_j to vary by workplace location in order to capture the fact that firms in different parts of the city may have different skill intensities.³⁹ Taking first order conditions of the producers problem, one finds that

$$w_{j,t}^h \tilde{L}_{Fj,t}^h = (1 - \rho_j) X_{jt}, \quad (12)$$

³⁹The vector of ρ_j for all j will be calibrated using the skill share of employment observed in 2010 for each workplace location.

$$w_{j,t}^l \tilde{L}_{Fj,t}^l = \rho_j X_{jt}. \quad (13)$$

Where X_{jt} is the total expenditure on variety j at time t . From the CES demand for varieties of the consumption good, we know that in equilibrium $X_{jt} = p_{jt}^{1-\sigma} X$, where $X = \sum_{i=1}^I \alpha \sum_{g \in \{h,l\}} \bar{y}_{igt}$ is the total expenditure on consumption in the economy, and \bar{y}_{igt} is the mean income of a worker of type g in location i at time t . Perfect competition will imply that the price of each variety is equal to its marginal cost at each time t , $p_{jt} = A_j^{-1} (w_{jt}^l)^{\rho_j} (w_{jt}^h)^{(1-\rho_j)}$. Combining these results we can express⁴⁰ labor demand at each location j at time t for each skill type g as a function of the wage vector $\mathbf{w}_t = \{\{w_{jt}^h\}_{j=1}^J, \{w_{jt}^l\}_{j=1}^J\}$,

$$\tilde{L}_{Fj,t}^g = f_{jgt}(\mathbf{w}_t) \quad (14)$$

Finally, we must relate the effective units of labor of each skill type to the physical units of labor of that skill type ($L_{Fj,t}^g$). Let $\bar{\varepsilon}_{jt}^g$ be the average worker-match productivity for a worker of skill type g , at time t in workplace location j . This average productivity can be computed as⁴¹

$$\bar{\varepsilon}_{jt}^g = T_g \sum_i^I \pi_{j|tig}^{-\frac{1}{\theta_g}} \frac{1}{d_{ijt}} \frac{\pi_{j|tig} L_{Rit}^g}{\sum_n^I \pi_{j|tn} L_{Rnt}^g}. \quad (15)$$

It follows then from the definition of the worker-match productivities that

$$L_{Fj,t}^g = \frac{\tilde{L}_{Fj,t}^g}{\bar{\varepsilon}_{jt}^g} \quad \forall g \in \{h, l\}.$$

5.7 Labor Market Clearing

From equation (10) we obtain the labor supply in workplace j at time t of skill type g , given a residential population distribution $\{L_{Ri,t}^g\}_{i=1}^I$ of skill type g . At the same time, from equation (14) we know that labor demand can be expressed as a function of the wage vector \bar{w}_t . Therefore, labor market clearing implies

$$L_{Fj,t}^g = \frac{f_{jgt}(\mathbf{w}_t)}{\bar{\varepsilon}_{jt}^g} = \sum_{i=1}^I \frac{(w_{j,t}^g/d_{ij,t})^\theta}{\sum_j \left(\frac{w_{j,t}^g}{d_{ij,t}} \right)^\theta} L_{Ri,t}^g. \quad (16)$$

5.8 Floorspace Market Clearing

Each residential location has a fixed amount of floorspace \bar{H}_{Ri} . Let $\bar{y}_{i,t}^g$ be the expected income of a resident of i of skill type g at time t , where the expectation is taken with respect to the distribution of

⁴⁰See Appendix C for the derivation.

⁴¹See Appendix C for derivation.

match productivities. From equation (4) we know that the aggregate demand for housing in location i is

$$H_{Ri}^S = \sum_{g \in \{h, l\}} \frac{L_{Ri,t}^g \bar{y}_{i,t}^g}{r_{Ri,t}} (1 - \alpha).$$

Solving for $\bar{y}_{i,t}^g$ we find that⁴²

$$H_{Ri}^S = \sum_{g \in \{h, l\}} \frac{L_{Ri,t}^g \tilde{T}_g \Phi_{Rgi,t}^{\frac{1}{\theta_g}}}{r_{Ri,t}} (1 - \alpha).$$

Market clearing for residential floorspace requires that the supply for residential floorspace in location i (\bar{H}_{Ri}) be equal to the demand for residential floorspace in location i , for all residential location, at every time t , which implies that

$$r_{Ri,t} = \frac{\sum_{g \in \{h, l\}} L_{Ri,t}^g \tilde{T}_g \Phi_{Rgi,t}^{\frac{1}{\theta_g}} (1 - \alpha)}{\bar{H}_{Ri}}. \quad (17)$$

5.9 Equilibrium Definitions

In this model, the endogenous state of the economy at time t is determined by the vector of residential labor allocation $\{L_{Ri,t}^g\}$, and the vector of workplace labor allocation $\{L_{Fj,t}^g\}$. The time varying fundamentals of this economy are the pairwise transport time⁴³ from each residential location to each workplace location, t_{ij} . The constant fundamentals are the pairwise moving costs μ_{in}^g , and the workplace productivities A_j . The parameters in this model are assumed constant and are: the semi-elasticity of commute costs with respect to commute times (κ), the residential location migration elasticities for each worker type (ν_g), the parameters that govern the distribution of idiosyncratic workplace match-productivities for each worker type (T_g and θ_g), the time discount factor (β), the parameters that determine the shape of the production function at each workplace location j , $\{\rho_{jg}\}$, the parameter that determines the shape of the utility function (α), and the elasticity of substitution of the CES consumption bundle (σ). Following Caliendo et al. (2019) I will now define three equilibrium concepts in this model (for a given value of the model parameters), a *temporary equilibrium*, a *sequential equilibrium*, and a *stationary equilibrium*.

Definition 1. Given a vector of residential location population $\{L_{Ri,t}^g\}$ at time t , a pairwise transport time matrix $\{d_{ij}\}$, and a vector of workplace productivities $\{A_j\}$, a **temporary equilibrium** is defined as a vector of wages for each worker type $g \in \{h, l\}$, $\{w_{j,t}^g\}$, and residential floorspace rents $\{r_{Ri,t}\}$ that satisfy the equilibrium conditions of the static sub-problem, which is determined by the labor market clearing condition expressed in equation (16) for each worker type $g \in \{h, l\}$, and the residential floorspace market clearing condition expressed in equation (17).

Note that in this simple framework, at any time t , once the residential location vector is determined, the static problem can be subsumed into finding the vector of wages that equalizes labor demand and labor supply in each workplace location for each worker type, and the vector of rents that equalizes

⁴²See Appendix C of this derivation.

⁴³The pairwise transport cost d_{ij} is calculated as $\exp(\kappa t_{ij})$, where $\kappa > 0$ is the semi-elasticity of commute costs with respect to commute times.

floorspace demand and floorspace supply in each residential location. Once all the wages and rents are determined for period t , individual consumption of the numeraire consumption good and of residential floorspace follows from the solution to the worker's consumption problem, and the market for the final consumption good must clear by Walras's Law. Having defined the temporary equilibrium, I now proceed to define the sequential competitive equilibrium for this model given a path of exogenous fundamentals, and given parameter values. Let $m_t^g = \{m_{in,t}^g\}_{i=1,n=1}^{I,I}$, $L_{Rt}^g = \{L_{Ri,t}^g\}_{i=1}^I$, $L_{Ft}^g = \{L_{Fj,t}^g\}_{j=1}^J$, $w_t^g = \{w_{j,t}^g\}_{j=1}^J$, and $V_t^g = \{V_{i,t}^g\}_{i=1}^I$ be the residential location migration shares, residential population, workplace population, wages, and lifetime expected utilities for each worker type $g \in \{h, l\}$ respectively. Following Caliendo et al. (2019) I define the sequential competitive equilibrium in this model as follows.

Definition 2. Given an initial distribution of residential population for each worker type L_{R0}^g , an initial distribution of employment for each worker type L_{F0}^g , and a known sequence of time-varying and non time-varying fundamentals ($\{d_{ij,t}\}_{i=1,j=1,t=1}^{I,J,\infty}$, $\{A_j\}_{j=1}^J$, and $\{\mu_{in}^g\}_{i=1,n=1}^{I,I}$), a sequential competitive equilibrium is a sequence of $\{L_{Rt}^g, L_{Ft}^g, m_t^g, w_t^g, V_t^g\}_{t=0,g \in \{h,l\}}^\infty$ that solves equations (7), (8), (11), and the temporary equilibrium at each time t .

We can now define a stationary equilibrium for this model as follows:

Definition 3. A stationary equilibrium of this model is a sequential competitive equilibrium such that all the elements of the vector $\{L_{Rt}^g, L_{Ft}^g, m_t^g, w_t^g, V_t^g\}_{t=0}^\infty$ are constant for all t and for all worker skill type g .

Note that, as always, in a stationary equilibrium all the fundamentals must be constant for all t , since a change in fundamentals would lead to changes in the endogenous variables of the model through time. Also, note that in a stationary equilibrium individual residents may still move from one residential location to another, or from one workplace location to another, in so far as the aggregate populations in each location, and the migration flows between locations for each worker skill type stay constant.

5.10 Model Solution

In this section I will describe how to solve for the full transitional dynamics of this model. The solution relies heavily on Caliendo et al. (2019), with some modifications to allow for the fact that in this model workers do not necessarily work in the same location as where they reside, as well as for the fact that in this model there are two types of workers (high-skilled workers and low-skilled workers). This numerical solution method relies on the fact that we can express the equilibrium conditions in first differences, and by employing this "dynamic hat algebra" we do not have to take a stance on the level of the fundamentals of this economy. Additionally, this approach does not require us to assume that the economy is in a steady state equilibrium at our initial period $t = 0$.

5.11 Equations in First Difference

In this section I will express the equations that govern the transition dynamics of this model (equations (7), (8), (11), and (17)) in first differences. For any time dependent variable y_t , denote $\dot{y}_{t+1} \equiv \frac{y_{t+1}}{y_t}$. I will also denote $u_{n,t}^g \equiv \exp(V_{n,t}^g)$ to simplify the notation. We can now express the transition dynamics in first difference as follows⁴⁴:

$$\dot{u}_{n,t+1}^g = \left[\frac{\exp\left(\tilde{T}_g \Phi_{Rgn,t+1}^{\frac{1}{\theta_g}} r_{Rn,t+1}^{\alpha-1}\right)}{\exp\left(\tilde{T}_g \Phi_{Rgn,t}^{\frac{1}{\theta_g}} r_{Rgn,t}^{\alpha-1}\right)} \right] \left[\sum_{k=1}^I m_{kn,t}^g \left(\dot{u}_{k,t+2}^g \right)^{\frac{\beta}{\nu_g}} \right]^{\nu_g}, \quad (18)$$

$$\dot{m}_{in,t+1}^g = \frac{\left(\dot{u}_{i,t+2}^g \right)^{\frac{\beta}{\nu_g}}}{\sum_{k=1}^I m_{kn,t}^g \left(\dot{u}_{k,t+2}^g \right)^{\frac{\beta}{\nu_g}}}, \quad (19)$$

$$\dot{r}_{Ri,t+1} = \frac{\sum_{g \in \{h,l\}} L_{Ri,t+1}^g \tilde{T}_g \Phi_{Rgi,t+1}^{\frac{1}{\theta_g}}}{\sum_{g \in \{h,l\}} L_{Ri,t}^g \tilde{T}_g \Phi_{Rgi,t}^{\frac{1}{\theta_g}}}. \quad (20)$$

5.12 Solution Algorithm

I will now summarize the solution algorithm used to calculate the solution to this dynamic discrete choice model.

1. Initiate the algorithm at $t = 0$ with a guess for a path of $\{\{\dot{u}_{t+1}^{g0}\}_{n=1}^I\}_{t=0}^\infty\}_{g \in \{h,l\}}$, such that $\dot{u}_{n,T+1}^g = 1$ for all T large enough, and for all n . Take as given $\{L_{R0}^g, L_{F0}^g, m_{-1}^g, \{d_{ij,t}\}_{i=1,j=1,t=1}^{I,J,\infty}, \{A_j\}_{j=1}^J, \{\bar{H}_{Ri}\}_{i=1}^I, \{r_{Ri,0}\}_{i=1}^I\}$.
2. For all $t \geq 0$, use $\{\dot{u}_{t+1}^{g0}\}_{n=1}^I\}_{t=0}^\infty$ to solve for $\{m_t^g\}_{t=1}^\infty$ using equation (19).
3. Use L_{R0}^g , $\{m_t\}_{t=1}^\infty$, and equation (11) to solve for $\{L_{Rt}^g\}_{t=0}^\infty$.
4. Use $\{L_{Rt}^g\}$ and L_{F0}^g to estimate model consistent wages for period zero ($t = 0$), $\{w_{j,0}^g\}_{j=1}^J$ using the labor market clearing condition for each skill type⁴⁵, (16).
5. Use $\{L_{Rt}^g\}$, $\{w_{j,0}^g\}_{j=1}^J$, L_{F0}^g , and vector equation implied by (16) to solve forward⁴⁶ for the model consistent $\{L_{Ft}^g\}_{t=1}^\infty$ and $\{\{w_{j,t}^g\}_{j=1}^J\}_{t=0}^\infty$.
6. Use $\{L_{Rt}^g\}$, $\{\Phi_{Rgt}\}$, and equation (20) to solve for $\{\dot{r}_{Rn,t+1}\}$. Then use $\{r_{Ri,0}\}_{i=1}^I$ and $\{\dot{r}_{Rn,t+1}\}$ to solve for $\{r_{Rn,t}\}$.

⁴⁴See Appendix C for the derivation of these equations.

⁴⁵See Appendix C for an explanation on how to obtain the model-consistent wages as a function of residential and workplace population for each skill type.

⁴⁶See Appendix C for a detailed explanation of this algorithm, as well as a proof of convergence and uniqueness.

7. For each t , use $\{\{w_{j,t+1}^g\}, \{m_t^g\}, \{d_{ij,t}\}, \{\dot{r}_{Rn,t+1}\}$, and $\{\dot{u}_{i,t+2}^g\}$ to calculate backwards $\{\dot{u}_{n,t+1}^g\}$ using equation (18) for each skill type g . This will result in a new sequence $\{\dot{u}_{n,t+1}^{g1}\}_{t=0}^\infty$.
8. Verify if $\{\dot{u}_{n,t+1}^{g1}\}_{t=0}^\infty \approx \{\dot{u}_{n,t+1}^{g0}\}_{t=0}^\infty$, if not, then start again from step 1, with $\{\dot{u}_{n,t+1}^{g1}\}_{t=0}^\infty$ as your new guess. If indeed $\{\dot{u}_{n,t+1}^{g1}\}_{t=0}^\infty \approx \{\dot{u}_{n,t+1}^{g0}\}_{t=0}^\infty$, then $\{\dot{u}_{n,t+1}^{g1}\}_{t=0}^\infty$ is the solution.

5.13 Welfare Gains

The expected utility at time t in location n for a worker of skill type g can be written as⁴⁷

$$V_{n,t}^g = \sum_{s=t}^{\infty} \beta^{s-t} \left[\tilde{T}_g \Phi_{Rgn,s}^{\frac{1}{\theta_g}} r_{Rn,s}^{\alpha-1} - \nu_g \ln(m_{nn,s}^g) \right]. \quad (21)$$

If we define $\hat{V}_{n,t}^g$ as the expected utility under a counterfactual evolution of the model's fundamentals, then we can define the compensating variation in consumption ($\delta_{n,t}^g$) as the constant increase in consumption that must be made each period under the counterfactual so as to make an agent of skill type g living in location n at time t indifferent between the counterfactual world and the realized equilibrium. In other words, $\delta_{n,t}^g$ is such that

$$V_{n,t}^g = \sum_{s=t}^{\infty} \beta^{s-t} \left[\delta_{n,t}^g + \tilde{T}_g \hat{\Phi}_{Rgn,s}^{\frac{1}{\theta_g}} r_{Rn,s}^{\alpha-1} - \nu_g \ln(\hat{m}_{nn,s}^g) \right].$$

Solving for $\delta_{n,t}^g$, this implies that

$$\delta_{n,t}^g = (1 - \beta) \sum_{s=t}^{\infty} \beta^{s-t} \left[\tilde{T}_g \left(\Phi_{Rgn,s}^{\frac{1}{\theta_g}} r_{Rn,s}^{\alpha-1} - \hat{\Phi}_{Rgn,s}^{\frac{1}{\theta_g}} \hat{r}_{Rn,s}^{\alpha-1} \right) - \nu_g \ln \left(\frac{m_{nn,s}^g}{\hat{m}_{nn,s}^g} \right) \right]. \quad (22)$$

By calculating a population-weighted average of the expected utility in each residential location at time t , we obtain a measure of average welfare at time t ,

$$W_t = \sum_{g \in \{h,l\}} \sum_{n=1}^I \frac{L_{n,0}^g}{\sum_{g \in \{h,l\}} \sum_{i=1}^I L_{i,0}^g} V_{n,t}^g. \quad (23)$$

Where we weight the expected utility in each residential location by the share of the population of that skill type living in that location at time $t = 0$. In the same way, we can calculate the average welfare in the counterfactual world as

$$\hat{W}_t = \sum_{g \in \{h,l\}} \sum_{n=1}^I \frac{L_{n,0}^g}{\sum_{g \in \{h,l\}} \sum_{i=1}^I L_{i,0}^g} \hat{V}_{n,t}^g. \quad (24)$$

⁴⁷See Appendix C for a derivation of this equation.

With these measures, we can calculate the proportional gains in average welfare at time t with respect to the counterfactual as simply

$$\Delta W_t = \frac{W_t}{\hat{W}_t} - 1.$$

We can repeat this same exercise by skill type to obtain the average expected utility in each residential location at time t for each skill level g as

$$W_t^g = \sum_{n=1}^I \frac{L_{n,0}^g}{\sum_{i=1}^I L_{i,0}^g} V_{n,t}^g, \quad (25)$$

and the average welfare by skill type in the counterfactual as

$$\hat{W}_t^g = \sum_{n=1}^I \frac{L_{n,0}^g}{\sum_{i=1}^I L_{i,0}^g} \hat{V}_{n,t}^g. \quad (26)$$

Comparing these two measures by skill type we can obtain the proportional gains in average welfare at time t for each skill type with respect to the counterfactual as

$$\Delta W_t^g = \frac{W_t^g}{\hat{W}_t^g} - 1. \quad (27)$$

6 Parameter Estimation

There are 10 key parameters that must be known in order to solve this model, $\{\beta, \alpha, \sigma, T_h, T_l, \kappa, \theta_h, \theta_l, \nu_h, \nu_l\}$. I assume the bi-annual discount factor, β , to be 0.92 (implying approximately a 4% real annual interest rate). I also assume the parameter that governs the intra-period utility function, α , to be equal to 0.7, which results in a expenditure share in housing of 0.3. I assume that the elasticity of substitution for the CES aggregator of the consumption bundle, σ is equal to 6. This number is chosen based on the choice by Tsivianidis (2019) for his Armington elasticity of substitution, who, in turn, chooses that number based on the median estimates from Feenstra et al. (2018). I fix T_l to be 1, and calibrate T_h such that the average wage premium in the city at $t = 0$ is equal to the observed wage premium calculated from the National Household Survey for 2010 (See Appendix C for details), which results in T_h being equal to 1.14. I take $\kappa = 0.01$ from Ahlfeldt et al. (2015).

In Subsection 6.1 I explain how I estimate the semi-elasticities of commute flows with respect to commute costs for each skill type (θ_h , and θ_l) by relying on the 2010 commuting survey for the city of Buenos Aires (ENMODO). Finally, in Subsection 6.2 I explain how I estimate ν_h and ν_l , which are the multiplicative inverse of the intra-city migration elasticities with respect to expected income for each skill type.

6.1 Estimating Commuting Semi-Elasticities

In order to calculate θ_h , and θ_l , I use data from the commuting survey for the city of Buenos Aires from 2010 (*ENMODO*). This commuting survey divided the city into 21 zones, and provides individual level data on commuting patterns for a sample of 22,500 households in the metropolitan region of Buenos Aires. Following Ahlfeldt et al. (2015), I take logs of equation 9, and add an error term that reflects the measurement error resulting from the different methods employed to measure commute times in the model and in the survey. This results in

$$\pi_{ij}^g = -\theta_g \times \kappa \tau_{ij}^g + \gamma_i^g + \zeta_j^g + e_{ij}^g, \quad (28)$$

where $\pi_{ij}^g = \log(\Pi_{j|gi0})$ is the natural logarithm of the commuting probability between i and j at time $t = 0$ for a skill type g , τ_{ij}^g is the commute time from i and j for a skill type g , γ_i^g is a fixed effect at the origin level for a skill type g , ζ_j^g is a fixed effect at the destination level for a skill type g , and e_{ij}^g is the error term. Aggregating this equation to the zone level results in an approximate equation (ignoring the Jensen inequality term) of the form

$$\pi_{IJ}^g = -\theta_g \times \kappa \tau_{IJ}^g + \gamma_I^g + \zeta_J^g + e_{IJ}^g. \quad (29)$$

I will estimate this equation using the bilateral commuting flows from the commuting survey in 2010. I estimate this equation using both a linear fixed effects estimator, as well as with a Poisson Pseudo Maximum Likelihood estimator, to address the concerns regarding the granularity of the commuting data (Dingel et al., 2020). Table 7 shows the results of these estimations for each skill type. From columns 2 and 4 we can see that $\theta_h \times \kappa = -0.029$, and $\theta_l \times \kappa = -0.038$. Using the fact that $\kappa = 0.01$, we find that $\theta_h = 2.9$, and $\theta_l = 3.8$. These results are very similar to the ones estimated by Tsivanidis (2019), who finds a θ_h equal to 2.7 and a θ_l equal to 3.3 using commuting data from Bogota.

6.2 Estimating Intra-City Migration Elasticities

I will estimate the intra-city migration elasticities by skill type ($1/\nu_h$ and $1/\nu_l$) by adapting the estimation method used in Caliendo et al. (2019), which is in itself an adapted version of Artuç et al. (2010). I show that we can derive an estimating equation from this model that relates current differences in migration flows to future differences in expected income, as well as future differences in migration flows. I then estimate this equation using an IV-GMM PPML estimator (Windmeijer and Santos Silva, 1997), using past migration flows by skill type to instrument for future migration flows, and lagged differences in commuter market access to instrument for the differences in commuter market access. The estimating equation⁴⁸ (which closely resembles the specification in Caliendo et al. (2019) but with expected income

⁴⁸See Appendix C for the derivation of this equation.

instead of future wages) is

$$\log \left(\frac{m_{in,t}^g}{m_{nn,t}^g} \right) = -\mu_{in}^g \frac{1-\beta}{\nu_g} + \frac{\beta}{\nu_g} \left[\tilde{T}_g \left(\Phi_{Rgi,t+1}^{\frac{1}{\theta_g}} r_{Ri,t+1}^{\alpha-1} - \Phi_{Rgn,t+1}^{\frac{1}{\theta_g}} r_{Rn,t+1}^{\alpha-1} \right) \right] + \beta \log \left(\frac{m_{in,t+1}^g}{m_{ii,t+1}^g} \right) + \omega_{t+1}^g. \quad (30)$$

Following Caliendo et al. (2019) and Artuç et al. (2010), I estimate this equation under the assumption that the average moving costs are equal for all location pairs (i, j) , so that $\mu_{ij}^g = \mu \forall (i, j) \in N \times N$, which allows me to define $\tilde{C}_g = -\mu \frac{1-\beta}{\nu_g}$, and obtain the following equation:

$$\log \left(\frac{m_{in,t}^g}{m_{nn,t}^g} \right) = \tilde{C}_g + \frac{\beta}{\nu_g} \left[\tilde{T}_g \left(\Phi_{Rgi,t+1}^{\frac{1}{\theta_g}} r_{Ri,t+1}^{\alpha-1} - \Phi_{Rgn,t+1}^{\frac{1}{\theta_g}} r_{Rn,t+1}^{\alpha-1} \right) \right] + \beta \log \left(\frac{m_{in,t+1}^g}{m_{ii,t+1}^g} \right) + \omega_{t+1}^g. \quad (31)$$

Where \tilde{C}_g is a constant and ω_{t+1}^g is a random term that includes any unexpected shock at time $t + 1$ that affects the relative migration flows at time $t + 1$. Estimating this equation for each skill type using bi-annual intra-city migration flows constructed from the individual-level data on residential locations obtained from the electoral register leads to an estimate of ν_h equal to 1.4, and a ν_l equal to 1.8. This implies that high-skilled workers have a higher intra-city migration elasticity than low-skilled workers (since the migration elasticity is the multiplicative inverse these parameters).

7 Model Results

Having estimated the necessary elasticities and key parameters in the model, I use the algorithm describe in Subsection 5.12 to solve numerically for the sequential competitive equilibrium (as defined in Subsection 5.9) that converges to a stationary equilibrium in 25 periods, which is equal to 50 years, since I choose each period to be equal to two years, in order to match the bi-annual individual-level migration data. I use data on employment and residential population by district⁴⁹ in 2011 to initialize the employment and population vectors, I then use the migration matrix estimated from individual level data at the district level between 2011 and 2013 to initialize the migration matrix in the model at $t = 0$. Finally, I calculate minimum commute times using ArcMaps's Network Analyst Tool for each period by adding sequentially each line that appeared in each bi-annual period, with these commute times I can calculate $\{d_{ij,t}\}$ for every $t = 0, 1, 2, 3, \dots$ ⁵⁰ When estimating a counterfactual scenario, I will use different commute times, calculated in the same way, under different assumptions regarding the changes in the transport infrastructure. These changes in the vector of time-varying fundamentals will lead to different sequential competitive equilibria and stationary equilibria.

⁴⁹In order to alleviate concerns regarding the sparsity of the migration matrix at the census tract level, I solve the model at a more aggregate spatial level, the electoral district. The main results hold when the model is solved at the census tract level (see Appendix D).

⁵⁰I will assume that $d_{ij,t} = d_{ij,3}$ for all $t \geq 4$.

7.1 Effects of BRT on Spatial Sorting: Model vs Data

In this section I compare the estimated effects of the changes in market access due to the construction of the BRT from the reduced form analysis (Section 4) to the estimated effects within the model. I first solve for the path of the endogenous variables in the model under the assumption that the commute times (and therefore the commute costs) change reflecting the construction of the BRT system. I then solve the model under the counterfactual assumption that no BRT line was built, and, therefore, commute times did not change over time.⁵¹ Having solved the model for both the scenario with the BRT, and the scenario where no BRT was built, I employ a difference-in-difference estimation procedure within the model, where I take the differential changes in market access in time, between $t = 0$ and $t = 4$,⁵² and between the model with the BRT and the model without the BRT (indexed as CF), and regress these differential changes in market access on the differential changes in the outcomes of interest. Within the model, I can observe the counterfactual trends of all the endogenous variables for every location by solving the counterfactual model. Therefore, by subtracting the changes that would have occurred even in the absence of the transport infrastructure improvements, I can isolate the direct effects of the transport infrastructure improvements in the model. The corresponding difference in difference estimating equation takes the following form:

$$\Delta \log(Y_{BRT}) - \Delta \log(Y_{CF}) = \alpha + \beta_1(\Delta \log(CMA_{BRT}) - \Delta \log(CMA_{CF})) + \beta_2 HS\ sh._0 + \beta_3(\Delta \log(CMA_{BRT}) - \Delta \log(CMA_{CF})) \times HS\ sh._0 + \epsilon. \quad (32)$$

Where $\Delta \log(Y_m)$ is the change between $t = 0$ and $t = 4$ in the log of the outcome of interest (high-skilled share, floorspace prices or population) for model m , which can either be *BRT* for the model that incorporates the BRT, or *CF* for the model that assumes no BRT lines were built; in the same way, $\Delta \log(CMA_m)$ is the change in log market access for each model; $HS\ sh._0$ is the high-skilled share at $t = 0$ in each district; and ϵ is the error term.

7.1.1 High-Skilled Share

From Table 8 we can see on the left the results from estimating equation 1 using the historical IV estimation method covered in Section 4 (column 4 of Table 4, and on the right we can see the estimation results from estimating equation 32 with the differential change in the high-skilled share as the dependent variable. We can see that the model produces similar estimates than the reduced form analysis, both in sign and in magnitude. In both cases we see that market access increased the high-skilled share more in places that had a higher initial level of high-skilled share.⁵³ The similarity of these results provide

⁵¹Note that, because the model does not assume that the economy starts at a stationary equilibrium, the endogenous variables will not stay constant over time even in the absence of changes in commute times.

⁵²Recall that each period in the model represents two years, so there are eight years between $t = 0$ and $t = 4$.

⁵³It is worth noting that changes in the high-skilled share were not directly targeted in the estimation of this model.

further evidence that the construction of the *Metrobus* BRT system increased the spatial segregation by skill type in the city.

7.2 Changes in Segregation by Skill Type

We have seen both through the lens of the model and through the reduced form analysis that the changes in market access driven by the construction of the BRT system lead to an increase in segregation by skill type in the short-run by increasing the high-skilled share more in places that had originally higher high-skilled share. However, we could also ask ourselves if this increase in segregation persists in the long-run (i.e. at the stationary equilibrium). To answer this question, I calculate the differential change in the high-skilled share between $t = 0$ and the values achieved at the stationary equilibrium for the model with the full BRT, and the model where not BRT line was put in place. I will then regress those differential changes for each place on the initial high-skilled share at $t = 0$, estimating the following equation:

$$\Delta \log(hs\ share_{BRT}) - \Delta \log(hs\ share_{CF}) = \alpha + \beta \log(hs\ share_0) + \epsilon. \quad (33)$$

By estimating equation 33, I find that, relative to a scenario where no BRT line had been built, the *Metrobus* BRT system did increase segregation by skill type in the long run. From Table 9 we can see that, indeed, places that started with a higher value of high-skilled share increased their high-skilled share by more. A 1% increase in the initial high-skilled share led to a 0.6% higher differential increase in the high-skilled share at the stationary equilibrium.

8 Welfare Results

In this section I analyze the impact on resident's welfare of the construction of the BRT system in Buenos Aires. One of the key contributions of this dynamic framework is that it allows me to quantify the average welfare gains for residents based on where they were living before the BRT system was built (which I refer to as "incumbents"), as opposed to doing comparative statics on the *ex post* equilibrium. In the following subsection I study the welfare gains by skill type for incumbents, and how these gains differ for different parts of the city. I then study the aggregate welfare gains by skill type in the entire city, as well as the average gains for people living close to the BRT lines at $t = 0$ and at the *ex post* stationary equilibrium.

8.1 Welfare Gains for Incumbents

Let $V_{n,0}^g$ be the expected utility of a resident of skill type g living in location i at time $t = 0$ in the scenario where the full BRT system will be built, as calculated in equation 21. Let us also calculate $\hat{V}_{n,0}^g$ as the expected utility at time $t = 0$ under the assumption that no BRT line will be built. Since residents are forward-looking (and have perfect foresight), these expected utilities will include the expected future utility flows under each scenario, and will, therefore, be different. By calculating $V_{n,0}^g/\hat{V}_{n,0}^g - 1$ we can measure the welfare gains in terms of expected utility for residents according to their place of residence before the BRT was put in place.

When analyzing the spatial distribution of the average welfare gains for incumbents by district (Figure 16), there are three findings that stand out. First, welfare gains were higher for both high- and low-skilled incumbents living closer to the BRT lines and further from the CBD, since these are the locations where commuter market access increased the most. Second, welfare gains for high- and low-skilled incumbents are highly spatially correlated. In fact, the Pearson correlation coefficient between high- and low-skilled gains by district is 0.97. Third, welfare gains for both skill types seem larger for incumbents living near the southernmost BRT line than for incumbent living near the northernmost BRT line, with incumbents living near the other BRT lines seeing an intermediate level of welfare gains on average.

From Figure 3 we see that different BRT lines cross through neighborhoods with different levels of high-skilled share at baseline. In particular, census tracts near (less than one kilometer) from the first, second, and fifth lines built have an average high-skilled share that is close to the median,⁵⁴ while census tracts near the third line built (the southernmost line) have, on average, much lower levels of high-skilled share,⁵⁵ and the census tracts near the fourth line built (the northernmost line) have the highest high-skilled share on average (Table 10).⁵⁶ With this information, I group the lines into three subsets: the southern line (third line to be built) constitutes one group, and represents the line built along neighborhoods with the lowest levels of high-skilled share in 2010; the first, second, and fifth lines to be built constitute the second group, and represent the lines that were built along neighborhoods with a medium level of high-skilled share; and the northern line (fourth to be built) constitutes the third group, and represents the line built along neighborhoods with the highest high-skilled share in the city.

By comparing the average welfare gains for incumbent residents living near⁵⁷ each group of lines (Figure 17), we can see that both high- and low-skilled incumbent residents that were living in locations with lower initial high-skilled share saw the largest welfare gains. In fact, high-skilled incumbent residents living near the southernmost line saw welfare gains on average 2.1 times those of the incumbent residents living near the northernmost line, while for low-skilled incumbent residents the gains were 1.8 times higher near the southern line. Gains on average for residents living near the lines that served

⁵⁴The median census tract had a high-skilled share of 0.5 according to the 2010 census.

⁵⁵The average census tract that is at most at one kilometer from the southern line has a high-skilled share of 0.31, placing it at the thirteenth percentile of the distribution of high-skilled share in the city in 2010.

⁵⁶The average census tract near the northern line had a high-skilled share of 0.63 in 2010, placing it at the seventy-third percentile of the distribution of high-skilled share in the city.

⁵⁷At most at one kilometer from a BRT line.

neighborhoods with a median level of high-skilled share saw welfare gains that were in between those of the southern and the northern line, on average.

8.2 Aggregate Welfare Results

Estimating ΔW_t^g from equation 27 at $t = 0$ for high- and low-skilled residents, I find that the aggregate welfare gains at $t = 0$ from the construction of the BRT system were 0.6% for both high- and low-skilled residents.⁵⁸ At the same time, estimating the same measure at $t = 25$, where the sequential competitive equilibrium is assumed to converge to a stationary equilibrium, I find that the average welfare gains at the stationary equilibrium are 0.7% for both high- and low-skilled residents. Additionally, I find that the *Metrobus* resulted in a net present value gain (net of construction costs) of \$13.26 billion measured in 2010.⁵⁹ This is equivalent to a constant increase in the 2010 GDP of the city of 0.4%.

From Figure 16 we can clearly see that the welfare gains were not distributed equally across the city, and in fact, in many parts of the city (further from the BRT), the gains were significantly lower than in districts that were close to a BRT line. One additional way to see this is to calculate the aggregate welfare gains for a subset of districts that are at most at a certain distance from a BRT line. Table 11 shows the aggregate welfare gains for residents (high- and low-skilled) living in districts at most at a certain distance from a line. We can see from this table that for residents living at most at 800 meters (about half a mile) from a BRT line at $t = 0$, welfare gains are much larger on average, with high-skilled residents seeing an average gain of 1.04% and low-skilled residents seeing an average gain of 0.94%. As we increase the maximum distance to a BRT line, the average welfare gains decrease, as would be expected.

9 Counterfactuals: Local Transport Infrastructure Improvements

In this section I study what would have happened to spatial sorting between high- and low-skilled residents if only a subset of lines were built, as opposed to the full BRT system. I construct three counterfactual scenarios: in the first scenario, only the southern line, that goes through the districts with the lowest high-skilled share in 2010, is built; in the second scenario, the three lines that go through districts that are close to the median value of the high-skilled distribution in 2010 (the first, second, and fifth lines to be built) are the only lines to be built; in the third scenario, only the northern line, that serves the districts with the highest high-skilled share on average, is built. I study the consequences of building these three different subsets of BRT lines on spatial sorting, and on welfare for incumbents that live near each group of BRT lines.

⁵⁸Average welfare gains for both high- and low-skilled residents are the same up to the fourth digit. This similarity is consistent with the findings of Tsivianidis (2019), where he finds that both high- and low-skilled residents of Bogota benefited about the same on average from the construction of a BRT in the city.

⁵⁹See Appendix D for details on this calculation.

9.1 Spatial Sorting in Each Counterfactual Scenario

Having solved the model for the sequential competitive equilibrium that converges to a stationary equilibrium under each counterfactual scenario, I compare the changes in the high-skilled share in each district between each of these counterfactuals and the counterfactual scenario where no BRT line was built. I estimate a version of equation 33, where the subscript *BRT* now refers to each counterfactual scenario where only a subset of the BRT lines are built. The results of running these regressions for each counterfactual scenario are shown in Table 12. We can see that, had the city built only the southernmost line (column 2), the high-skilled share would have increased more in districts that had an originally lower level of high-skilled share. This is consistent with the fact that the only transport infrastructure improvement taking place in this scenario is in districts that are, on average, at the lower end of the distribution of high-skilled share in baseline. This result indicates that gentrification⁶⁰ would have occurred around the southern line, had that been the only line that was built.

If we look at column 3 in Table 12, we can see that, if only the three lines that run through districts with medium levels of high-skilled share in baseline were built, we would have still seen a similar pattern of spatial sorting, with high-skilled share increasing more in places that had a higher initial level of high-skilled share. Finally, from column 4 of the same table, we see that the northern line, which serves the districts with the highest initial high-skilled share, would have had no significant effect on spatial sorting as a whole in the city, although this could be in part due to the smaller length of this line, which implies that it affected a smaller area of the city.

9.2 Welfare Gains in Each Counterfactual Scenario

As would be expected given the more local nature of the transport infrastructure improvements in these counterfactual scenarios, we can see in Figures 18, 20, 22 that the largest welfare gains in each counterfactual scenario were for incumbents near the BRT lines that were built in each case. This is consistent with the fact that welfare gains are higher for residents living closer to the transport infrastructure improvements.

Interestingly, when we compare the gains for incumbents that were living near the southern line (Figure 19) between the scenario where only that line was built, and the scenario where all BRT lines were built, we can see that the welfare gains are 31% lower for high-skilled residents and 30% lower for low-skilled residents. In comparison, the welfare gains for incumbent residents living near the BRT lines that were built in the second scenario only saw a decrease of 3% for high-skilled workers, and 5% for low-skilled workers (Figure 21). The decrease in welfare for incumbent residents living near the built BRT lines in the third counterfactual scenario was in between decreases in the other two scenarios, with a decrease of 20% for high-skilled residents and 19% for low-skilled residents.

⁶⁰Defined narrowly in this case as the increase in the high-skilled share in places that had a low level of high-skilled share initially.

Part of these decreases in welfare would come from the decrease in expected utility conditional on moving in the future, since under the counterfactual scenarios, commuter market access increase in fewer parts of the city. However, the fact that the highest decreases in welfare arise from the scenario where only the southern line was built suggests that, at least in part, the gentrification caused by only building that one line decreased the welfare gains for incumbent residents, relative to a situation where other lines were the full BRT system was built, and no gentrification occurred in these districts.

10 Conclusion

In this paper, I make three contributions to the understanding of the effects of improving the urban transit infrastructure. First, I show that migration response to these improvements by high- and low-skilled workers depend on the initial characteristics of the neighborhoods that are being targeted by these improvements. For the same level of increase in market access, neighborhoods with an initial proportion of high-skilled share at the eightieth percentile of the distribution see increases in the high-skilled share that are, on average, six times those of neighborhoods at the twentieth percentile of the distribution. This differential effect led to an increase in spatial segregation in the city.

Second, I develop a dynamic quantitative spatial equilibrium framework that allows us to quantify the welfare effects of these transport projects on the residents that were living near these improvements before they were put in place. This is particularly significant because transport infrastructure projects are a form of place based policy, and as such, policy makers chose the placement of these projects in order to target the residents that are living in the neighborhoods that are closer to these transport improvements. Therefore, being able to quantify the welfare gains of these incumbent residents is of direct policy relevance. In the case of Buenos Aires, I find that the BRT system increased welfare more for both high- and low-skilled residents in neighborhoods that had an initially low high-skilled share. Comparing residents living near the southern line, which runs through the neighborhoods with the highest proportion of low-skilled residents, to the residents living near the northern line, which runs through neighborhoods with the highest proportion of high-skilled residents, we find that the residents living near the southern line saw welfare gains that are twice those of the residents living near the northern line.

Third, I study the counterfactual welfare effects for incumbent residents living near the BRT lines of more localized transport infrastructure improvements. Due to budgetary and political considerations, governments might decide to prioritize transport improvements in poorer areas, where the share of low-skilled workers is higher. I show that, in the case of Buenos Aires, building a single line that ran through the neighborhoods with the highest proportion of low-skilled workers would have still benefited incumbent residents living near the line, but the welfare gains would have been 31% lower for high-skilled residents, and 31% lower for low-skilled residents. Furthermore, this more localized transit improvement would have led to a gentrification of the targeted neighborhoods, as opposed to the more comprehensive plan that was put in place, which had the opposite effect for neighborhoods in the lowest quintile of the high-skilled share distribution. This finding suggests that the transit-induced gentrification hypothesis might

hold for localized transit improvements, but by building a whole network of transit improvements, the city produced the opposite effect, increasing the spatial segregation by skill type in the city.

References

- AGCBA. Informe final de auditoría con informe ejecutivo. Technical report, Buenos Aires, Argentina, 2015.
- AGCBA. Informe final de auditoría con informe ejecutivo. Technical report, Buenos Aires, Argentina, 2019.
- Gabriel M. Ahlfeldt, Stephen J. Redding, Daniel M. Sturm, and Nikolaus Wolf. The Economics of Density: Evidence From the Berlin Wall. *Econometrica*, 83(6):2127–2189, 2015. ISSN 0012-9682. doi: 10.3982/ECTA10876. URL <https://www.econometricsociety.org/doi/10.3982/ECTA10876>.
- Treb Allen and Costas Arkolakis. The Welfare Effects of Transportation Infrastructure Improvements. Working paper, 2019. URL <http://www.nber.org/papers/w25487>.
- Treb Allen, Costas Arkolakis, and Xiangliang Li. Optimal City Structure. Working paper, 2016.
- Milena Almagro and Tomás Domínguez-Iino. Location Sorting and Endogenous Amenities: Evidence from Short-Term Rentals in Amsterdam. Working paper, 2019.
- Guillermo Alves, Lucila Berniell, Dolores de la Mata, D Fernandez, C Juncosa, S Rotondo, et al. Distribución espacial del empleo formal en la ciudad autónoma de buenos aires: un diagnóstico a partir de registros administrativos. 2018.
- Erhan Artuç, Shubham Chaudhuri, and John McLaren. Trade shocks and labor adjustment: A structural empirical approach. *American Economic Review*, 100(3):1008–1045, jun 2010. ISSN 00028282. doi: 10.1257/aer.100.3.1008. URL <http://pubs.aeaweb.org/doi/10.1257/aer.100.3.1008>.
- Clare Balboni. In Harm’s Way? Infrastructure Investments and the Persistence of Coastal Cities. Working paper, 2019.
- Clare Balboni, Gharad Bryan, Melanie Morten, and Bilal Siddiqi. Transportation, Gentrification, and Urban Mobility: The Inequality Effects of Place-Based Policies. Working paper, 2020.
- Eleni Bardaka, Michael S Delgado, and Raymond JGM Florax. Causal identification of transit-induced gentrification and spatial spillover effects: The case of the denver light rail. *Journal of Transport Geography*, 71:15–31, 2018.
- Nathaniel Baum-Snow. Did highways cause suburbanization? *The quarterly journal of economics*, 122(2):775–805, 2007.
- Nathaniel Baum-Snow and Matthew A Turner. Transport infrastructure and the decentralization of cities in the people’s republic of china. *Asian development review*, 34(2):25–50, 2017.

Nathaniel Baum-Snow, Matthew Freedman, and Ronni Pavan. Why has urban inequality increased? *American Economic Journal: Applied Economics*, 10(4):1–42, oct 2018. ISSN 19457790. doi: 10.1257/app.20160510.

Claudia N. Berg, Uwe Deichmann, Yishen Liu, and Harris Selod. Transport policies and development. *Journal of Development Studies*, 53:465–480, 4 2017. ISSN 17439140. doi: 10.1080/00220388.2016.1199857.

Gharad Bryan and Melanie Morten. The aggregate productivity effects of internal migration: Evidence from indonesia. *Journal of Political Economy*, 127(5):2229–2268, 2019.

Gharad Bryan, Edward Glaeser, and Nick Tsivanidis. Cities in the developing world. *Annual Review of Economics*, 12:273–297, 2020.

Lorenzo Caliendo, Maximiliano Dvorkin, and Fernando Parro. Trade and Labor Market Dynamics: General Equilibrium Analysis of the China Trade Shock. *Econometrica*, 87(3):741–835, 2019. ISSN 0012-9682. doi: 10.3982/ecta13758.

Karen Chapple and Anastasia Loukaitou-Sideris. *Transit-oriented displacement or community dividends?: Understanding the effects of smarter growth on communities*. MIT Press, 2019.

Victor Couture, Cecile Gaubert, Jessie Handbury, and Erik Hurst. Income Growth and the Distributional Effects of Urban Spatial Sorting. Working paper, 2018.

H David, Christopher J Palmer, and Parag A Pathak. Gentrification and the amenity value of crime reductions: Evidence from rent deregulation. Technical report, National Bureau of Economic Research, 2017.

Casey Dawkins and Rolf Moeckel. Transit-induced gentrification: Who will stay, and who will go? *Housing Policy Debate*, 26(4-5):801–818, 2016.

Klaus Desmet, Robert E Kopp, Scott A Kulp, Dávid Krisztián Nagy, Michael Oppenheimer, Esteban Rossi-Hansberg, and Benjamin H Strauss. Evaluating the economic cost of coastal flooding. *American Economic Journal: Macroeconomics*, forthcoming.

Jonathan I Dingel, Felix Tintelnot, and Kenneth C Griffin. Spatial Economics for Granular Settings. Working paper, 2020.

Kacie Dragan, Ingrid Ellen, and Sherry A Glied. Does gentrification displace poor children? new evidence from new york city medicaid data. Technical report, National Bureau of Economic Research, 2019.

Gilles Duranton and Matthew A Turner. Urban growth and transportation. *Review of Economic Studies*, 79(4):1407–1440, 2012.

Pablo Fajgelbaum and Stephen Redding. Trade, Structural Transformation and Development: Evidence from Argentina 1869-1914. Working paper, 2018.

Robert C Feenstra, Philip Luck, Maurice Obstfeld, and Katheryn N Russ. In search of the armington elasticity. *Review of Economics and Statistics*, 100(1):135–150, 2018.

- Takao Fujimoto and Ulrich Krause. Strong ergodicity for strictly increasing nonlinear operators. *Linear Algebra and its Applications*, 71:101–112, 1985.
- Stephen Gibbons and Stephen Machin. Valuing rail access using transport innovations. *Journal of urban Economics*, 57(1):148–169, 2005.
- Edward L. Glaeser, Matthew E. Kahn, and Jordan Rappaport. Why do the poor live in cities? The role of public transportation. *Journal of Urban Economics*, 63(1):1–24, jan 2008. ISSN 00941190. doi: 10.1016/j.jue.2006.12.004.
- Marco Gonzalez-Navarro and Matthew A Turner. Subways and urban growth: Evidence from earth. *Journal of Urban Economics*, 108:85–106, 2018.
- Eric Hannon, Jan Tijs Nijssen, Sebastian Stern, and Ben Sumers. The effects of roads on trade and migration: Evidence from a planned capital city. Technical report, McKinsey & Company, 2020.
- Stephan Hebllich, Stephen J Redding, and Daniel M Sturm. The making of the modern metropolis: evidence from london. *The Quarterly Journal of Economics*, 135(4):2059–2133, 2020.
- Dorota Kamrowska-Zaluska. Buenos aires—toward comprehensive development and sustainable mobility. In *IOP conference series: materials science and engineering*, number 6, page 062022. IOP Publishing, 2017.
- Melanie Morten and Jaqueline Oliveira. The effects of roads on trade and migration: Evidence from a planned capital city. *NBER Working Paper*, 22158:43, 2018.
- Miguel Padeiro, Ana Louro, and Nuno Marques da Costa. Transit-oriented development and gentrification: a systematic review. *Transport Reviews*, 39(6):733–754, 2019.
- Rahul Pathak, Christopher K Wyczalkowski, and Xi Huang. Public transit access and the changing spatial distribution of poverty. *Regional Science and Urban Economics*, 66:198–212, 2017.
- Stephen J Redding and Matthew A Turner. Transportation costs and the spatial organization of economic activity. In *Handbook of regional and urban economics*, volume 5, pages 1339–1398. Elsevier, 2015.
- Mark Roberts, Martin Melecky, Théophile Bougna, and Yan Xu. Transport corridors and their wider economic benefits: A quantitative review of the literature. *Journal of Regional Science*, 60:207–248, 3 2020. ISSN 14679787. doi: 10.1111/jors.12467.
- Eleanor Sanderson and Frank Windmeijer. A weak instrument f-test in linear iv models with multiple endogenous variables. *Journal of Econometrics*, 190(2):212–221, 2016.
- Christopher Severen. Commuting, Labor, and Housing Market Effects of Mass Transportation: Welfare and Identification. Working paper, 2018.
- Dhan Zunino Singh. The tales of two mobility infrastructures: The street and the underground railway of buenos aires, 1880s–1940s. In *Architectures of Hurry—Mobilities, Cities and Modernity*, pages 65–82. Routledge, 2018.

James Stock and Motohiro Yogo. Asymptotic distributions of instrumental variables statistics with many instruments. *Identification and inference for econometric models: Essays in honor of Thomas Rothenberg*, pages 109–120, 2005.

Yichen Su. The rising value of time and the origin of urban gentrification. *Available at SSRN 3216013*, 2020.

Shadi O Tehrani, Shuling J Wu, and Jennifer D Roberts. The color of health: Residential segregation, light rail transit developments, and gentrification in the united states. *International Journal of Environmental Research and Public Health*, 16(19):3683, 2019.

Nick Tsivanidis. Evaluating the Impact of Urban Transit Infrastructure: Evidence from Bogotá's Trans-Milenio. Working paper, 2019.

UN. 2018 revision of world urbanization prospects, 2018.

Frank AG Windmeijer and Joao MC Santos Silva. Endogeneity in count data models: an application to demand for health care. *Journal of applied econometrics*, 12(3):281–294, 1997.

11 Tables

Mode of Transport	Low-Skilled	High-Skilled	Total
Car / motorcycle	16.5%	22.9%	19.3%
Taxi	2.1%	3.7%	2.8%
Bus	37.1%	39.3%	38.1%
Subway	4.4%	14.5%	8.8%
Train	1.6%	3.2%	2.3%
Walking / bicycle	38.1%	16.3%	28.5%
Other	0.2%	0.0%	0.1%

Table 1: Percentage of trips made by mode of transport by skill type. Percentages calculated from the 2010 mobility survey for the metropolitan region of Buenos Aires (*Encuesta de Movilidad Domiciliaria*, or *EnMoDo*), taking all trips with origin and destination within the city of Buenos Aires, for people of age 18 or above. Any person with at least some post-secondary education was categorized as high-skilled, and every person with no more than secondary education was categorized as low-skilled.

Code	Occupation Description
1	Managers
2	Professional
3	Technicians and associate professionals
4	Clerical support workers
5	Service and sales workers
6	Skilled agricultural, forestry and fishery workers
7	Craft and related trades workers
8	Plant and machine operators, and assemblers
9	Elementary occupations
0	Armed forces occupations

Table 2: International Standard Classification of Occupations (ISCO) one-digit occupation groups.

	$\Delta \log(\text{hs share})$				
	1	2	3	4	5
	OLS	IV	OLS	IV	IV
$\Delta \log(CMA)$	-0.122 (0.087)	0.202 (0.096)**	-2.797 (0.564)***	-2.308 (0.522)***	-2.609 (1.197)**
hs share_0	0.192 (0.038)***	0.296 (0.044)***	0.153 (0.078)**	0.113 (0.052)**	0.191 (0.097)**
$\Delta \log(CMA) \times \text{hs sh. avg}_0$			4.629 (0.895)***	4.143 (0.847)***	3.489 (1.925)*
cons	-0.457 (0.026)***	-0.538 (0.031)***	-0.445 (0.053)***	-0.419 (0.036)***	-0.404 (0.063)***
Neigh. FE	NO	NO	NO	NO	YES
F first	-	1470	-	791	277
N	2,282	2,282	2,282	2,282	2,282

Table 4: Reduced Form Results: regressions of change in high skill share between 2011 and 2017 on change in market access between 2011 and 2017, initial average high skill share for contiguous census tracts, and the interaction term. The instrument used for the IV regressions is a measure of change of log CMA where the 2017 CMA is calculated assuming the BRT lines were built following the 1938 tramway lines. Cragg-Donald Wald F statistics from the first stage regression are reported for each IV estimation. Robust standard errors in parentheses. * p<0.10, ** p<0.05, *** p<0.01.

	(1) $\Delta \log(CMA)$	(2) $\Delta \log(CMA)$	(3) $\Delta \log(CMA) \times \text{hs sh. avg}_0$	(4) $\Delta \log(CMA)$	(5) $\Delta \log(CMA) \times \text{hs sh. avg}_0$
$\Delta \log(CMA_{\text{inst}})$	0.661*** (0.0172)	2.156*** (0.141)	0.736*** (0.0828)	1.912*** (0.137)	0.810*** (0.0815)
hs share_0	-0.200*** (0.0110)	-0.0110 (0.0207)	-0.0345** (0.0122)	0.193*** (0.0202)	0.113*** (0.0120)
$\Delta \log(CMA_{\text{inst}}) \times \text{hs share}_0$		-2.392*** (0.224)	-0.537*** (0.132)	-2.322*** (0.213)	-0.857*** (0.126)
Constant	0.121*** (0.00763)	0.000891 (0.0135)	0.0180** (0.00795)	-0.0807*** (0.0140)	-0.0428*** (0.00831)
F - stat	1470	791	791	277	277
Neighborhood FE	NO	NO	NO	YES	YES
N	2282	2282	2282	2282	2282

Table 3: First stage regressions with historical IV instrument. Each column shows a regression of one of the endogenous regressors from Tables 4, 5, and 6 on the instrumented changes in market access, where the instrument is constructed assuming the BRT system was built following the 1938 tramway lines, as well as the instrumented market access interacted with the initial share of high-skilled residents. Cragg-Donald Wald F statistics are reported for each regression. Robust standard errors in parentheses. * p<0.10, ** p<0.05, *** p<0.01.

	$\Delta \log(\text{floorspace_price})$				
	1	2	3	4	5
	OLS	IV	OLS	IV	IV
$\Delta \log(CMA)$	-0.310 (0.134)**	0.314 (0.084)***	-4.059 (1.097)***	-3.550 (1.012)***	-5.299 (1.420)***
hs share ₀	0.080 (0.051)	0.281 (0.071)***	-0.161 (0.065)**	-0.001 (0.055)	-0.480 (0.093)***
$\Delta \log(CMA) \times \text{hs sh. avg.}_0$			6.552 (1.735)***	6.376 (1.611)***	9.379 (2.235)***
cons	0.104 (0.033)***	-0.051 (0.047)	0.250 (0.044)***	0.131 (0.038)***	0.361 (0.057)***
Neigh. FE	NO	NO	NO	NO	YES
F first	-	1470	-	791	277
N	2,282	2,282	2,282	2,282	2,282

Table 5: Reduced Form Results: regressions of change in floorspace prices between 2011 and 2017 on change in market access between 2011 and 2017, initial average high skill share for contiguous census tracts, and the interaction term. The instrument used for the IV regressions is a measure of change of log CMA where the 2017 CMA is calculated assuming the BRT lines were built following the 1938 tramway lines. Floorspace prices are calculated as the average sale price per square meter, according to geo-referenced online asking price data for the city of Buenos Aires. Cragg-Donald Wald F statistics from the first stage regression are reported for each IV estimation. Robust standard errors in parentheses. * p<0.10, ** p<0.05, *** p<0.01.

	IV regressions		
	$\Delta \log(\text{HS pop.})$	$\Delta \log(\text{LS pop.})$	$\Delta \log(\text{Tot. pop.})$
$\Delta \log(CMA)$	-1.429 (0.553)***	-0.679 (0.668)	-1.198 (0.505)**
$hs \text{ share}_0$	0.200 (0.056)***	0.129 (0.071)*	0.266 (0.050)***
$\Delta \log(CMA) \times hs \text{ sh. avg.}_0$	3.500 (0.934)***	2.376 (1.142)**	3.167 (0.850)***
cons	-0.471 (0.039)***	-0.528 (0.047)***	-0.547 (0.034)***
F first	791	791	791
N	2,282	2,282	2,282

Table 6: Reduced Form Results: regressions of change in high-skilled population (column 1), low-skilled population (column 2), and total population (column 3) between 2011 and 2017 on change in market access between 2011 and 2017, initial average high skill share for contiguous census tracts, and the interaction term. The instrument used for the IV regressions is a measure of change of log CMA where the 2017 CMA is calculated assuming the BRT lines were built following the 1938 tramway lines. Cragg-Donald Wald F statistics from the first stage regression are reported for each IV estimation. Robust standard errors in parentheses. * p<0.10, ** p<0.05, *** p<0.01.

	ln Bilateral Commuting Prob. 2010			
	High-skilled		Low-skilled	
trip time	-0.037 (0.014)***	-0.029 (0.012)**	-0.047 (0.009)***	-0.038 (0.009)***
Estimation	OLS	PPML	OLS	PPML
Fixed Effects	Yes	Yes	Yes	Yes
R ²	0.48	-	0.28	-
N	415	415	424	424

Table 7: Estimation of bilateral commuting probabilities using equation 9. Robust standard errors in parentheses. * p<0.10, ** p<0.05, *** p<0.01.

Reduced Form (IV)		Model	
	$\Delta \log(\text{hs share})$		$\Delta \log(\text{hs share}_{BRT}) - \Delta \log(\text{hs share}_{CF})$
$\Delta \log(CMA)$	-2.308 (0.522)***	$\Delta \log(CMA_{BRT}) - \Delta \log(CMA_{CF})$	-2.202 (0.623)***
hs share_0	0.113 (0.052)**	hs share_0	-0.026 (0.036)
$\Delta \log(CMA) \times \text{hs sh. avg.}_0$	4.143 (0.847)***	$\Delta \log(CMA_{BRT}) - \Delta \log(CMA_{CF}) \times \text{hs share}_0$	6.169 (1.651)***
cons	-0.419 (0.036)***	cons	-0.012 (0.020)
R^2	-	R^2	0.29
N	2,282	N	167

Table 8: Reduced form results versus model estimation. The left-hand side shows the results from column 4 of table 4, while the right-hand side shows the results from the difference in difference estimation within the model, comparing changes between $t = 0$, and $t = 0$, and between the model with the BRT system, and the counterfactual without a BRT system put in place. Robust standard errors in parentheses. * p<0.10, ** p<0.05, *** p<0.01.

$\Delta \log(\text{hs share}_{BRT}) - \Delta \log(\text{hs share}_{CF})$	
$\log(\text{hs share}_0)$	0.585 (0.139)***
cons	0.403 (0.088)***
R^2	0.11
N	167

Table 9: Measuring increase in segregation at the stationary equilibrium. This table shows the result from estimating a difference in difference regression within the model, where I difference the changes between the initial high-skilled share and the high-skilled share at the stationary equilibrium, between the model with the BRT, and the counterfactual model without the BRT. Robust standard errors in parentheses. * p<0.10, ** p<0.05, *** p<0.01.

Order Built	1	2	3	4	5
Line Name	J. B. Justo	9 de Julio	Sur	Cabildo	San Martin
Median HS share	0.46	0.54	0.33	0.65	0.48
Mean HS share	0.48	0.55	0.31	0.63	0.48

Table 10: High-skilled share by BRT line. Each column shows the median and mean high-skilled share for census tracts that are at most one kilometer from a BRT line. The high-skilled share was calculated as the proportion of population in each census tract with at least some post-secondary education, according to the 2010 national census data.

Distance to Line (m)	(1)		(2)		(3)	(4)
	Avg. Welfare HS close to line	Avg. Welfare HS far from line	Avg. Welfare LS close to line	Avg. Welfare LS far from line		
400	1.04	0.59	0.94	0.59		
800	1.03	0.55	1.02	0.55		
1200	0.92	0.48	0.9	0.48		
1600	0.87	0.37	0.85	0.37		
2000	0.76	0.35	0.76	0.35		
2400	0.67	0.36	0.68	0.36		
2800	0.61	0.39	0.61	0.39		
3200	0.59	0.7	0.59	0.63		
3600	0.59	0.71	0.59	0.61		

Table 11: Average welfare for high- and low-skilled incumbents by distance to a BRT line. Columns 1 and 3 show the welfare gains for incumbents living at most at the distance shown in the “Distance to line” column from a BRT line at time $t = 0$, while columns 2 and 4 show the average welfare gains for incumbent residents of places farther than that distance at time $t = 0$.

	$\Delta \log(hs\ share_{BRT}) - \Delta \log(hs\ share_{CF})$			
	(1)	(2)	(3)	(4)
	Full BRT	Low HS share	Medium HS share	High HS share
$\log(hs\ share_0)$	0.585 (0.139)***	-1.216 (0.734)*	0.412 (0.068)***	-0.261 (0.243)
cons	0.403 (0.088)***	-0.807 (0.464)*	0.284 (0.042)***	-0.170 (0.154)
R^2	0.11	0.12	0.15	0.04
N	167	167	167	167

Table 12: Spatial sorting for counterfactual scenarios. This table shows the result from estimating a difference in difference regression within the model, where I difference the changes between the initial high-skilled share and the high-skilled share at the stationary equilibrium, between the model with only a subset of BRT lines, and a counterfactual model with no BRT lines. Robust standard errors in parentheses. * p<0.10, ** p<0.05, *** p<0.01.

12 Figures

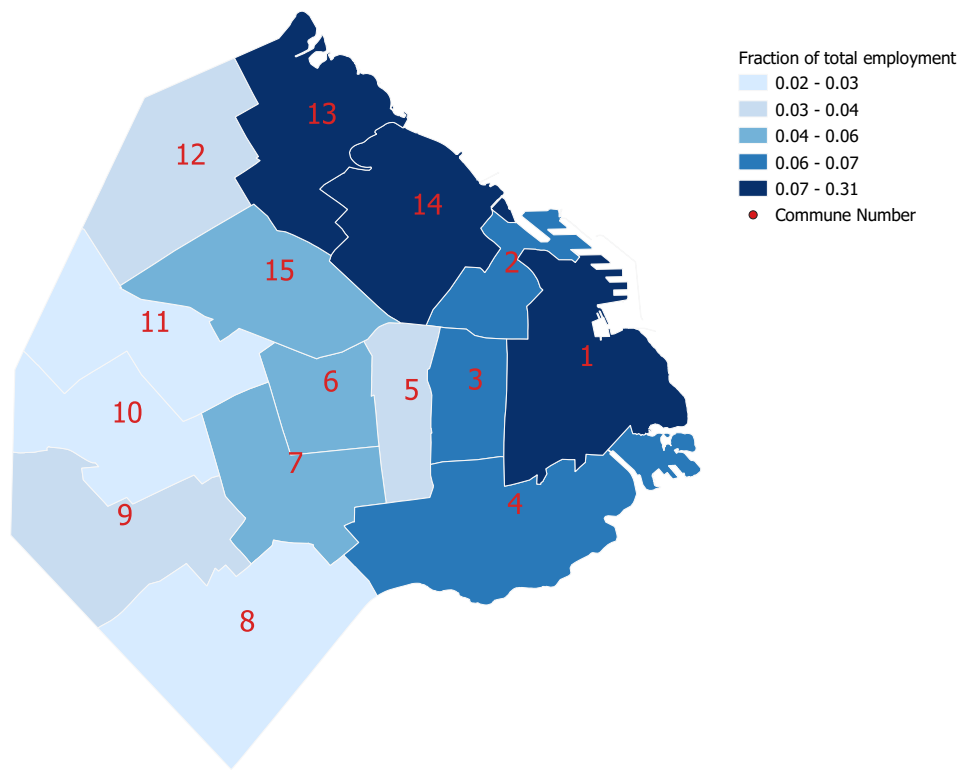


Figure 1: Fraction of total employment population by commune.

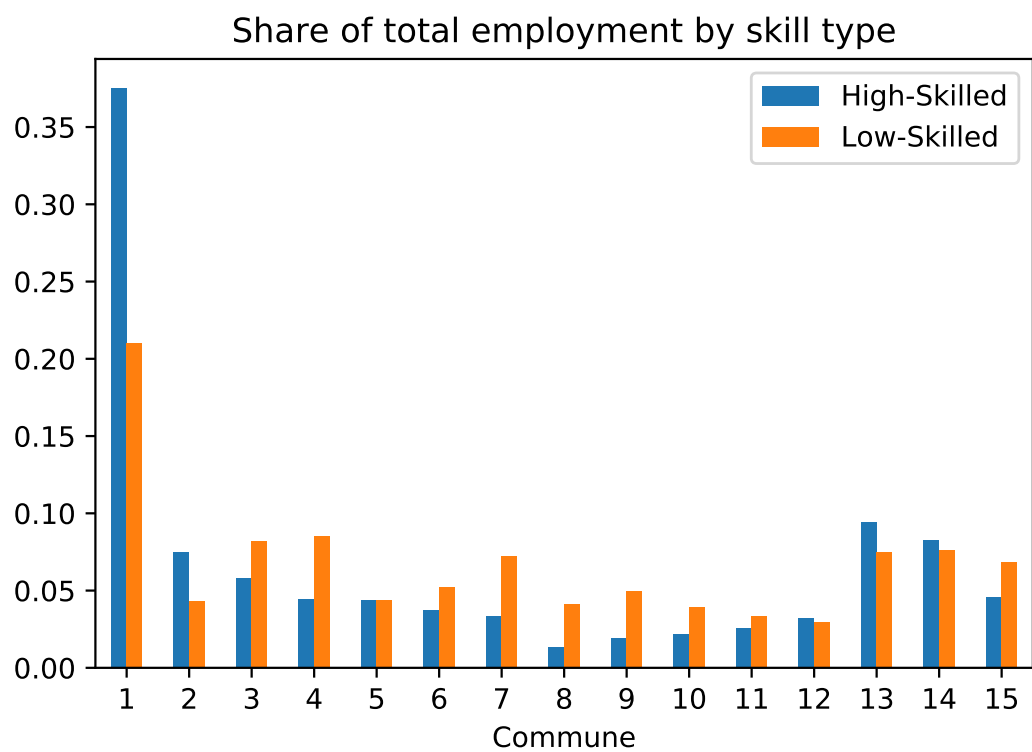


Figure 2: Share of total employment by skill type for each commune.

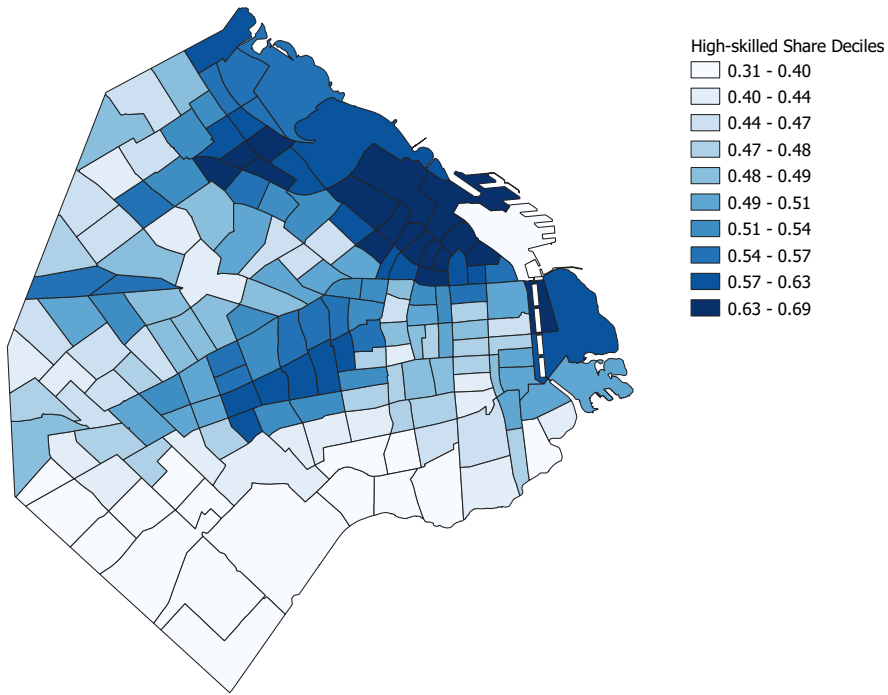


Figure 3: Share of high-skilled residents living in each district in 2011.

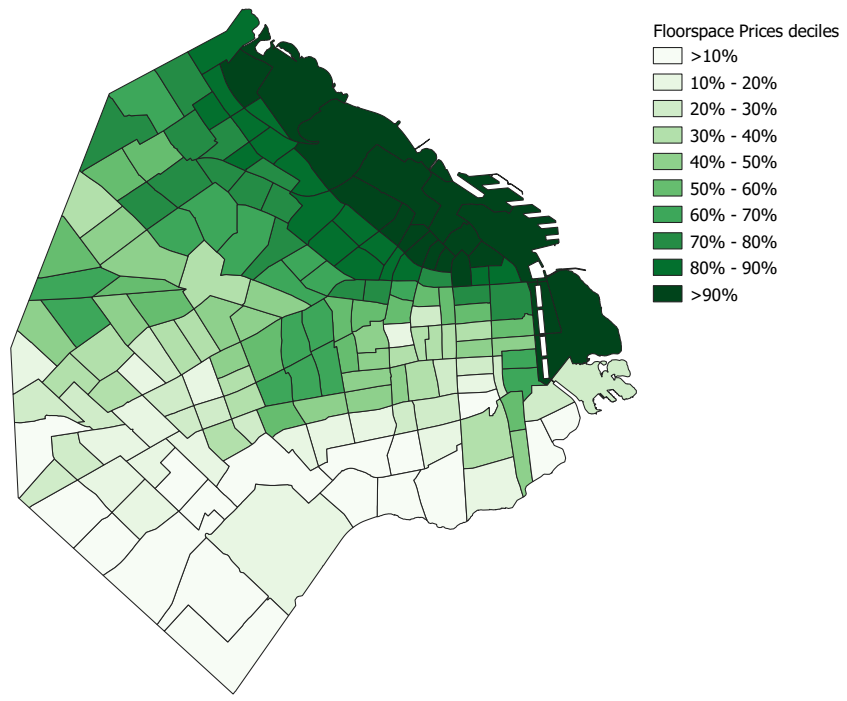


Figure 4: Percentiles of floorspace prices, calculated as the average sale price per square meter, by district in 2011.

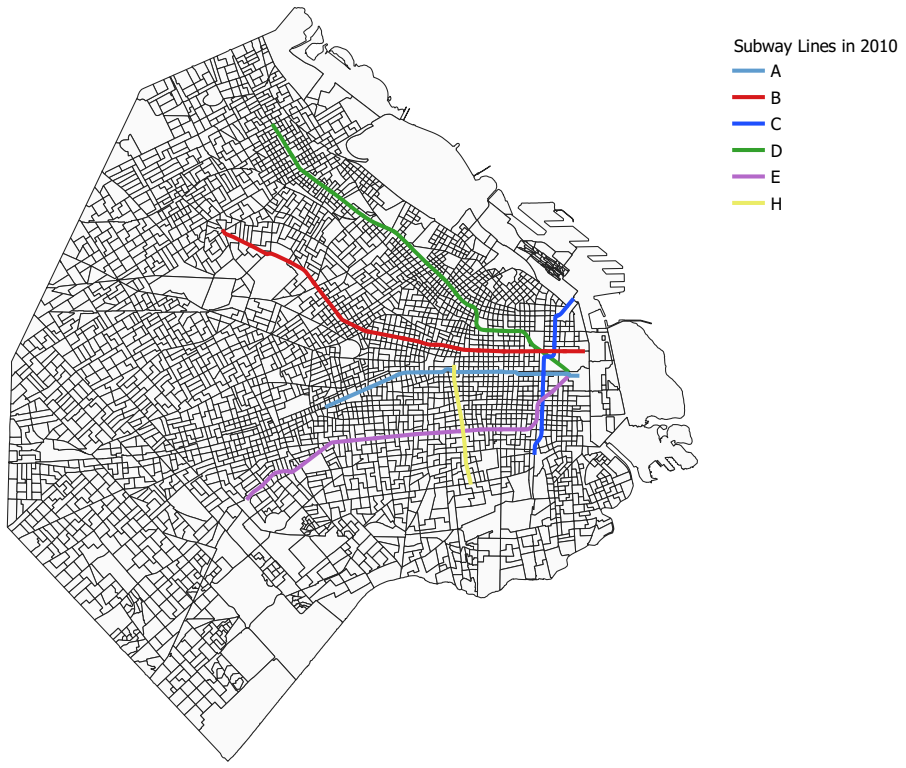


Figure 5: Subway lines built up to 2010 in the city of Buenos Aires.

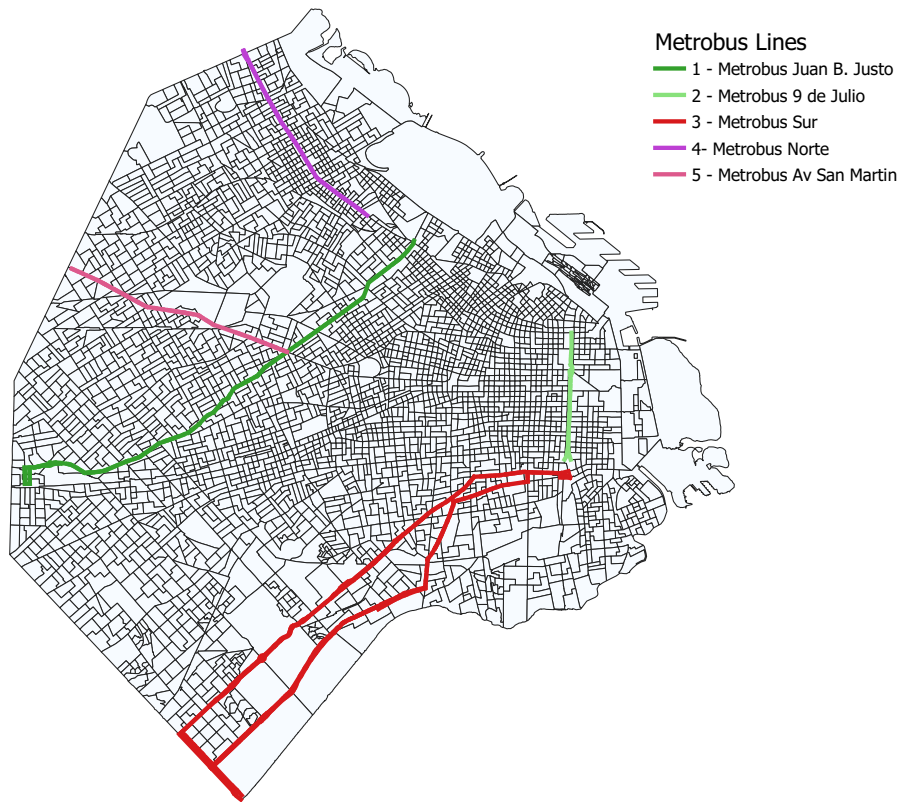


Figure 6: *Metrobus* lines built between 2011 and 2017 in the city of Buenos Aires, numbered by the order in which they were constructed.

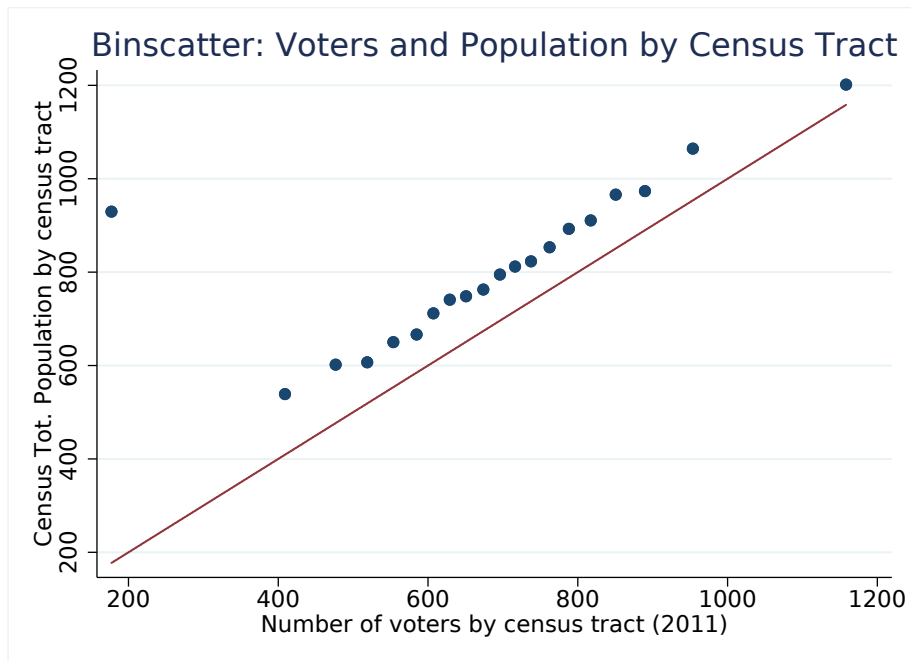


Figure 7: Binscatter of the 2010 census population by census tract compared to the number of geocoded voters by census tract. The red line is a 45 degree line.

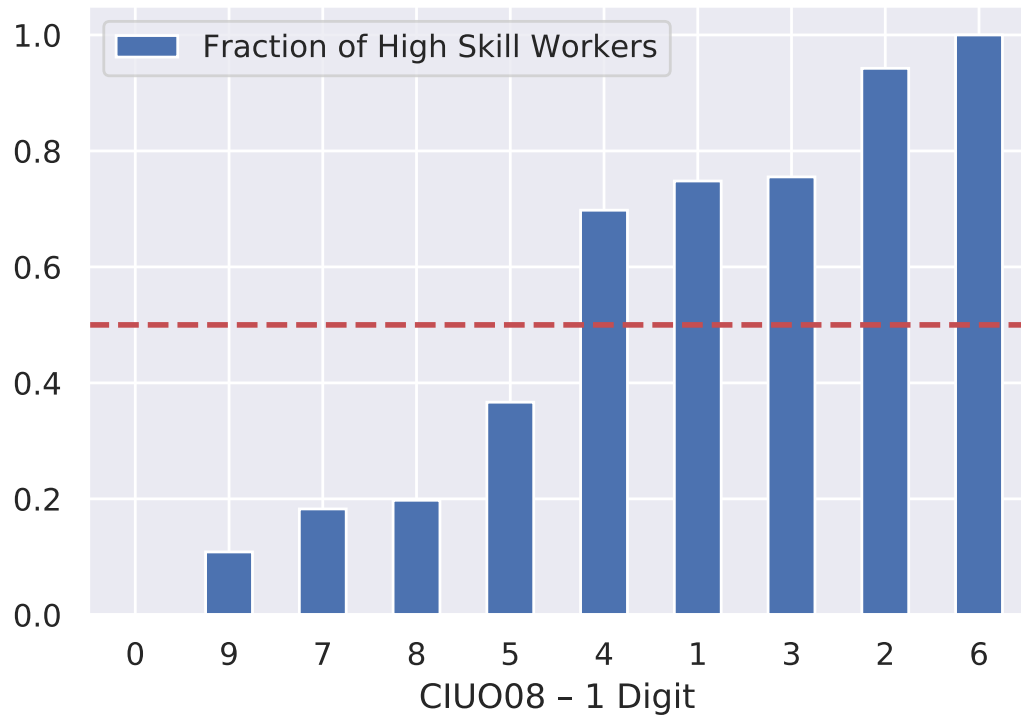


Figure 8: High-skill share by occupations at 1 digit ISCO classification in 2011. Calculated from the first-trimester wave of the National Household Survey (*Encuesta Permanente de Hogares*) in 2011.

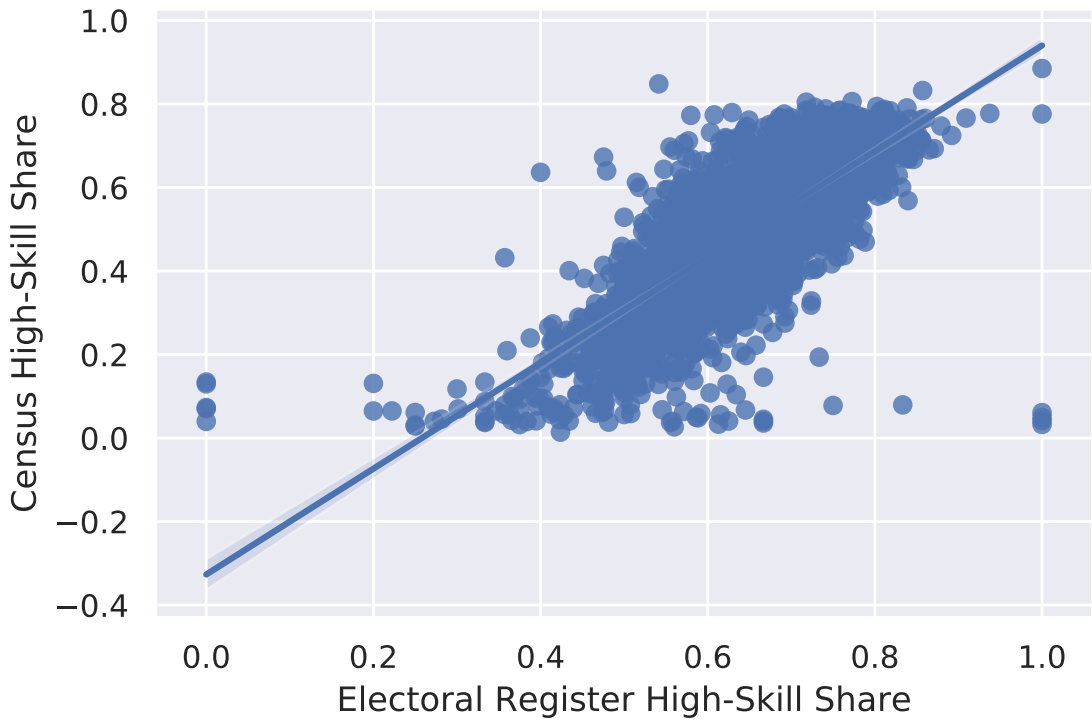


Figure 9: High-skilled share in 2010 census versus electoral register data in 2011. Regression at the census tract level of high-skilled share observed in the 2010 census on the high-skilled share measure constructed from the individual level data from the 2011 electoral register. The slope of the regression line is 1.2, and is significant at a 1% level. The R-squared of the regression is 0.6.

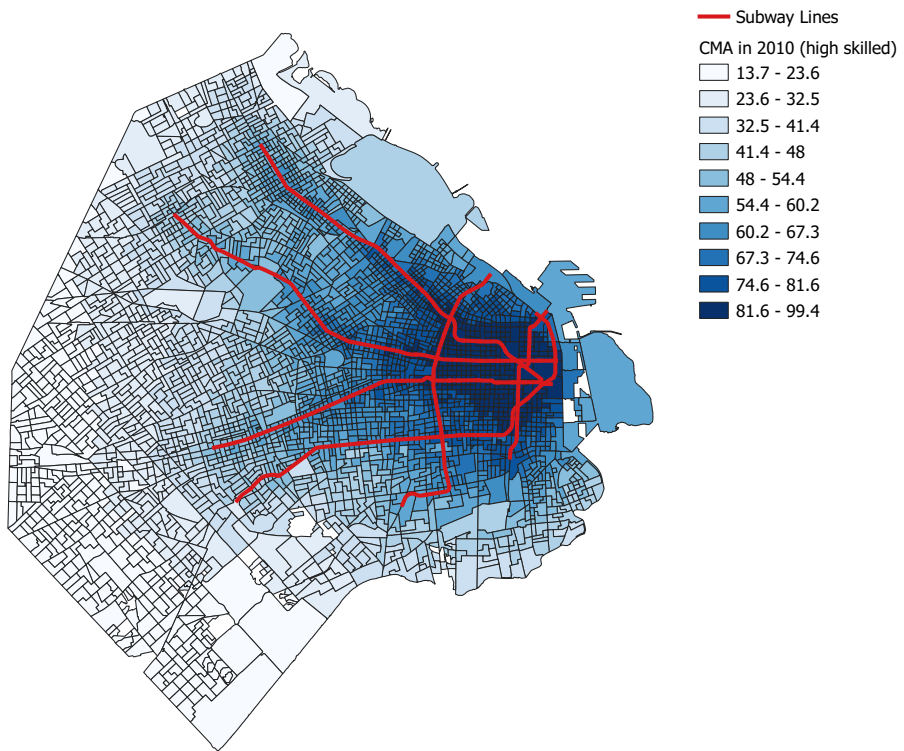


Figure 10: Commuter Market Access of high-skilled workers in 2011.

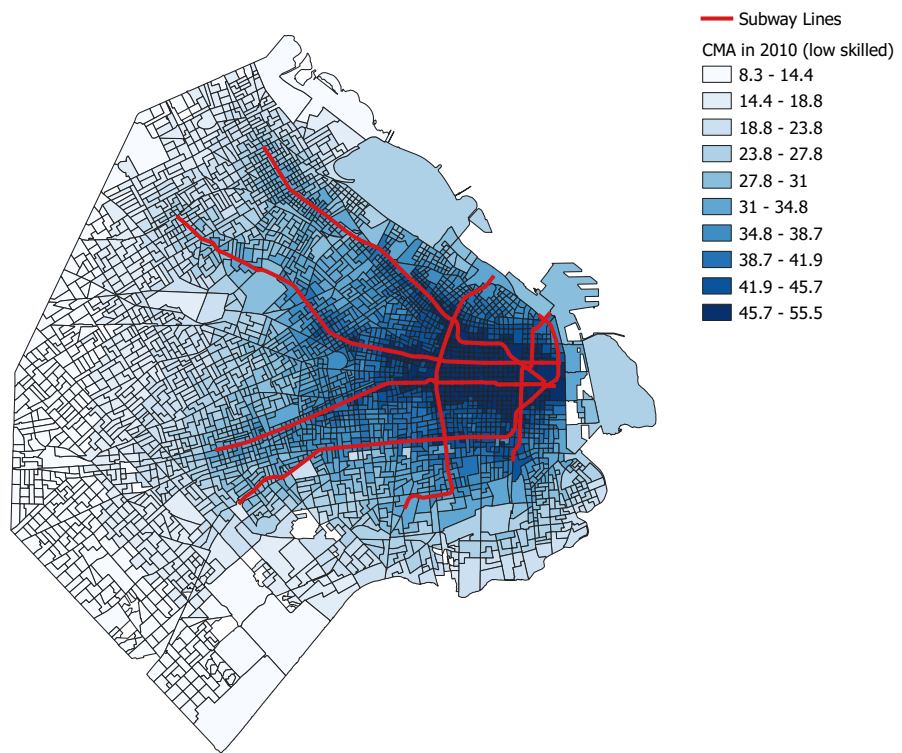


Figure 11: Commuter Market Access of low-skilled workers in 2011.

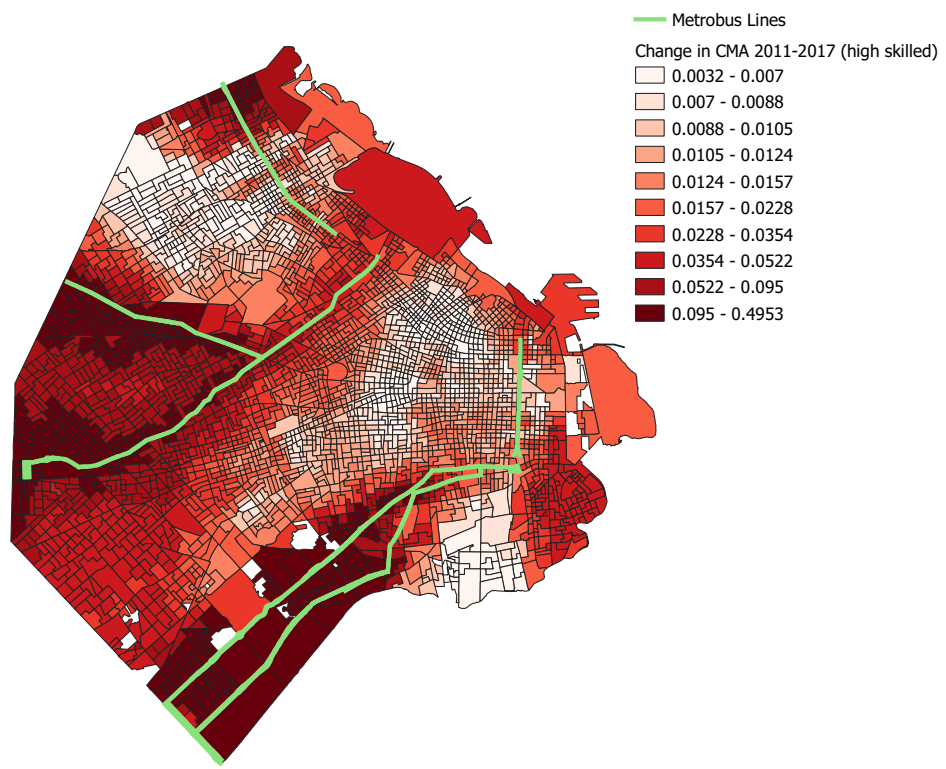


Figure 12: Proportional change in Commuter Market Access for high-skilled workers between 2011 and 2017.

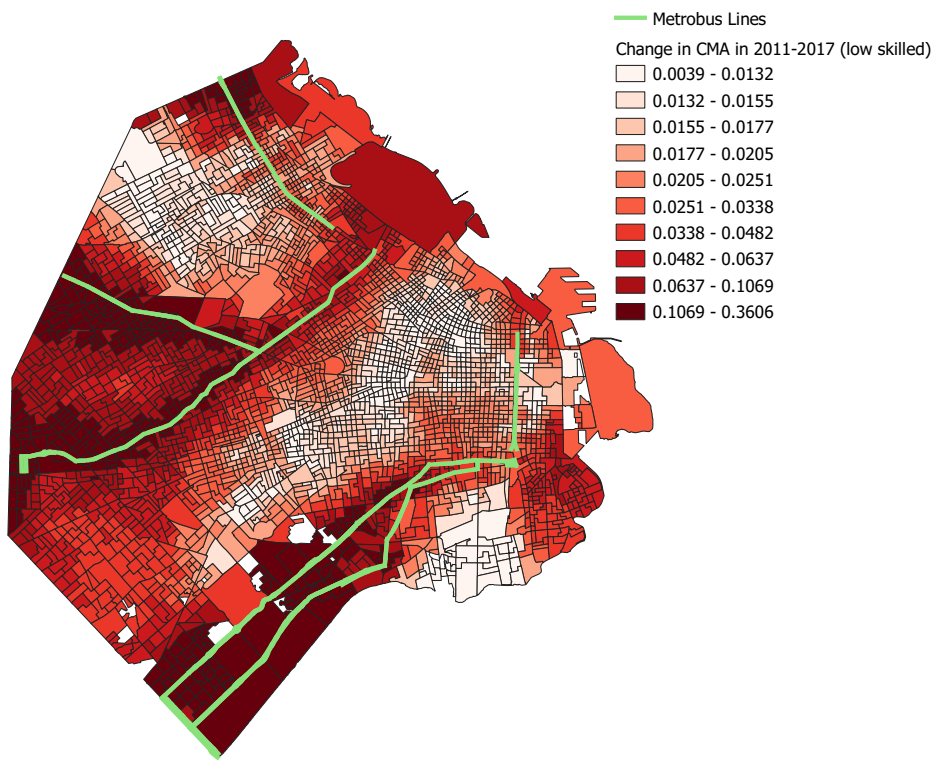


Figure 13: Proportional change in Commuter Market Access for low-skilled workers between 2011 and 2017.

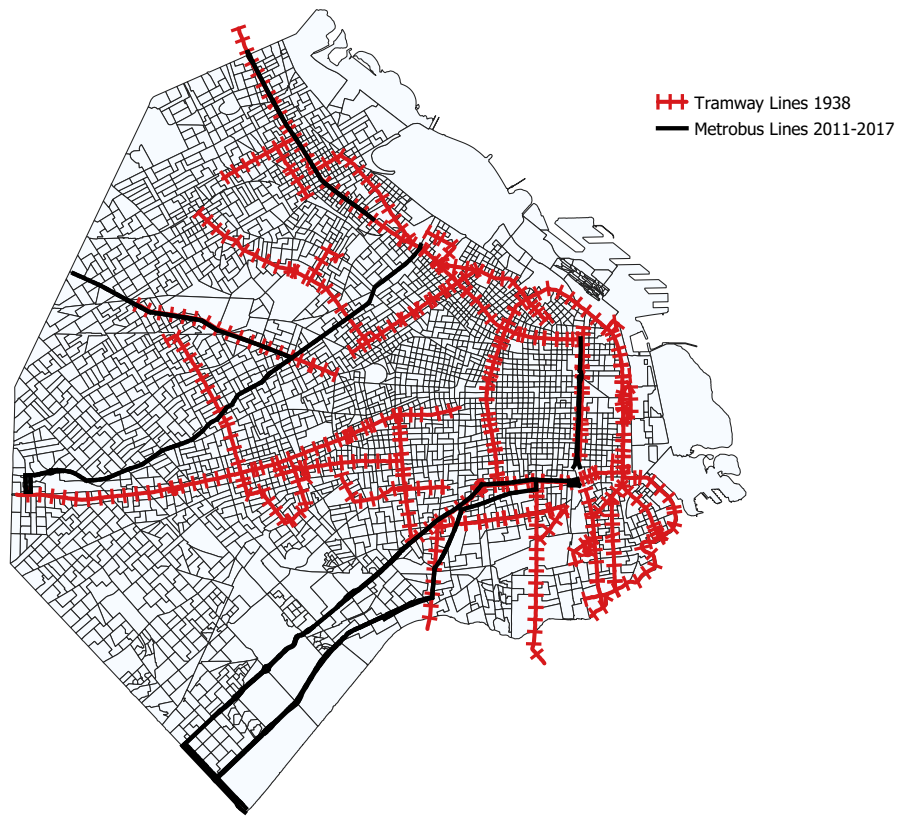


Figure 14: Tramway lines running through two-way avenues in 1938, and *Metrobus* BRT lines built up to 2017.

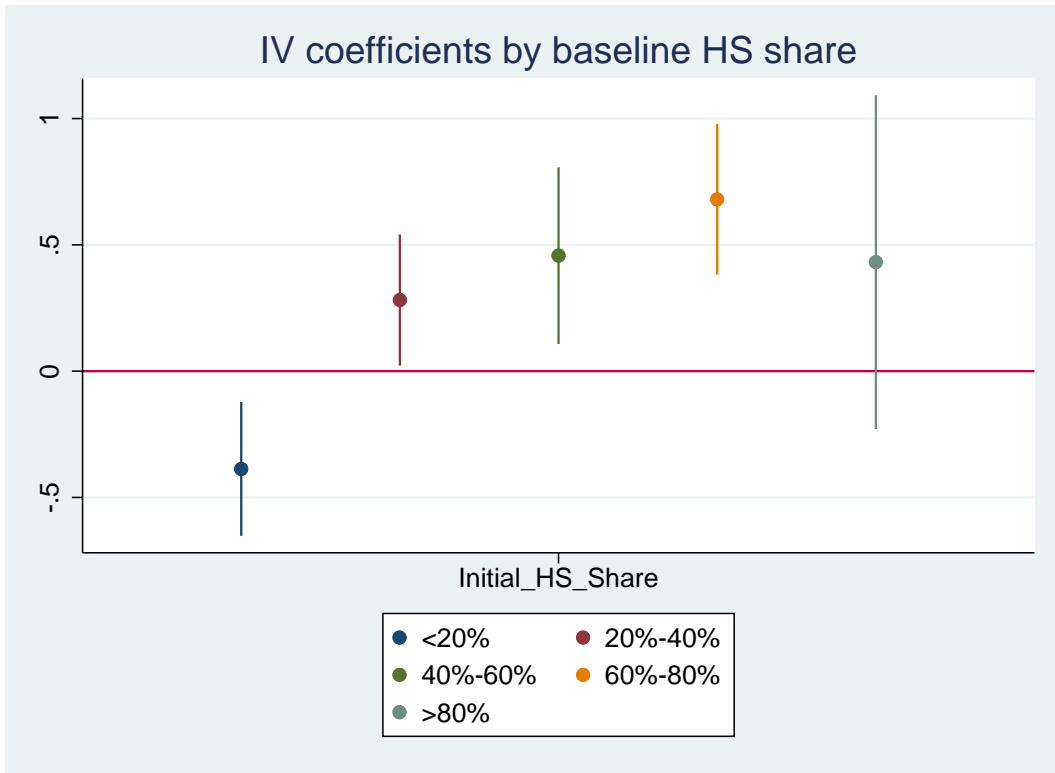


Figure 15: Coeff. of regressing $\Delta \log(\text{hs_share})$ on $\Delta \log(CMA)$ for census tracts in different parts of the distribution of initial HS share of contiguous census tracts.

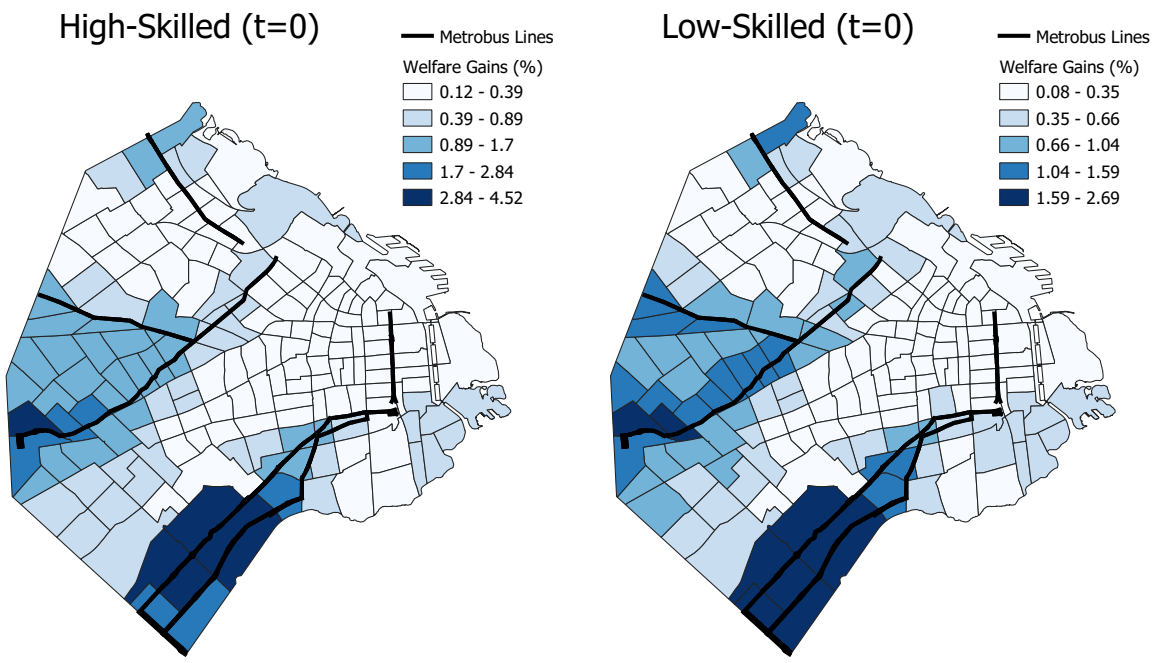


Figure 16: Average welfare gains (in percentage terms) for high-skilled and low-skilled incumbents at $t = 0$ by district.

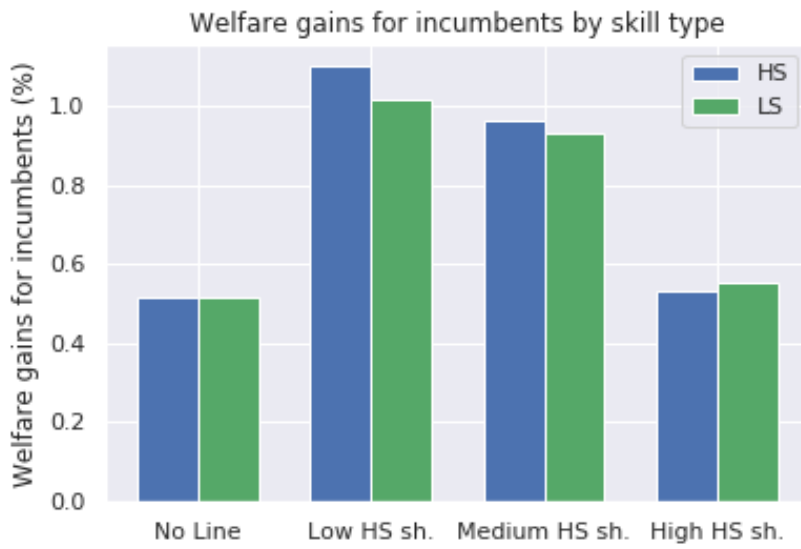


Figure 17: Average welfare gains for incumbent residents at $t = 0$ by line group and skill type.

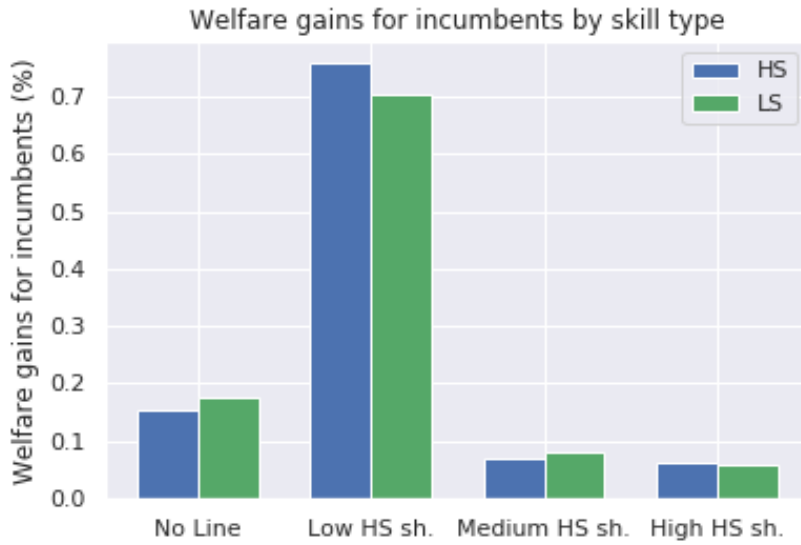


Figure 18: Average welfare gains for incumbent residents at $t = 0$ by line group and skill type in the counterfactual scenario where only the southern line that goes through the districts with the lowest high-skilled share is built.

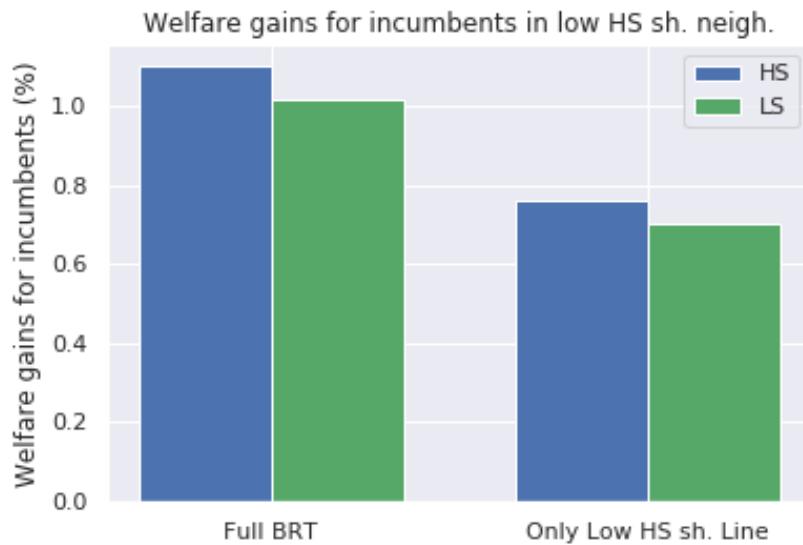


Figure 19: Comparison of welfare gains for each skill type between model with full BRT, and model where only the southern line that goes through the districts with the lowest high-skilled share is built.

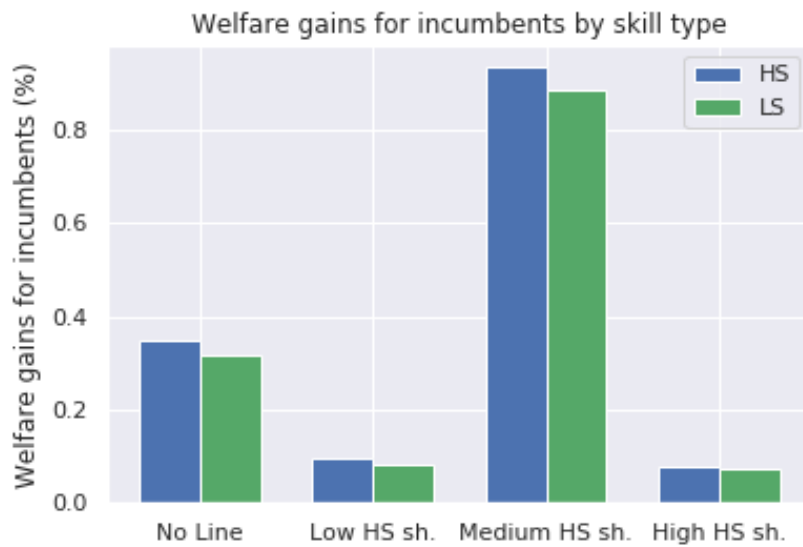


Figure 20: Average welfare gains for incumbent residents at $t = 0$ by line group and skill type in the counterfactual scenario where only the lines that go through the districts with the medium level of high-skilled share are built.

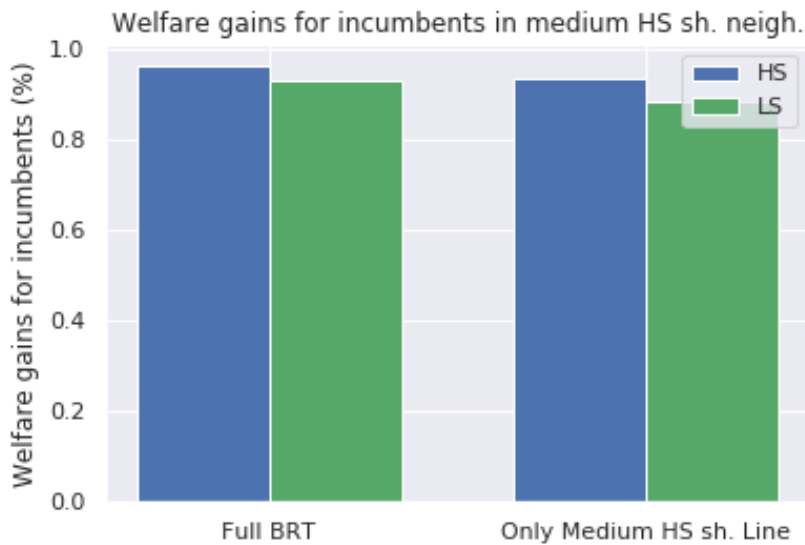


Figure 21: Comparison of welfare gains for each skill type between model with full BRT, and model where only the lines that go through the districts with the medium level of high-skilled share are built.

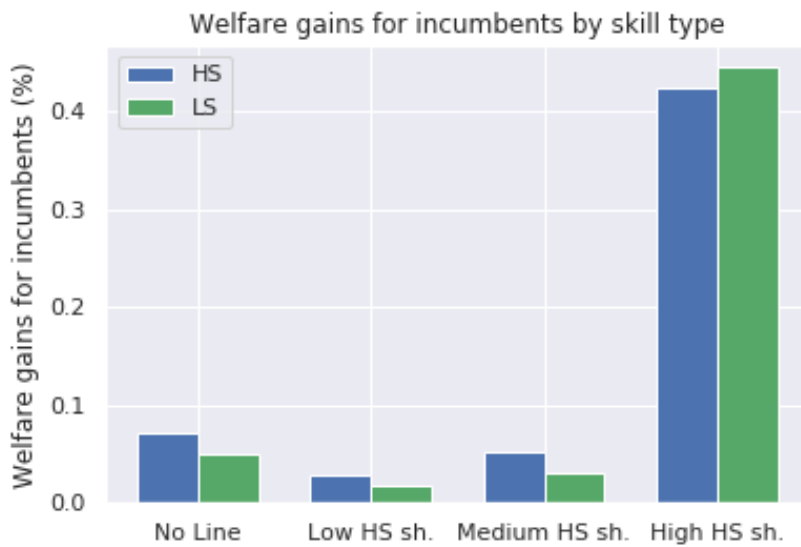


Figure 22: Average welfare gains for incumbent residents at $t = 0$ by line group and skill type in the counterfactual scenario where only the line that goes through the districts with the highest high-skilled share is built.

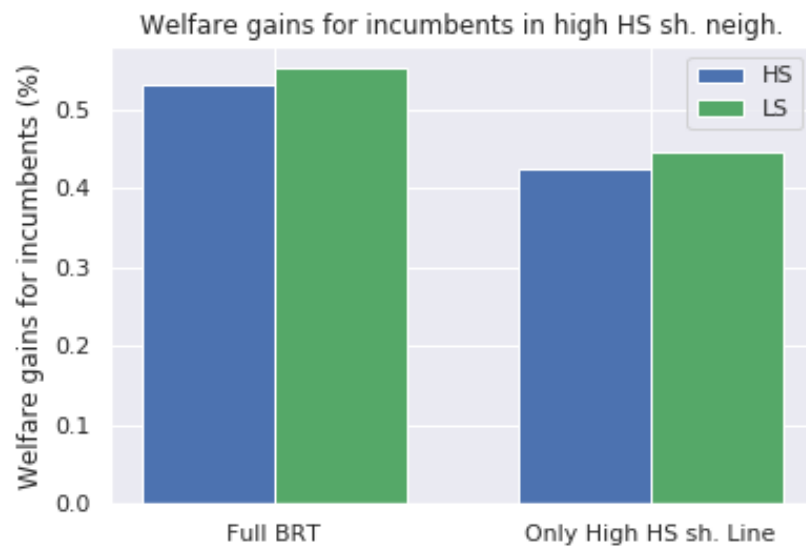


Figure 23: Comparison of welfare gains for each skill type between model with full BRT, and model where only the line that goes through the districts with the highest high-skilled share is built.

A Data Appendix

A.1 Electoral Register Data

The electoral register (*padrón electoral*) for the city of Buenos Aires contains information on each citizen eligible for voting⁶¹ that resides in the city of Buenos Aires, which amounts to approximately 2.5 million individuals.⁶² This register contains the full name, sex of birth, year of birth, national ID number, residential address, and a description of occupation.⁶³ I use the full name, national ID number, and sex of birth to uniquely identify each citizen across registers.⁶⁴ This allows me to merge the 2011, 2013, 2015, and 2017 registers into a panel data set that contains addresses for each individual for every year that they appear in the data set.

A.1.1 Geocoding Observations

I assign geographical coordinates (latitude and longitude) to every street address that can be identified within the electoral register for each year using a combination of two geocoding services, the government of the city of Buenos Aires geocoding API⁶⁵, and the HERE geocoding API.⁶⁶ After extensive string cleaning and normalization, I was able to geocode 139,263 distinct addresses.⁶⁷ I discard government addresses and police stations, which are often used to provide an address for people who do not have a fixed residential address.⁶⁸ Finally, close to 5% of the individuals in the data set had residential addresses that could not be geocoded. Most of these individuals live in informal settlements, and therefore do not have standardized addresses that could be interpreted by the geocoding services. In the end, I obtain geocoded addresses that give me the street level location of the residential address for 2,382,326 individuals in 2011, 2,438,693 individuals in 2013, 2,446,541 individuals in 2015, and 2,461,564 individuals in 2017.

⁶¹Every Argentine citizen over 18 years of age was eligible for voting in 2011. Starting in the 2013 elections, eligibility was extended to all citizens over 16 years of age. Since I restrict myself to a balanced panel of individuals that can be tracked between 2011 and 2017, I don't include individuals that are less than 18 years of age in 2013.

⁶²The total number of voters registered in the city changes by less than 1% between 2011 and 2017.

⁶³This description of occupation was only available in the 2011 register, so I don't have any time-series variation on occupation by individual.

⁶⁴The national ID number and sex of birth are enough to uniquely identify 98% of the observations, for the remaining observations I use the full name to supplement the merging procedure.

⁶⁵Available here: <https://usig.buenosaires.gob.ar/apis/>

⁶⁶Available here: <https://developer.here.com/products/geocoding-and-search>

⁶⁷These addresses do not contain the exact apartment number for multi-family residential buildings.

⁶⁸Keeping these addresses does not change the main results of the paper, but increases the population substantially in certain census tracts in 2011 relative to the population observed in the 2010 census.

A.1.2 Classifying Occupations

The electoral register for the year 2011 includes a variables that describes the occupation of each person in the register. These descriptions were grouped into 4522 distinct occupations, which were then classified manually into one of the ten one-digit groups from the International Standard Classification of Occupations (ISCO). In order to guarantee the quality of the classification, I only classified occupations when it was clear they belonged to a group, and when the original description was informative. Slightly more than half of the sample (1,305,217) had an occupation value of “student” (*estudiante* in Spanish). I decided to drop these individuals from my main analysis, since it wasn’t clear what occupation or education level they might have. For another 399,185 individuals, no occupation was listed. In total, I was able to reliably identify an occupation for 607,775 individuals. I will track these individuals through time in order to construct the migration probabilities that will be used in the estimation of the model.

A.2 Construction of Employment Measure by District

The city’s Annual Household Survey (*Encuesta Anual de Hogares*) allows me to calculate a measure of employment by skill type by commune. However, there are only 15 communes within the city, and, in order to capture changes in market access, it is convenient to have a smaller measure of employment at a smaller spatial unit.⁶⁹ In order to obtain a measure of employment at the district level,⁷⁰ I combine the measure of employment at the commune level with the land use map from 2010-2011 by skill type (L_c^g). I use the land use map to count the number of plots in each commune that are used for commercial or productive uses (l_c^g), I then count the number of plots in each district, within a commune, that are used for commercial or productive uses ($l_{v,c}^g$). With these three measures, I estimate the employment by skill type as

$$L_{v,C} = L_C \times \frac{l_{v,C}}{l_C}.$$

The underlying assumption is that workers of a given skill type within a commune are distributed between districts in proportion to the fraction of the total land used for commercial and productive uses in the commune that is in that district.

A.3 Commute Times

In order to calculate the commute times used in the model τ_{ij} , I create a model of the city’s transport network using ArcMap’s Network Analyst Tool and GIS data on the street grid, the subway lines, the bus lines, the BRT lines, and the above-ground trains. I assign an average speed for subways, trains, buses, and walking within the network based on the average speeds calculated by mode of transport in the 2010

⁶⁹ Alternatively, one could calculate average commute times for different points within a larger spatial unit, and use this average commute time as the commute time from any residential location to an employment location defined at the commune level. Both the reduced form and the quantitative results remain qualitatively similar when employing this alternative method.

⁷⁰There are 167 districts, or an average of 11.13 districts per commune.

commuting survey (*ENMODO*). With this transport network put in place, I estimate commute times as the times for the minimum-time routes between the centroids of each residential location (defined either as a census tract or a district) to the centroid of each employment location (district), where the minimum-time route is calculated using the shortest path Dijkstra algorithm. I first calculate these commute times in a model of the city's transport network that does not include the BRT lines, and then, I add each lines sequentially according the the time they were inaugurated. Once a line or a set of lines have been added, I assume that buses that run through those lines increase their speed according the the increases in speed measures by the City Government, and re-calculate the minimum commute times.

B Supplementary Reduced Form Results

B.1 Reduced Form Results Using Low-Skilled CMA

	$\Delta \log(\text{hs share})$				
	1	2	3	4	5
	OLS	IV	OLS	IV	IV
$\Delta \log(CMA_l)$	-0.024 (0.076)	0.424 (0.088)***	-2.634 (0.646)***	-1.088 (0.708)	-2.450 (1.369)*
hs share_0	0.224 (0.037)***	0.362 (0.047)***	0.170 (0.085)**	0.237 (0.071)***	0.157 (0.114)
$\Delta \log(CMA) \times \text{hs sh. avg}_0$			4.362 (0.992)***	2.379 (1.117)**	3.660 (2.111)*
constant	-0.481 (0.025)***	-0.591 (0.033)***	-0.457 (0.058)***	-0.508 (0.048)***	-0.400 (0.078)***
Neigh. FE	NO	NO	NO	NO	YES
N	2,282	2,282	2,282	2,282	2,282

* $p < 0.1$; ** $p < 0.05$; *** $p < 0.01$

Table B.1: Reduced Form Results: regressions of change in high skill share between 2011 and 2017 on change in market access for low-skilled workers between 2011 and 2017, initial average high skill share for contiguous census tracts, and the interaction term. The instrument used for the IV regressions is a measure of change of $\log CMA_l$ where the 2017 CMA_l is calculated assuming the BRT lines were built following the 1938 tramway lines. Cragg-Donald Wald F statistics from the first stage regression are reported for each IV estimation. Robust standard errors in parentheses. * $p < 0.10$, ** $p < 0.05$, *** $p < 0.01$.

	$\Delta \log(\text{floorspace price})$				
	1 OLS	2 IV	3 OLS	4 IV	5 IV
$\Delta \log(CMA_l)$	-0.178 (0.107)*	0.470 (0.078)***	-4.609 (1.150)***	-1.871 (1.246)	-5.907 (1.659)***
hs share ₀	0.125 (0.057)**	0.325 (0.079)***	-0.202 (0.070)***	0.132 (0.086)	-0.528 (0.119)***
$\Delta \log(CMA) \times \text{hs sh. avg}_0$			7.375 (1.781)***	3.684 (1.932)*	10.021 (2.495)***
constant	0.071 (0.037)*	-0.088 (0.053)*	0.277 (0.048)***	0.041 (0.059)	0.392 (0.078)***
Neigh. FE	NO	NO	NO	NO	YES
N	2,282	2,282	2,282	2,282	2,282

* $p < 0.1$; ** $p < 0.05$; *** $p < 0.01$

Table B.2: Reduced Form Results: regressions of change in floorspace prices between 2011 and 2017 on change in market access for low-skilled workers between 2011 and 2017, initial average high skill share for contiguous census tracts, and the interaction term. The instrument used for the IV regressions is a measure of change of $\log CMA_l$ where the 2017 CMA_l is calculated assuming the BRT lines were built following the 1938 tramway lines. Floorspace prices are calculated as the average sale price per square meter, according to geo-referenced online asking price data for the city of Buenos Aires. Cragg-Donald Wald F statistics from the first stage regression are reported for each IV estimation. Robust standard errors in parentheses. * $p < 0.10$, ** $p < 0.05$, *** $p < 0.01$.

C Theory Appendix

C.1 Derivation of Value Function

In this section I show how to go from equation (6) to equation (7). Consider

$$V_{n,t}^g = E_0 \left[\max_{\{i\}} \left\{ \frac{w_{j,t}^g \varepsilon_{j,t}}{d_{ij,t}} \right\} \right] + E_0 \left[\max_{\{j\}} \left\{ \beta V_{i,t+1}^g - \mu_{ni}^g + \eta_{i,t}^g \right\} \right].$$

I will first show that

$$E_0 \left[\max_{\{i\}} \left\{ \frac{w_{j,t}^g \varepsilon_{j,t}}{d_{ij,t}} \right\} \right] = \tilde{T} \Phi_{Rn,t}^{\frac{1}{\theta}}.$$

Let $y_j = \frac{w_j \varepsilon_j}{d_{nj}}$, where I drop the time subscript for clarity. We will assume ε_j is distributed extreme value type II, so that $F(\varepsilon_j) = \exp((-T\varepsilon)^{-\theta})$. Then, the CDF of y_j is

$$\begin{aligned} G_j(y) &= P(y_j \leq y) \\ &= P\left(\frac{w_j \varepsilon_j}{d_{nj}} \leq y\right) \\ &= P\left(\varepsilon_j \leq y \frac{d_{nj}}{w_j}\right) \\ &= e^{-\left(Ty \frac{d_{nj}}{w_j}\right)^{-\theta}}. \end{aligned}$$

Let $\tilde{y} = \max_j\{y_j\}$, then we can define the CDF of \tilde{y} as

$$\begin{aligned} G(y) &= P(\tilde{y} \leq y) \\ &= \prod_{j=1}^J P(y_j \leq y) \\ &= \prod_{j=1}^J \exp\left[\left(\frac{-y}{T^{-1} \frac{w_j}{d_{nj}}}\right)^{-\theta}\right] \\ &= \exp\left[-\sum_{j=1}^J \left(\frac{y}{T^{-1} \frac{w_j}{d_{nj}}}\right)^{-\theta}\right] \\ &= \exp\left[-y^{-\theta} T^{-\theta} \sum_{j=1}^J \left(\frac{w_j}{d_{nj}}\right)^\theta\right] \\ &= \exp\left(-\left(\frac{y}{T^{-1} \left[\sum_{j=1}^J \left(\frac{w_j}{d_{nj}}\right)^\theta\right]^{\frac{1}{\theta}}}\right)^{-\theta}\right). \end{aligned}$$

Which implies that \tilde{y} is distributed Frechet with a shape parameter θ and a scale parameter $T^{-1} \left[\sum_{j=1}^J \left(\frac{w_j}{d_{nj}}\right)^\theta\right]^{\frac{1}{\theta}}$. This implies that the expected value of \tilde{y} is

$$\begin{aligned} E\left(\max_{j=1}^J \left\{\frac{w_j \varepsilon_j}{d_{nj}}\right\}\right) &= E(\tilde{y}) = T^{-1} \Gamma\left(1 - \frac{1}{\theta}\right) \left[\sum_{j=1}^J \left(\frac{w_j}{d_{nj}}\right)^\theta\right]^{\frac{1}{\theta}} \\ &= \tilde{T} \Phi_{Rn}^{\frac{1}{\theta}}. \end{aligned}$$

Where $\tilde{T} = T^{-1} \Gamma\left(1 - \frac{1}{\theta}\right)$, and $\Phi_{Rn} = \sum_{j=1}^J \left(\frac{w_j}{d_{nj}}\right)^\theta$.

For the second term in (6), recall that $\eta_{i,t}^g$ is distributed extreme value type I with parameters $(-\gamma\nu_g, \nu_g)$, where γ is the Euler-Mascheroni constant. Let us define

$$\mathcal{O}_{n,t}^g = E_0 \left[\max_{\{j\}} \{\beta V_{i,t+1}^g - \mu_{ni}^g + \eta_{i,t}^g\} \right].$$

We can rewrite this expression as

$$\begin{aligned} \mathcal{O}_{n,t}^g &= E \left\{ \sum_{i=1}^I \beta V_{i,t+1}^g - \mu_{ni}^g + \eta_{i,t}^g \right\} \times \Pr[(\beta V_{i,t+1}^g - \mu_{ni}^g + \eta_{i,t}^g) \geq \beta V_{m,t+1}^g - \mu_{nm}^g + \eta_{m,t}^g \forall m = 1, \dots, N] \\ &= \sum_{i=1}^I \int (\beta V_{i,t+1}^g - \mu_{ni}^g + \eta_{i,t}^g) f(\eta_{i,t}^g) \times \prod_{m \neq i} F(\beta(V_{i,t+1}^g - V_{m,t+1}^g) - (\mu_{ni}^g - \mu_{nm}^g) + \eta_{i,t}^g) d\eta_{i,t}^g \\ &= \sum_{i=1}^I \int (\beta V_{i,t+1}^g - \mu_{ni}^g + \eta_{i,t}^g) \frac{1}{\nu_g} \exp\left(\frac{\eta_{i,t}^g}{\nu_g} - \gamma\right) \times \\ &\quad \times \exp\left(-\sum_{i=1}^I \exp\left(-\frac{\beta(V_{i,t+1}^g - V_{m,t+1}^g) - (\mu_{ni}^g - \mu_{nm}^g) + \eta_{i,t}^g}{\nu_g} - \gamma\right)\right) d\eta_{i,t}^g. \end{aligned}$$

Where the last step used the fact that the pdf of $\eta_{i,t}^g$ is

$$f(x) = \frac{1}{\nu_g} \exp\left(-\frac{x}{\nu_g} - \gamma - \exp\left(-\frac{x}{\nu_g} - \gamma\right)\right)$$

and the CDF of $\eta_{i,t}^g$ is

$$F(x) = \exp\left(-\exp\left(-\frac{x}{\nu_g} - \gamma\right)\right).$$

Let us define $b_{i,t}^g = \frac{\eta_{i,t}^g}{\nu_g} + \gamma$, $a_{im,t}^g = \frac{\beta(V_{i,t+1}^g - V_{m,t+1}^g) - (\mu_{ni}^g - \mu_{nm}^g) + \eta_{i,t}^g}{\nu_g}$, $\tilde{a}_{i,t}^g = \ln \sum_{m=1}^I \exp(a_{im,t}^g)$, and $\tilde{b}_{i,t}^g = b_{i,t}^g - \tilde{a}_{i,t}^g$. First consider the change of variables using $b_{i,t}^g$:

$$\begin{aligned} \mathcal{O}_{n,t}^g &= \sum_{i=1}^I \int (\beta V_{i,t+1}^g - \mu_{ni}^g + \nu_g(b_{it}^g - \gamma)) \exp\left(-b_{i,t}^g - \sum_{i=1}^I \exp(a_{im,t}^g - b_{i,t}^g)\right) db_{i,t}^g \\ &= \sum_{i=1}^I \int (\beta V_{i,t+1}^g - \mu_{ni}^g + \nu_g(b_{it}^g - \gamma)) \exp(-b_{i,t}^g - \exp(-(b_{i,t}^g - \tilde{a}_{i,t}^g))) db_{i,t}^g. \end{aligned}$$

Doing a second change of variables using $\tilde{b}_{i,t}^g$ we obtain:

$$\mathcal{O}_{n,t}^g = \sum_{i=1}^I \exp(\tilde{a}_{i,t}^g) (\beta V_{i,t+1}^g - \mu_{ni}^g + \nu_g(\tilde{a}_{it}^g - \gamma)) + \nu_g \int \tilde{b}_{i,t}^g \exp(-\tilde{b}_{i,t}^g - \exp(-\tilde{b}_{i,t}^g)) d\tilde{b}_{i,t}^g.$$

Using the fact that $\gamma = \int x \exp(-x - \exp(-x))$, we obtain

$$\mathcal{O}_{n,t}^g = \sum_{i=1}^I \exp(\tilde{a}_{i,t}^g) (\beta V_{i,t+1}^g - \mu_{ni}^g + \nu_g \tilde{a}_{it}^g).$$

Substituting in for $\tilde{a}_{i,t}^g$, we find that

$$\mathcal{O}_{n,t}^g = \nu_g \ln \sum_{i=1}^I (\exp(\beta V_{i,t+1}^g - \mu_{ni}^g))^{\frac{1}{\nu_g}}.$$

Combining the first and second term, we arrive at equation (7).

C.2 Deriving Neighborhood Migration Flows

Let $m_{in,t}^g$ be the fraction of residents of type g that are residing in location n at the beginning of period t , and move to location i by the end of period t . Since there is a continuum of agents in each residential location at any time t , we can apply the strong law of large numbers and express this fraction as the probability that any worker living in location n chooses to move to location i at the end of time t , or

$$\begin{aligned} m_{in,t}^g &= P [(\beta V_{i,t+1}^g - \mu_{in} + \eta_{i,t}^g) \geq (\beta V_{m,t+1}^g - \mu_{mn}^g + \eta_{m,t}^g) \forall m = 1, \dots, N] \\ &= \int_{-\infty}^{\infty} f(\eta_{i,t}^g) \prod_{m \neq i} F(\beta(V_{i,t+1}^g - V_{m,t+1}^g) - (\mu_{in}^g - \mu_{mn}^g) + \eta_{i,t}^g) d\eta_{i,t}^g. \end{aligned}$$

Let $z_{im,t}^g = \beta(V_{i,t+1}^g - V_{m,t+1}^g) - (\mu_{in}^g - \mu_{mn}^g)$, then

$$\begin{aligned} m_{in,t}^g &= \int_{-\infty}^{\infty} f(\eta_{i,t}^g) \prod_{m \neq i} F(z_{im,t}^g + \eta_{i,t}^g) d\eta_{i,t}^g \\ &= \int \frac{1}{\nu} \left(\frac{-\eta_{i,t}^g}{\nu_g} - \gamma - \exp\left(\frac{-\eta_{i,t}^g}{\nu_g} - \gamma\right) \right) \prod_{m \neq i} \exp\left(-\exp\left(\frac{-z_{im,t}^g}{\nu_g} - \frac{\eta_{i,t}^g}{\nu_g} - \gamma\right)\right) d\eta_{i,t}^g \\ &= \int \frac{1}{\nu_g} \exp\left(\frac{-\eta_{i,t}^g}{\nu_g} - \gamma\right) \prod_{m \neq i} \exp\left(-\exp\left(\frac{-z_{im,t}^g}{\nu_g} - \frac{\eta_{i,t}^g}{\nu_g} - \gamma\right)\right) d\eta_{i,t}^g \\ &= \int \frac{1}{\nu_g} \exp\left(\frac{-\eta_{i,t}^g}{\nu_g} - \gamma\right) \exp\left(-\sum_{m=1}^N \exp\left(\frac{-z_{im,t}^g}{\nu_g} - \frac{\eta_{i,t}^g}{\nu_g} - \gamma\right)\right) d\eta_{i,t}^g. \end{aligned}$$

Define $\lambda_t^g = \log\left(\sum_{m=1}^N \exp\left(\frac{-z_{im,t}^g}{\nu_g}\right)\right)$, $x_t^g = \frac{\eta_{i,t}^g}{\nu_g} + \gamma$, $y_t^g = x_t^g - \lambda_t^g$. Note that

$$\frac{dx_t^g}{d\eta_{i,t}^g} = \frac{1}{\nu_g} \Rightarrow d\eta_{i,t}^g = \nu_g dx_t^g,$$

$$\text{and } \frac{dy_t^g}{d\eta_{i,t}^g} = \frac{dx_t^g}{d\eta_{i,t}^g} \Rightarrow dy_t^g = dx_t^g.$$

Therefore, we can rewrite $m_{in,t}^g$ as

$$\begin{aligned}
m_{in,t}^g &= \int_{-\infty}^{\infty} \frac{1}{\nu_g} \exp(-x_t^g) \exp(-\exp(\lambda_t^g) \exp(-x_t^g)) \nu_g dx_t^g \\
&= \int \exp(-y_t^g - \lambda_t^g) \exp(-\exp(\lambda_t^g) \exp(-y_t^g - \lambda_t^g)) dy_t^g \\
&= \exp(\lambda_t^g) \int \exp(-y_t^g - \exp(y_t^g)) dy_t^g \\
&= \exp(-\lambda_t^g) [\exp(-\exp(y_t^g))] |_{-\infty}^{\infty} \\
&= \exp(-\lambda_t^g) \\
&= \frac{1}{\sum_{m=1}^n \exp\left(\frac{-z_{in,t}^g}{\nu_g}\right)} \\
&= \frac{1}{\sum_{m=1}^n \exp\left[\frac{1}{\nu_g}(-\beta(V_{i,t+1}^g - V_{m,t+1}^g) + (\mu_{in}^g - \mu_{mn}^g)\right]} \\
&= \frac{[\exp(\beta V_{i,t+1}^g - \mu_{in}^g)]^{\frac{1}{\nu_g}}}{\sum_{m=1}^n [\exp((\beta V_{m,t+1}^g) - \mu_{mn}^g)]^{\frac{1}{\nu_g}}}.
\end{aligned}$$

C.3 Deriving Labor Demand

From the first order conditions of the producers problem, we know that

$$w_{j,t}^h \tilde{L}_{Fj,t}^h = (1 - \rho_j) X_{jt},$$

$$w_{j,t}^l \tilde{L}_{Fj,t}^l = \rho_j X_{jt}.$$

Where X_{jt} is the total expenditure on variety j at time t . From the CES demand for varieties of the consumption good, we know that in equilibrium $X_{jt} = p_{jt}^{1-\sigma} X$, where $X = \sum_{i=1}^I \alpha \sum_{g \in \{h,l\}} \bar{y}_{igt}$ is the total expenditure on consumption in the economy, and \bar{y}_{igt} is the mean income of a worker of type g in location i at time t . Perfect competition will imply that the price of each variety is equal to its marginal cost at each time t , $p_{jt} = A_j^{-1} (w_{jt}^l)^{\rho_j} (w_{jt}^h)^{(1-\rho_j)}$. Combining these results and re-arranging terms we get

$$\tilde{L}_{Fj,t}^l = \frac{\rho_j}{w_j^l} \left(\frac{(w_j^l)^{\rho_j} (w_j^h)^{(1-\rho_j)}}{A_j} \right)^{(1-\sigma)} \sum_i \sum_g \alpha \tilde{T}_g \left(\sum_s \left(\frac{w_s^g}{d_{is}} \right)^{\theta_g} \right)^{\frac{1}{\theta_g}} L_{Ri,t}^g, \quad (34)$$

$$\tilde{L}_{Fj,t}^h = \frac{1 - \rho_j}{w_j^h} \left(\frac{(w_j^l)^{\rho_j} (w_j^h)^{(1-\rho_j)}}{A_j} \right)^{(1-\sigma)} \sum_i \sum_g \alpha \tilde{T}_g \left(\sum_s \left(\frac{w_s^g}{d_{is}} \right)^{\theta_g} \right)^{\frac{1}{\theta_g}} L_{Ri,t}^g. \quad (35)$$

Let $\mathbf{w}_t = \{\{w_{jt}^h\}_{j=1}^J, \{w_{jt}^l\}_{j=1}^J\}$, note that the right-hand side of equations 34 and 35 depends on \mathbf{w}_t , the residential population vector for high- and low-skilled workers at time t (which is assumed to be known to the producer at time t), and known parameters. Therefore, we can define

$$f_{jlt}(\mathbf{w}_t) = \frac{\rho_j}{w_j^l} \left(\frac{(w_j^l)^{\rho_j} (w_j^h)^{1-\rho_j}}{A_j} \right)^{(1-\sigma)} \sum_i \sum_g \alpha \tilde{T}_g \left(\sum_s \left(\frac{w_s^g}{d_{is}} \right)^{\theta_g} \right)^{\frac{1}{\theta_g}} L_{Ri,t}^g, \quad (36)$$

$$f_{jht}(\mathbf{w}_t) = \frac{1-\rho_j}{w_j^h} \left(\frac{(w_j^l)^{\rho_j} (w_j^h)^{1-\rho_j}}{A_j} \right)^{(1-\sigma)} \sum_i \sum_g \alpha \tilde{T}_g \left(\sum_s \left(\frac{w_s^g}{d_{is}} \right)^{\theta_g} \right)^{\frac{1}{\theta_g}} L_{Ri,t}^g. \quad (37)$$

C.4 Deriving Average Match Productivity

Consider

$$\begin{aligned} \bar{\varepsilon}_{jt}^g &= E[\varepsilon|g, t, \text{ choose j}] \\ &= \sum_{i=1}^I E[\varepsilon|g, t, \text{ choose j if living in i}] Pr(i|j, g, t) \\ &= \sum_{i=1}^I T_g \Pi_{j|git}^{-\frac{1}{\theta_g}} \frac{1}{d_{ij,t}} Pr(i|j, g, t). \end{aligned}$$

Where the last equality comes from the properties of ϵ being a random variable distributed Fréchet, conditional on $\frac{w_{j,t}^g \varepsilon_{j,t}}{d_{ij,t}}$ being the maximal element of $\left\{ \frac{w_{s,t}^g \varepsilon_{s,t}}{d_{sj,t}} \right\}_{s=1}^I$. Solving for $Pr(i|j, g, t)$, we get

$$\begin{aligned} Pr(i|j, g, t) &= \Pi_{i|gjt} \\ &= \frac{\Pi_{j|git} \Pi_{git}}{\sum_{r=1}^I \Pi_{j|grt} \Pi_{grt}} \\ &= \frac{\Pi_{j|git} L_{Ri,t}^g}{\sum_{r=1}^I \Pi_{j|grt} L_{Rr,t}^g}. \end{aligned}$$

Which implies that

$$\bar{\varepsilon}_{jt}^g = T_g \sum_i \pi_{j|tig}^{-\frac{1}{\theta_g}} \frac{1}{d_{ij,t}} \frac{\pi_{j|tig} L_{Ri,t}^g}{\sum_n \pi_{j|tn} L_{Rn,t}^g}. \quad (38)$$

C.5 Derivation of Equations in First Difference

C.5.1 Deriving Equation 18

Let us first define $\dot{u}_{n,t+1}^g = \exp(V_{n,t+1}^g - V_{n,t}^g)$. Then, from equation 7 we get

$$(\dot{u}_{n,t+1}^g)^{\frac{1}{\nu_g}} = \left[\frac{\exp\left(\tilde{T}_g \Phi_{Rgn,t+1}^{\frac{1}{\theta_g}} r_{Rn,t+1}^{\alpha-1}\right)}{\exp\left(\tilde{T}_g \Phi_{Rgn,t}^{\frac{1}{\theta_g}} r_{Rgn,t}^{\alpha-1}\right)} \right]^{\frac{1}{\nu_g}} \left[\frac{\sum_{i=1}^I (\exp(\beta V_{i,t+2}^g - \mu_{in}^g))^{\frac{1}{\nu_g}}}{\sum_{i=1}^I (\exp(\beta V_{i,t+1}^g - \mu_{in}^g))^{\frac{1}{\nu_g}}} \right].$$

Multiplying and dividing each term in the sum $\sum_{i=1}^I (\exp(\beta V_{i,t+2}^g - \mu_{in}^g))^{\frac{1}{\nu_g}}$ by $(\exp(\beta V_{i,t+1}^g - \mu_{in}^g))^{\frac{1}{\nu_g}}$ we obtain

$$(\dot{u}_{n,t+1}^g)^{\frac{1}{\nu_g}} = \left[\frac{\exp\left(\tilde{T}_g \Phi_{Rgn,t+1}^{\frac{1}{\theta_g}} r_{Rn,t+1}^{\alpha-1}\right)}{\exp\left(\tilde{T}_g \Phi_{Rgn,t}^{\frac{1}{\theta_g}} r_{Rgn,t}^{\alpha-1}\right)} \right]^{\frac{1}{\nu_g}} \left[\frac{\sum_{k=1}^I \left(\exp(\beta V_{k,t+2}^g - \mu_{kn}^g) \right)^{\frac{1}{\nu_g}} \frac{(\exp(\beta V_{k,t+1}^g - \mu_{kn}^g))^{\frac{1}{\nu_g}}}{(\exp(\beta V_{k,t+1}^g - \mu_{kn}^g))^{\frac{1}{\nu_g}}}}{\sum_{i=1}^I (\exp(\beta V_{i,t+1}^g - \mu_{in}^g))^{\frac{1}{\nu_g}}} \right].$$

Reordering terms, and using the fact that

$$m_{kn,t}^g = \frac{\left[\exp(\beta \beta V_{k,t+1}^g - \mu_{kn}^g) \right]^{\frac{1}{\nu_g}}}{\sum_{m=1}^n \left[\exp((\beta \beta V_{m,t+1}^g) - \mu_{mn}^g) \right]^{\frac{1}{\nu_g}}},$$

we obtain

$$\begin{aligned} (\dot{u}_{n,t+1}^g)^{\frac{1}{\nu_g}} &= \left[\frac{\exp\left(\tilde{T}_g \Phi_{Rgn,t+1}^{\frac{1}{\theta_g}} r_{Rn,t+1}^{\alpha-1}\right)}{\exp\left(\tilde{T}_g \Phi_{Rgn,t}^{\frac{1}{\theta_g}} r_{Rgn,t}^{\alpha-1}\right)} \right]^{\frac{1}{\nu_g}} \left[\sum_{k=1}^I m_{kn,t}^g \frac{\left(\exp(\beta V_{k,t+2}^g - \mu_{kn}^g) \right)^{\frac{1}{\nu_g}}}{\left(\exp(\beta V_{k,t+1}^g - \mu_{kn}^g) \right)^{\frac{1}{\nu_g}}} \right] \\ &= \left[\frac{\exp\left(\tilde{T}_g \Phi_{Rgn,t+1}^{\frac{1}{\theta_g}} r_{Rn,t+1}^{\alpha-1}\right)}{\exp\left(\tilde{T}_g \Phi_{Rgn,t}^{\frac{1}{\theta_g}} r_{Rgn,t}^{\alpha-1}\right)} \right]^{\frac{1}{\nu_g}} \left[\sum_{k=1}^I m_{kn,t}^g \left(\exp(\beta (V_{k,t+2}^g - V_{k,t+1}^g)) \right)^{\frac{1}{\nu_g}} \right] \\ &= \left[\frac{\exp\left(\tilde{T}_g \Phi_{Rgn,t+1}^{\frac{1}{\theta_g}} r_{Rn,t+1}^{\alpha-1}\right)}{\exp\left(\tilde{T}_g \Phi_{Rgn,t}^{\frac{1}{\theta_g}} r_{Rgn,t}^{\alpha-1}\right)} \right]^{\frac{1}{\nu_g}} \left[\sum_{k=1}^I m_{kn,t}^g \left(\dot{u}_{k,t+2}^g \right)^{\frac{\beta}{\nu_g}} \right]. \end{aligned}$$

Which implies that

$$\dot{u}_{n,t+1}^g = \left[\frac{\exp\left(\tilde{T}_g \Phi_{Rgn,t+1}^{\frac{1}{\theta_g}} r_{Rn,t+1}^{\alpha-1}\right)}{\exp\left(\tilde{T}_g \Phi_{Rgn,t}^{\frac{1}{\theta_g}} r_{Rgn,t}^{\alpha-1}\right)} \right] \left[\sum_{k=1}^I m_{kn,t}^g \left(\dot{u}_{k,t+2}^g \right)^{\frac{\beta}{\nu_g}} \right]^{\nu_g}. \quad (39)$$

C.5.2 Deriving Equation 19

Let us define $\dot{m}_{in,t+1}^g = \frac{m_{in,t+1}^g}{m_{in,t}^g}$. Then, from equation 8

$$\begin{aligned} \dot{m}_{in,t+1}^g &= \frac{\frac{[\exp(\beta V_{i,t+2}^g - \mu_{in}^g)]^{\frac{1}{\nu_g}}}{\sum_{m=1}^N [\exp(\beta V_{m,t+2}^g - \mu_{mn}^g)]^{\frac{1}{\nu_g}}}}{\frac{[\exp(\beta V_{i,t+1}^g - \mu_{in}^g)]^{\frac{1}{\nu_g}}}{\sum_{m=1}^N [\exp(\beta V_{m,t+1}^g - \mu_{mn}^g)]^{\frac{1}{\nu_g}}}} \\ &= \frac{(\exp(\beta(V_{i,t+2}^g - V_{i,t+1}^g)))^{\frac{1}{\nu_g}}}{\sum_{k=1}^I m_{kn,t}^g (\exp(\beta(V_{k,t+2}^g - V_{k,t+1}^g)))^{\frac{1}{\nu_g}}} \\ &= \frac{(\dot{u}_{i,t+2}^g)^{\frac{\beta}{\nu_g}}}{\sum_{k=1}^I m_{kn,t}^g (\dot{u}_{k,t+2}^g)^{\frac{\beta}{\nu_g}}}. \end{aligned}$$

C.5.3 Deriving Equation 20

Let us define $\dot{r}_{Ri,t+1} = \frac{r_{Ri,t+1}}{r_{Ri,t}}$. From equation 17 we obtain

$$\begin{aligned} \dot{r}_{Ri,t+1} &= \frac{\frac{\sum_{g \in \{h,l\}} L_{Ri,t+1}^g \tilde{T}_g \Phi_{Rgi,t+1}^{\frac{1}{\theta_g}} (1-\alpha)}{H_{Ri}}}{\frac{\sum_{g \in \{h,l\}} L_{Ri,t}^g \tilde{T}_g \Phi_{Rgi,t}^{\frac{1}{\theta_g}} (1-\alpha)}{H_{Ri}}} \\ &= \frac{\sum_{g \in \{h,l\}} L_{Ri,t+1}^g \tilde{T}_g \Phi_{Rgi,t+1}^{\frac{1}{\theta_g}}}{\sum_{g \in \{h,l\}} L_{Ri,t}^g \tilde{T}_g \Phi_{Rgi,t}^{\frac{1}{\theta_g}}}. \end{aligned}$$

C.6 Numerical Solution Algorithm

In this section I provide a more detailed explanation of the numerical solution algorithm implemented in the main quantitative model of this paper.

1. Initiate the algorithm at $t = 0$ with a guess for a path of $\{\{\dot{u}_{t+1}^{g0}\}_{n=1}^I\}_{t=0}^\infty\}_{g \in \{h,l\}}$, such that $\dot{u}_{n,T+1}^g = 1$ for all T large enough, and for all n . Take as given $\{L_{R0}^g, L_{F0}^g, m_{-1}^g, \{d_{ij,t}\}_{i=1,j=1,t=1}^{I,\infty}, \{A_j\}_{j=1}^J, \{\rho_j\}_{j=1}^J, \{\bar{H}_{Ri}\}_{i=1}^I, \{r_{Ri,0}\}_{i=1}^I\}$.
2. For all $t \geq 0$, use $\{\{\dot{u}_{t+1}^{g0}\}_{n=1}^I\}_{t=0}^\infty$ to solve for $\{m_t^g\}_{t=1}^\infty$ using equation (19).
3. Use $L_{R0}^g, \{m_t\}_{t=1}^\infty$, and equation (11) to solve for $\{L_{Rt}^g\}_{t=0}^\infty$.
4. Use $\{L_{Rt}^g\}$ and L_{F0}^g to estimate model consistent wages for period zero ($t = 0$), $\{w_{j,0}^g\}_{j=1}^J$ using the labor market clearing condition for each skill type, (16).

This step follows closely the way equilibrium wages are obtained in Ahlfeldt et al. (2015) using employment population and residential population vectors for $t = 0$. The key here is that these vectors are observed in the data, and so we can find the wages at $t = 0$ that are consistent with the distribution of employment and residential population observed in the data, conditional on the estimated parameters.

5. Use $\{L_{Rt}^g\}, \{w_{j,0}^g\}_{j=1}^J, L_{F0}^g$, and vector equation implied by (16) to solve forward for the model consistent $\{L_{Ft}^g\}_{t=1}^\infty$ and $\{\{w_{j,t}^g\}_{j=1}^J\}_{t=0}^\infty$.

In this section I implement a numerical algorithm to find model-consistent wages for high- and low-skilled workers by inverting the labor demand functions from equations 36 and 37. See Subsection C.6.1 for details on this algorithm.

6. Use $\{L_{Rt}^g\}, \{\Phi_{Rgt}\}$, and equation (20) to solve for $\{\dot{r}_{Rn,t+1}\}$. Then use $\{r_{Ri,0}\}_{i=1}^I$ and $\{\dot{r}_{Rn,t+1}\}$ to solve for $\{r_{Rn,t}\}$.
7. For each t , use $\{\{w_{j,t+1}^g\}, \{m_t^g\}, \{d_{ij,t}\}, \{\dot{r}_{Rn,t+1}\}$, and $\{\dot{u}_{i,t+2}^g\}$ to calculate backwards $\{\dot{u}_{n,t+1}^g\}$ using equation (18) for each skill type g . This will result in a new sequence $\{\dot{u}_{n,t+1}^{g1}\}_{t=0}^\infty$.
8. Verify if $\{\dot{u}_{n,t+1}^{g1}\}_{t=0}^\infty \approx \{\dot{u}_{n,t+1}^{g0}\}_{t=0}^\infty$, if not, then start the again from step 1, with $\{\dot{u}_{n,t+1}^{g1}\}_{t=0}^\infty$ as your new guess. If indeed $\{\dot{u}_{n,t+1}^{g1}\}_{t=0}^\infty \approx \{\dot{u}_{n,t+1}^{g0}\}_{t=0}^\infty$, then $\{\dot{u}_{n,t+1}^{g1}\}_{t=0}^\infty$ is the solution.

C.6.1 Algorithm for Model-Consistent Wages

In order to calculate model-consistent wages at time $t > 0$ using the residential population vector at time t , $\{L_{Ri,t}^g\}$ for residents of both skill types, I use equations 36 and 37, as well as the labor market clearing condition (equation 16) to express wages for both skill types as a function of the full vector of wages, the full vector of residential population, and estimated parameters.

Take 16 for each skill type g , and replace $\tilde{L}_{Fj,t}^g$ with $f_{jgt}(\mathbf{w}_t)$ from equations 36 and 37. Rearranging terms we get

$$(w_{j,t}^l)^{\theta_l+1+(\sigma-1)\rho_j} = \frac{\rho_j}{\bar{\varepsilon}_{j,t}^l} \left(\frac{(w_{j,t}^h)(1-\rho_j)}{A_j} \right)^{(1-\sigma)} \sum_i \sum_g \alpha \tilde{T}_g \left(\sum_s \left(\frac{w_{s,t}^g}{d_{is,t}} \right)^{\theta_g} \right)^{\frac{1}{\theta_g}} \left[\sum_i \frac{L_{Ri,t}^l}{(d_{ij,t})^{\theta_l}} \Phi_{Ril,t} \right]^{-1},$$

and

$$(w_{j,t}^h)^{\theta_h+1+(\sigma-1)(1-\rho_j)} = \frac{(1-\rho_j)}{\bar{\varepsilon}_{j,t}^h} \left(\frac{(w_{j,t}^l)_j^\rho}{A_j} \right)^{(1-\sigma)} \sum_i \sum_g \alpha \tilde{T}_g \left(\sum_s \left(\frac{w_{s,t}^g}{d_{is,t}} \right)^{\theta_g} \right)^{\frac{1}{\theta_g}} \left[\sum_i \frac{L_{Ri,t}^h}{(d_{ij,t})^{\theta_h}} \Phi_{Rih,t} \right]^{-1}.$$

Which imply that

$$w_{j,t}^l = \left[\frac{\rho_j}{\bar{\varepsilon}_{j,t}^l} \left(\frac{(w_{j,t}^h)(1-\rho_j)}{A_j} \right)^{(1-\sigma)} \sum_i \sum_g \alpha \tilde{T}_g \left(\sum_s \left(\frac{w_{s,t}^g}{d_{is,t}} \right)^{\theta_g} \right)^{\frac{1}{\theta_g}} \left[\sum_i \frac{L_{Ri,t}^l}{(d_{ij,t})^{\theta_l}} \Phi_{Ril,t} \right]^{-1} \right]^{\frac{1}{\theta_l+1+(\sigma-1)\rho_j}}, \quad (40)$$

and

$$w_{j,t}^h = \left[\frac{(1-\rho_j)}{\bar{\varepsilon}_{j,t}^h} \left(\frac{(w_{j,t}^l)_j^\rho}{A_j} \right)^{(1-\sigma)} \sum_i \sum_g \alpha \tilde{T}_g \left(\sum_s \left(\frac{w_{s,t}^g}{d_{is,t}} \right)^{\theta_g} \right)^{\frac{1}{\theta_g}} \left[\sum_i \frac{L_{Ri,t}^h}{(d_{ij,t})^{\theta_h}} \Phi_{Rih,t} \right]^{-1} \right]^{\frac{1}{\theta_h+1+(\sigma-1)(1-\rho_j)}}. \quad (41)$$

Stacking all the wages for high- and low-skilled into one vector of length $2 \times J$, $\mathbf{w}_t = \{\{w_{jt}^h\}_{j=1}^J, \{w_{jt}^l\}_{j=1}^J\}$, we get

$$\mathbf{w}_t = \mathbf{g}(\mathbf{w}_t). \quad (42)$$

Where $\mathbf{g} : \mathbb{R}^{2J} \rightarrow \mathbb{R}^{2J}$ is a vector function such that

$$\mathbf{g}_{g,t} = \begin{cases} \left[\frac{(1-\rho_j)}{\bar{\varepsilon}_{j,t}^h} \left(\frac{(w_{j,t}^l)_j^\rho}{A_j} \right)^{(1-\sigma)} \sum_i \sum_g \alpha \tilde{T}_g \left(\sum_s \left(\frac{w_{s,t}^g}{d_{is,t}} \right)^{\theta_g} \right)^{\frac{1}{\theta_g}} \left[\sum_i \frac{L_{Ri,t}^h}{(d_{ij,t})^{\theta_h}} \Phi_{Rih,t} \right]^{-1} \right]^{\frac{1}{\theta_h+1+(\sigma-1)(1-\rho_j)}} & \text{if } g = h \\ \left[\frac{\rho_j}{\bar{\varepsilon}_{j,t}^l} \left(\frac{(w_{j,t}^h)(1-\rho_j)}{A_j} \right)^{(1-\sigma)} \sum_i \sum_g \alpha \tilde{T}_g \left(\sum_s \left(\frac{w_{s,t}^g}{d_{is,t}} \right)^{\theta_g} \right)^{\frac{1}{\theta_g}} \left[\sum_i \frac{L_{Ri,t}^l}{(d_{ij,t})^{\theta_l}} \Phi_{Ril,t} \right]^{-1} \right]^{\frac{1}{\theta_l+1+(\sigma-1)\rho_j}} & \text{if } g = l. \end{cases}$$

In this way we have defined the full vector of wages as a fixed point that solves the vector equation $\mathbf{w}_t = \mathbf{g}(\mathbf{w}_t)$. In order to obtain a unique (to-scale) \mathbf{w}_t , we can start with any initial vector, and apply iteratively $\mathbf{g}(\mathbf{w}_t)$ until the difference between one iteration and the previous is small enough, where I define the difference in terms of the L^2 distance between vectors. This algorithm will result in a unique (to-scale) vector that solved the vector equation $\mathbf{w}_t = \mathbf{g}(\mathbf{w}_t)$. This follows from the fact that $\mathbf{g}(\mathbf{x})$ is strictly increasing in \mathbf{x} , and weakly homogenous, which implies that $\mathbf{g}(\lambda \mathbf{x}) = f(\lambda) \mathbf{g}(\mathbf{x})$, for $f : \mathbb{R}_+ \rightarrow \mathbb{R}_+$ such

that $\frac{f(\lambda)}{\lambda}$ is strictly increasing and $f(0) = 0$. With these properties, Fujimoto and Krause (1985) show that there must exist a unique up-to-scale solution to $\mathbf{w}_t = \mathbf{g}(\mathbf{w}_t)$.

C.7 Deriving Expected Utility Expression

From equation (8), and the assumption that the mobility costs are zero for non-movers ($\mu_{nn} = 0$) we know that

$$m_{nn,t}^g = \frac{(\exp(\beta V_{n,t+1}^g))^{\frac{1}{\nu}}}{\sum_{m=1}^I (\exp(\beta V_{m,t+1}^g - \mu_{mn}^g))^{\frac{1}{\nu_g}}}.$$

Taking logs at both sides we get

$$\ln(m_{nn,t}^g) = \frac{1}{\nu_g} (\beta V_{n,t+1}^g) - \ln \left(\sum_{m=1}^I (\exp(\beta V_{m,t+1}^g - \mu_{mn}^g))^{\frac{1}{\nu_g}} \right).$$

From (7) we know that

$$V_{n,t}^g = \tilde{T}_g \Phi_{Rgn,t}^{\frac{1}{\theta}} r_{Rn,t}^{\alpha-1} + \nu_g \ln \left(\sum_{m=1}^I (\exp(\beta V_{m,t+1}^g - \mu_{mn}^g))^{\frac{1}{\nu_g}} \right)$$

which, along with the previous equation implies that

$$V_{n,t}^g = \tilde{T}_g \Phi_{Rgn,t}^{\frac{1}{\theta}} r_{Rn,t}^{\alpha-1} + \beta V_{n,t+1}^g - \nu_g \ln(m_{nn,t}^g).$$

Iterating this equation forward and substituting we obtain

$$V_{n,t}^g = \sum_{s=t}^{\infty} \beta^{s-t} \left[\tilde{T}_g \Phi_{Rgn,s}^{\frac{1}{\theta}} r_{Rn,t}^{\alpha-1} - \nu_g \ln(m_{nn,s}^g) \right]. \quad (43)$$

C.8 Calibrating Additional Parameters

I fix $T_l = 1$, and I calibrate T_h in order to equalize the average wage premium in the model to the average average wage premium in the city according to the 2011 first quarter National Household Survey (*Encuesta Permanente de Hogares*). Let \hat{WP} be the observed average wage premium, I calculate T_h so that

$$\hat{WP} = \frac{T_h \sum_i \Phi_{Rih0}^{1/\theta_h} \lambda_{ih}}{\sum_i \Phi_{Ril0}^{1/\theta_l} \lambda_{il}}, \quad (44)$$

where

$$\lambda_{ig} = \frac{L_{Ri}^g}{L_{Ri}^h + L_{Ri}^l}.$$

This results in $T_h = 1.146$.

In order to calculate $\{\rho_j\}_{j=1}^J$, and $\{A_j\}_{j=1}^J$, I first estimate $\{w_{j0}^g\}_{j=1,g \in \{h,l\}}^J$ using equation 16; the residential population vector for $t = 0$, $\{L_{Ri,t}^g\}$, by skill type; and the employment population vector for $t = 0$, $\{L_{Fj,t}^g\}$, both of which are observed data. I calculate the model-consistent wages following the algorithm used in Ahlfeldt et al. (2015). With this wage vector, and the employment population at $t = 0$, I estimate the $\{\rho_j\}_{j=1}^J$ from the following equation:

$$\frac{\tilde{L}_{Fj0}^h w_{j0}^h}{\tilde{L}_{Fj0}^l w_{j0}^l} = \frac{1 - \rho_j}{\rho_j},$$

and I estimate the vector of total factor productivities, $\{A_j\}_{j=1}^J$, from the following equation:

$$A_j = \left[\frac{\tilde{L}_{Fj0}^l w_{j0}^l}{\rho_j} [(w_{j0}^l)^{\rho_j} (w_{j0}^h)^{(1-\rho_j)}]^{\sigma-1} \left[\sum_i \sum_{g \in \{h,l\}} \alpha \tilde{T}_g \left(\sum_s \left(\frac{w_{s0}^g}{d_{is0}} \right)^{\theta_g} \right)^{\frac{1}{\theta_g}} L_{Ri0}^g \right]^{-1} \right]^{\frac{1}{\sigma-1}}.$$

I will do this by first calculating

$$X = \sum_i \sum_{g \in \{h,l\}} \alpha \tilde{T}_g \left(\sum_j \left(\frac{w_{j0}^g}{d_{ij0}} \right)^{\theta_g} \right)^{\frac{1}{\theta_g}} L_{Ri0}^g,$$

and then calculating

$$A_j = \left[\frac{\tilde{L}_{Fj0}^l w_{j0}^l}{\rho_j} [(w_{j0}^l)^{\rho_j} (w_{j0}^h)^{(1-\rho_j)}]^{\sigma-1} [X]^{-1} \right]^{\frac{1}{\sigma-1}}$$

for each $j = 1, \dots, J$

C.9 Derivation of Estimating Equation for Migration Elasticities

From equation 8 we know that

$$\ln(m_{nn,t}^g) = \frac{1}{\nu_g} (\beta V_{n,t+1}^g) - \ln \left(\sum_{m=1}^I (\exp(\beta V_{m,t+1}^g - \mu_{mn}^g))^{\frac{1}{\nu_g}} \right),$$

and

$$\ln(m_{in,t}^g) = \frac{1}{\nu_g} (\beta V_{n,t+1}^g - \mu_{in}) - \ln \left(\sum_{m=1}^I (\exp(\beta V_{m,t+1}^g - \mu_{mn}^g))^{\frac{1}{\nu_g}} \right).$$

Which implies that

$$\ln \left(\frac{m_{in,t}^g}{m_{nn,t}^g} \right) = \frac{1}{\nu_g} (\beta (V_{i,t+1}^g - V_{n,t+1}^g) - \mu_{in}),$$

so that

$$\begin{aligned} \ln \left(\frac{m_{in,t}^g}{m_{nn,t}^g} \right) &= \frac{\beta}{\nu_g} \left(\tilde{T}_g \left(\Phi_{Rgi,t+1}^{\frac{1}{\theta}} r_{Ri,t+1}^{\alpha-1} - \Phi_{Rgn,t+1}^{\frac{1}{\theta}} r_{Rn,t+1}^{\alpha-1} \right) \right. \\ &\quad \left. + \nu_g \left(\ln \left(\sum_{m=1}^I (\exp(\beta V_{m,t+2}^g - \mu_{mi}^g))^{\frac{1}{\nu_g}} \right) - \ln \left(\sum_{m=1}^I (\exp(\beta V_{m,t+2}^g - \mu_{mn}^g))^{\frac{1}{\nu_g}} \right) \right) - \frac{\mu_{in}}{\beta} \right). \end{aligned} \quad (45)$$

Now consider that

$$\ln \left(\frac{m_{in,t+1}^g}{m_{ii,t+1}^g} \right) = -\frac{\mu_{in}}{\nu_g} + \left(\ln \left(\sum_{m=1}^I (\exp(\beta V_{m,t+2}^g - \mu_{mi}^g))^{\frac{1}{\nu_g}} \right) - \ln \left(\sum_{m=1}^I (\exp(\beta V_{m,t+2}^g - \mu_{mn}^g))^{\frac{1}{\nu_g}} \right) \right),$$

which implies that

$$\nu_g \ln \left(\frac{m_{in,t+1}^g}{m_{ii,t+1}^g} \right) + \mu_{in} = \nu_g \left(\ln \left(\sum_{m=1}^I (\exp(\beta V_{m,t+2}^g - \mu_{mi}^g))^{\frac{1}{\nu_g}} \right) - \ln \left(\sum_{m=1}^I (\exp(\beta V_{m,t+2}^g - \mu_{mn}^g))^{\frac{1}{\nu_g}} \right) \right).$$

Combining this result with the expression for $\ln \left(\frac{m_{in,t}^g}{m_{nn,t}^g} \right)$ derived above, we obtain

$$\ln \left(\frac{m_{in,t}^g}{m_{nn,t}^g} \right) = \frac{\beta}{\nu_g} \left(\tilde{T}_g \left(\Phi_{Rgi,t+1}^{\frac{1}{\theta}} r_{Ri,t+1}^{\alpha-1} - \Phi_{Rgn,t+1}^{\frac{1}{\theta}} r_{Rn,t+1}^{\alpha-1} \right) + \beta \ln \left(\frac{m_{in,t+1}^g}{m_{ii,t+1}^g} \right) \right) - \mu_{in} \frac{1-\beta}{\nu_g}. \quad (46)$$

Taking expectation at time t of equation 46 we get

$$E_t \left[\ln \left(\frac{m_{in,t}^g}{m_{nn,t}^g} \right) \right] = E_t \left[\frac{\beta}{\nu_g} \left(\tilde{T}_g \left(\Phi_{Rgi,t+1}^{\frac{1}{\theta}} r_{Ri,t+1}^{\alpha-1} - \Phi_{Rgn,t+1}^{\frac{1}{\theta}} r_{Rn,t+1}^{\alpha-1} \right) + \beta \ln \left(\frac{m_{in,t+1}^g}{m_{ii,t+1}^g} \right) \right) - \mu_{in} \frac{1-\beta}{\nu_g} \right].$$

Which can be interpreted as the linear regression equation:

$$\log \left(\frac{m_{in,t}^g}{m_{nn,t}^g} \right) = -\mu_{in}^g \frac{1-\beta}{\nu_g} + \frac{\beta}{\nu_g} \left[\tilde{T}_g \left(\Phi_{Rgi,t+1}^{\frac{1}{\theta_g}} r_{Ri,t+1}^{\alpha-1} - \Phi_{Rgn,t+1}^{\frac{1}{\theta_g}} r_{Rn,t+1}^{\alpha-1} \right) \right] + \beta \log \left(\frac{m_{in,t+1}^g}{m_{ii,t+1}^g} \right) + \omega_{t+1}^g. \quad (47)$$

D Supplementary Quantitative Results

D.1 Model Results at the Census Tract Level

Reduced Form (IV)		Model	
		$\Delta \log(hs\ share_{BRT}) - \Delta \log(hs\ share_{CF})$	
$\Delta \log(CMA)$	-2.308 (0.522)***	$\Delta \log(CMA_{BRT}) - \Delta \log(CMA_{CF})$	-2.79 (0.34)***
hs share ₀	0.113 (0.052)**	hs share ₀	-0.05 (0.02)
$\Delta \log(CMA) \times hs\ sh.\ avg_{t=0}$	4.143 (0.847)***	$\Delta \log(CMA_{BRT}) - \Delta \log(CMA_{CF}) \times hs\ share_{0}$	5.66 (0.65)***
cons	-0.419 (0.036)***	cons	-0.01 (0.01)
N	2,282	N	2,282

Table D.1: Reduced form results versus model estimation at census tract level. The left-hand side shows the results from column 4 of table 4, while the right-hand side shows the results from the difference in difference estimation within the model at the census tract level, comparing changes between $t = 0$, and $t = 0$, and between the model with the BRT system, and the counterfactual without a BRT system put in place. Robust standard errors in parentheses. * $p < 0.10$, ** $p < 0.05$, *** $p < 0.01$.

D.2 Calculations for GDP Gains Net of Construction Costs

Let X_t be the aggregate income in the city at time t ,

$$\sum_i \sum_{g \in \{h,l\}} \alpha \tilde{T}_g \left(\sum_j \left(\frac{w_{j,t}^g}{d_{ij,t}} \right)^{\theta_g} \right)^{\frac{1}{\theta_g}} L_{Ri,t}^g.$$

We can calculate the net present value of the benefits of the *Metrobus*, net of construction costs by calculating the discounted sum of the excess growth in aggregate income in the city and subtracting the discounted sum of the construction costs:

$$NPV_{GDP\ gains} = \left[\sum_{t=0}^{\infty} \beta^t \left(\frac{X_t}{X_0} - \frac{\hat{X}_t}{X_0} \right) \right] GDP_0 - \sum_{t=0}^4 C_t.$$

Where \hat{X}_t is the aggregate income at time t under the counterfactual scenario where no BRT was put in place, GDP_0 is the two year GDP for 2010 and 2011 for the city of Buenos Aires, and C_t is the estimated

construction cost measured in 2010 dollars for the bi-annual period that corresponds to each period t in the model. These construction costs are estimated by taking the average construction cost per kilometer, obtained from AGCBA (2015), and AGCBA (2019), and multiplying this number by the total number of kilometers built in each bi-annual period. Table D.2 shows the resulting estimated values. Once a net present value is obtained (measures in 2010 dollars), I calculate the fifty-year annuity payment that would lead to the same net present value, at an annual discount rate of $\beta^{-\frac{1}{2}}$, and express this annuity payment in terms of the city's 2010 GDP.

NPV of benefits of BRT (mm US dollars 2010)	13387
NPV of Construction Costs (mm US dollars 2010)	121
NPV of net gains of BRT (mm US dollars 2010)	13266
NPV gains as 2010 GDP constant growth equivalent (%)	0.4

Table D.2: Net present value of GDP gains from the *Metrobus* lines built between 2011 and 2017, net of construction costs.